BIOMATERIAL INTEGRATION WITHIN 3D STEM CELL

AGGREGATES FOR DIRECTED DIFFERENTIATION

A Thesis
Presented to
The Academic Faculty

by

Andrés Miguel Bratt-Leal

In Partial Fulfillment
of the Requirements for the Degree
Doctor of Philosophy in the
College of Engineering

Georgia Institute of Technology
December 2011

BIOMATERIAL INTEGRATION WITHIN 3D STEM CELL

AGGREGATES FOR DIRECTED DIFFERENTIATION

Approved by:

Dr. Todd McDevitt, Advisor
Department of Biomedical Engineering
Georgia Institute of Technology

Dr. Johnna Temenoff
Department of Biomedical Engineering
Georgia Institute of Technology

Dr. William Murphy
Department of Biomedical Engineering
University of Wisconsin

Dr. Andrés García
School of Mechanical Engineering
Georgia Institute of Technology

Dr. Athanassios Sambanis
School of Chemical and
Biomolecular Engineering
Georgia Institute of Technology

Date Approved: November 8, 2011

To my parents – Héctor and Carol

ACKNOWLEDGEMENTS

First, I would like to acknowledge the contributions of my committee members, Dr. Andrés García, Dr. Johnna Temenoff, Dr. Athanassios Sambanis, Dr. William Murphy and finally my advisor, Dr. Todd McDevitt. I appreciate the thoughtful insight, advice and critiques on various aspects of this project. Dr. García has played a large role in my academic career both as a professor for my biomaterials and cell engineering classes, and as a mentor during my participation in the tissue engineering training grant and beyond. Besides his valuable input on thesis work, I learned a lot from him at biomaterials related conferences and I really appreciate the time he spent leading the tissue engineering journal clubs. I've also enjoyed playing basketball with Dr. García, even though we've never been on the same team, it's always fun playing against a great competitor. Dr. Temenoff has contributed greatly to the project in terms of sharing her expertise in the areas of glycosaminoglycans and controlled release. I've spent a lot of time with the Temenoff lab and I have enjoyed our collaborations on extensions of this project to GAG materials and their applications to embryonic and mesenchymal stem cell spheroids. I appreciate all the advice that Dr. Temenoff has given me and also her sense of humor. I'd also like to thank Dr. Sambanis for being a great teacher. When I was a student in his class I was impressed by his thoughtfulness and I knew that I wanted to work with him in the future. I'm glad that his area of expertise is applicable to this project because I would have asked him to be on my committee in any case and I am grateful for the broad perspective he has provided to this work. Dr. Murphy served on my committee from Wisconsin and I appreciate the input he has given on this project. He

provided great advice on the presentation of this work and it's relation to developmental biology. His expertise on growth factor interactions and biomaterials are also appreciated. I wish that I had talked to Dr. Murphy earlier in my thesis project because he had some really great ideas for experiments.

I'm also very grateful for the opportunities provided to me while working in Todd's lab. Todd has been a great advisor, mentor, and teacher. Reflecting now, I better appreciate Todd's attention to detail and stringent requirements for manuscripts, abstracts and posters and I know that his training has prepared me well for my future endeavors. Todd is very passionate about research but he also cares about a well-rounded graduate experience and future careers of his students. Todd will definitely fight for his students and is protective of their research time. Beyond that, I've enjoyed getting to know Todd and Meg personally at various lab functions outside of research, and I know that we will be friends long past my time at Georgia Tech. Meg attended several of my oral presentations and I appreciate all the encouragement that she provided. Meg is a lot of fun to be around and I always appreciated her culinary talent.

I'd also like to thank Dr. Peter Zandstra and Dr. Kelly Purpura for their contributions to my thesis. Besides the numerous conference calls we spent discussing morphogen delivery from gelatin microparticles, Kelly and I frequently were in touch over email and video chat and talking with Kelly was always helpful in sorting out experimental design and data.

There are many individuals in the BME department, IBB and bioengineering program who deserve acknowledgement and thanks. In particular, Aqua Asberry in the histology lab and Steve Woodard in the confocal labs have been extremely helpful. I

beyond. The amount of competitive eating that went on in my time here was outstanding, especially when Rich was around. Sitting next to Rich for 4 years was always entertaining and definitely made lab fun to come to every day. I hope he knows that a picture I spent hours making of two Rich's will forever follow him wherever he goes.

Lab members here before me including Rekha Nair, Rich, Carolyn, Alyssa and Ima Ebong were excellent role models and I learned a lot about research from them and they made me feel welcome from the first day I stepped into lab. Thanks also to the friends that I made when I first moved to Atlanta that have since graduated including Blaine Zern, Torrence Welch, John Wilson, Mary Milner, Adam Higgins, Sarah Stabenfeldt, Chris Lessing, Chris Wilson, Hillary Irons, Meg Oest, Scott Robinson and Andrew Smith. I was fortunate enough to meet a lot of great people who made me part of their group of friends and always were willing to pass on advice from their time as graduate students. GB Fest, music with ESB, Brock's, fry parties and ABC were all amazing.

Thanks also to all the great friends I've made at Georgia Tech and Emory. Particularly, I spent a lot of time with Jeremy Lim, Erin Spinner, Chris and Ashley Brown, Randy Ankeny, Casey Holliday, Jason Weaver, Priya Santhanam, Jay Sy, Rachel Whitmire, Barbara and Ken. The times we spent celebrating quals, defenses, marriages, Halloween and other random events were memorable and I can't imagine the last 5 years without you guys. Jeremy, I really appreciate how great a friend you've been, the times we've had (robots in Chicago, Hawks, Braves and GT games, intramurals to name a few) and I hope you know you are stuck with me bugging you to come to Cali.

I want to thank Erin Spinner for all that we shared during graduate school. Erin's dedication and focus to her work is impressive and I've learned a lot from her. She was always willing to listen to me practice a presentation and gave great advice on how to improve my presentation style, which I really appreciated. Besides inspiring me to try and keep up with her pace in graduate school, she is a great travel partner and our trip to India is one that I will never forget. Her love and support made everything easier, especially during the last few months before my defense, and our time apart made it even more obvious how much she means to me.

My parents, Héctor and Carol, have always supported me in everything I've done and their love and support during graduate school was all that I could've asked for. Graduate school is full of ups and downs and my parents were always there to help me celebrate my successes and to provide encouragement and inspiration when I needed it. My parents are my friends and role models and I know that their advice comes from unselfish love with my best interests in mind. To my sisters, Claire and Valerie, my grandmother Arlene, and my uncle Alonso, thank you for your love and support.

TABLE OF CONTENTS

x

xi

LIST OF FIGURES

xv

xvi

LIST OF ABBREVIATIONS

AFP	α-Fetoprotein
bFGF	Basic Fibroblast Growth Factor
BMP-4	Bone Morphogenetic Protein-4
CM	Conditioned Medium
EB	Embryoid Body
ESC	Embryonic Stem Cell
GAG	Glycosaminoglycan
IGF-II	Insulin-Like Growth Factor II
IGFBP	Insulin-Like Growth Factor Binding Proteins
IPSC	Induced Pluripotent Stem Cell
LIF	Leukemia Inhibitory Factor
MagMP	Magnetic Microparticle
MP	Microparticle
MSC	Mesenchymal Stem Cell
PCR	Polymerase Chain Reaction
PLGA	poly(lactic-co-glycolic acid)
SEM	Scanning Electron Microscopy
TPO	Thrombopoeitin
VE-cadherin	Vascular Endothelial Cadherin
VEGF	Vascular Endothelial Growth Factor

SUMMARY

The derivation of embryonic stem cells (ESCs), first from mice blastocysts in 1981 then eventually from human blastocysts in 1998 has created an invaluable resource for scientific study and discovery. ESC models allow for *in vitro* study of normal and pathological mammalian embryological development and have created a platform on which therapies can be tested on human cells before trial in the clinic. Directed differentiation of ESCs towards functional, adult-cell types holds the promise of cell-based regenerative medicine with goals of curing diseases and restoration of function, rather than pharmacological treatment of symptoms or mitigation of side-effects. Already two clinical trials using human ESC derived adult cell types have begun in the United States to determine the safety and efficacy of ESC-derived cell therapies.

Even with successful derivation of adult cell types including cardiomyocytes, oligodendrocytes, retinal epithelial cells and others, further improvement in differentiation protocols is necessary to generate the large number of cells needed for clinical relevance. Additionally, directed differentiation of ESCs towards heterogeneous cell types, organized in 3D for construction of neo-tissues would be of great value for both research diagnostics, including limiting the need for animal studies, and for regenerative therapies. Differentiation of ESCs is commonly initiated through the formation of aggregates grown in suspension culture, termed embryoid bodies (EBs). Differentiation within EBs can be directed by the addition of soluble growth factors to the surrounding medium; however, barriers to free diffusion within the aggregates limit the effectiveness of this method. Recently, engineered biomaterials incorporated within

aggregates of ESCs have been utilized to gain access to the interior microenvironment. The goal of this work was to develop a method to incorporate biomaterial microparticles (MPs) within stem cell aggregates and to evaluate their use for local control of the cellular microenvironment for directed differentiation. The central hypothesis was that incorporation of biomaterials within EBs would induce efficient differentiation by controlled presentation of morphogens.

The effects of unloaded MPs on ESC differentiation were first determined by controlled incorporation of poly(lactic-co-glycolic acid) (PLGA), agarose and gelatin MPs. Previously reported methods of material incorporation within EBs were not adequate for incorporation of the three materials, therefore, a forced aggregation culture technique was modified to allow for robust and controlled incorporation of the MPs within EBs. Forced aggregation allowed for controlled study of EBs containing roughly the same number of MPs fabricated from the different material types. EB formation, cell viability, and gross morphology were not affected by the presence of the MPs. Further analysis of gene expression and patterns of phenotypic marker expression revealed alterations in the differentiation profile in response to material incorporation. Specifically, endoderm genes, including α-fetoprotein (AFP), and mesoderm genes, including myosin light chain-2V (MLC-2V), were increased in presence of gelatin MPs. Patterns of phenotypic marker expression of AFP and α-sarcomeric actin, analyzed by whole-mount immunostaining, were also altered in MP treated groups.

It was hypothesized that the materials could be interacting with endogenously produced growth factors, thereby altering the microenvironment and modulating EB differentiation. In order to test this hypothesis, gelatin MPs were modified with heparin,

xix

a sulfated glycosaminoglycan known to regulate growth factor interactions *in vivo.* Incorporation of heparin-modified gelatin MPs altered the secretion of growth factors by the EBs into the surrounding medium and gene expression was altered at days 7 and 11. The spatial expression pattern of vascular endothelial cadherin, a marker expressed by endothelial cells, was found to co-localize with the heparin-gelatin MPs, but not with unmodified gelatin MPs, further suggesting the MPs can influence the local microenvironment with EBs.

The ability of MPs to direct ESC differentiation was investigated by incorporation of growth factor loaded MPs within EBs. MPs were loaded with bone morphogenetic protein-4 (BMP-4), a protein which promotes mesoderm differentiation of ESCs, or with Noggin, a BMP-4 inhibitor. BMP-4 loaded MPs were capable of inducing mesoderm gene expression (Brachyury-T and fetal liver kinase-1) while at the same time inhibiting expression of an ectoderm marker (Pax-6) compared to untreated EBs. Noggin loaded MPs did not reduce mesoderm gene expression compared to untreated EBs but did increase the expression of Pax-6. Further analysis was performed on EBs formed from ESCs genetically engineered to express green fluorescent protein when Brachyury-T is expressed. EBs with BMP-4 loaded gelatin MPs contained a higher percentage of cells differentiated towards a mesoderm lineage (~50%) compared to soluble BMP-4 treatment (~40%) and untreated EBs (~25%). In this study, the amount of BMP-4 used for soluble delivery was over 10 fold greater than that used via MPs, indicating the potential applicability of MP based delivery methods for directed differentiation in large scale bioreactor systems.

Finally, magnetic MPs (magMPs) were incorporated within EBs for controlled heterogeneity within cell constructs. The number of incorporated magMPs was controlled by the seed ratio (cells:magMPs) used prior to EB formation. Similar to PLGA, agarose and gelatin MPs tested previously, magMP incorporation did not affect EB formation, viability or gross morphology. After formation, EBs containing magMPs could be manipulated using magnets placed outside the culture dish. The sensitivity of EBs to applied magnetic fields was controlled by the number of magMPs incorporated within the aggregates. Magnets placed on the outside of culture vessels were used to pattern populations of EBs both in static and in hydrodynamic culture systems. Cell construct heterogeneity could be controlled by taking advantage of E-cadherin based agglomeration of ESC aggregates placed in contact under static conditions. By using magnetic guidance to control the precise spatial location of EBs, a single construct could be created from 4 EBs formed from fluorescently labeled ESC populations. Interestingly, the fluorescently labeled cells remained in the approximate location of their original EB, thereby creating distinct quadrants, visualized by fluorescent microscopy, in the resulting construct. This same principle was used to create larger constructs from heterogeneous populations of hundreds of EBs demonstrating the flexibility of magnetic manipulation across broad length scales.

Overall, the results indicated that PSC differentiation within spheroids is sensitive to various types of biomaterials. Incorporation of MPs within EBs can be used to direct ESC differentiation by control of the cellular environment from microscale interactions, by delivery of soluble factors, to macroscale interactions, by control of EB position in static and suspension cultures.

CHAPTER 1

INTRODUCTION

Embryonic stem cells (ESCs) are pluripotent cells with the potential to serve as a limitless source for a range of cellular therapies. Limitations in current approaches to controlling ESC differentiation have prevented wide-scale application of ESC derived cells in clinical trials. Complex, multi-step protocols exist to increase the efficiency of directed differentiation in monolayer culture; however, such methods have only been successfully applied only to select cell types. Recently, interest has grown in manipulation and engineering of the three-dimensional microenvironment of ESC spheroids, termed embryoid bodies (EBs), in order to develop scalable differentiation methods more broadly applicable to the production of a wide range of mature cell types. Current approaches to directing EB behavior focus on "outside-in" methods including: manipulation of media components and control of EB size. Both these methods act directly on cells of only the exterior of the spheroids leading to non-uniform treatment of cells and gradients in signaling. Conversely, our lab has developed methods to incorporate biomaterial morphogen delivery vehicles within EBs as an "inside-out" approach to more efficiently control the local microenvironment of cells in the EB interior for directed differentiation. **The <u>objective</u> of this work was to efficiently direct ESC differentiation within EBs through incorporation of biomaterial microparticles. The <u>central hypothesis</u> was that incorporation of biomaterial microparticles within EBs would induce efficient differentiation by spatially and temporally controlled presentation of morphogenic factors.** The objective was

1

accomplished and the central hypothesis was tested through completion of the following specific aims:

Specific Aim 1.   Determine the effects of unloaded biomaterial MPs on EB differentiation. The working hypothesis was that the presence of unloaded biomaterial microparticles within EBs can influence ESC differentiation. The number of MPs incorporated per EB was determined for PLGA, agarose and gelatin MPs as a function of loading conditions. The effects of incorporation on EB differentiation were tested using equal incorporation amounts of comparably sized particles allowing for comparisons between materials. Material effects were further analyzed by incorporation of heparin-modified gelatin MPs. The material effects on differentiation were assessed using gross morphological analysis as well as qtPCR and immunofluorescent staining of early germ lineage markers for endoderm, mesoderm and ectoderm.

Specific Aim 2. Investigate the efficacy of MP delivery of single morphogens for directed differentiation within EBs. The working hypothesis was that morphogens delivered locally within EBs via incorporated MPs would result in more efficient differentiation, requiring less growth factor compared to soluble delivery. BMP-4 was delivered via gelatin MPs for directed mesodermal differentiation. In parallel, Noggin, a naturally secreted agonist of BMP4, loaded particles were also examined for their ability to inhibit mesoderm differentiation and promote ectoderm differentiation. Differentiation was assessed through gene and protein expression analysis of mesodermal and neural markers as well as morphological hallmarks of differentiation including neurite outgrowth.   Cells genetically engineered to express green fluorescent protein upon

2

Brachyury-T expression, a marker of early mesoderm differentiation, were utilized to examine spatial patterns of differentiation in all conditions.

Specific Aim 3. Examine the ability of microparticle incorporation to manipulate EBs on micro and macro scales. The working hypothesis was that controlled incorporation of magnetic MPs within EBs can modulate EB sensitivity to magnetic fields, allowing subsequent magnetic manipulation of spheroid location and merging. The application of magnetic fields was examined as a method to control spatial positioning of single spheroids as well as populations of spheroids in dynamic and static suspension culture. Magnetic fields were used to control the aggregation of heterogeneous EBs to form a single construct for complex, multi-signal control of the microenvironment. The effects of magnetic MP incorporation were determined by gene expression analysis, analysis of EB morphology and cell viability.

The work is significant because it is the first study to utilize and analyze the effects of multiple materials incorporated within stem cell aggregates. Material specific effects on ESC differentiation led to development of heparin-modified particles for directed interaction between endogenously secreted factors and the microparticles within 3D constructs. Efficient capture or presentation of endogenously secreted factors could enable large-scale differentiation of ESCs in suspension with minimal growth factor supplementation. In addition, the use of MPs to control growth factor presentation in combination with magnetic manipulation of spheroids is an enabling technology expected to yield insights for the transformation of ESCs into neo-tissues with applications to stem cell biology and tissue engineering.

3

CHAPTER 2

BACKGROUND[*]

Embryonic stem cells

Embryonic stem cells (ESCs) are capable of extensive self-renewal *in vitro* and differentiate into cells constituting all three primitive germ layers– mesoderm, ectoderm and endoderm, as well as germ cells (sperm and ova). ESCs, isolated from the inner cell mass of blastocyst stage embryos, were first derived from mouse embryos[1-3], followed by the derivation of primate[4, 5] and human[6, 7] ESC lines. Recently, an alternative method for deriving pluripotent cells by retroviral transduction of a combination of embryonic genes into somatic cells was reported, first by Yamanaka's group, followed shortly thereafter by several other groups independently[8-12]. The "induced" pluripotent stem (iPS) cells created from both mouse and human somatic cells appear similar to ESCs in terms of both self-renewal and differentiation capacity.

A functional test of pluripotency is whether introduction of the cells into a blastocyst stage embryo results in a chimera with ESCs (or iPS cells) contributing to all tissues of the organism[13, 14]. Similarly, ESCs injected into various tissue sites of adult organisms spontaneously form teratomas, benign tumors composed of a disorganized mix of cells from all three germ layers. Blastocyst injection and teratoma studies demonstrate

---

[*] Modified from :
Bratt-Leal, AM, Carpenedo RL, McDevitt TC. *Engineering the embryoid body microenvironment.* Biotechnology Progress. (2009) **25**(1): 43-51
Bratt-Leal, AM, Carpenedo RL, McDevitt TC. *Integration of materials into 3D stem cell environments.* Biomaterials as Stem Cell Niche. K. Roy, Editor. Springer: Berlin. p. 45-59 (2010)

4

that the environment into which pluripotent cells are introduced can influence differentiation, however, *in vivo* studies are limited in their ability to attain mechanistic insights into the effects of environmental factors on stem cell differentiation. In contrast, differentiation of ESCs *in vitro*, affords more controlled methods to present morphogenic cues in the stem cell microenvironment and directly assess differentiated cell phenotypes. Common formats to induce ESC differentiation *in vitro* include monolayer culture on defined matrices[15], co-culture with heterotypic cell types[16] and the formation of cell aggregates grown in suspension termed embryoid bodies (EBs)[3]. Culture of ESCs in planar formats (i.e. monolayer, co-culture) attempt to provide a more defined substrate for ESC attachment and uniform exposure to soluble media components, while the 3D aggregates of ESCs formed by EB culture techniques more accurately recapitulate the complex assembly of cell adhesions and intercellular signaling of early embryogenesis.

Culture in two or three dimensions

Traditionally, two-dimensional culture (2-D) is used to maintain cells in an undifferentiated state whereas three-dimensional (3-D) culture techniques are more commonly implemented in differentiation protocols. For example, ESCs are commonly differentiated through the formation of 3-D multicellular aggregates, referred to as embryoid bodies (EBs)[3]. Spheroid culture provides a platform for scalable culture of cells because they can be grown in suspension and require a lower tissue culture surface area-to-volume ratio compared to cells in monolayer. The 3D spheroid microenvironment is complex and becomes more so as differentiation progresses. Differentiating cells

5

deposit extracellular matrix and are subjected to homo- and heterotypic cell-cell interactions, as well as autocrine and paracrine factors.

Soluble factors added to the culture media are more accessible to cells grown in monolayer and the temporal resolution of these factors can be fairly well controlled by simply exchanging the culture media at specific times[17]. In contrast, 3-D culture provides more physiological cues such as increased cell-cell interactions and the potential for increased cell-extracellular matrix interaction; however, diffusion limitations complicate 3-D cultures of cells. Concentration gradients of soluble factors added to the media, which result from the diffusion properties of 3-D cellular aggregates or constructs, can result in differences in the microenvironment depending on the spatial positioning of cells. Stem cells can be very sensitive to small perturbations in the biochemical composition of their surroundings and the effects of soluble factors often vary in a dose-dependent manner. This limited control of the 3D environment has necessitated the development of biomaterial technologies to engineer the microenvironment of 3D culture systems in order to further develop stem cell differentiation protocols.

Embryoid body development

The *in vitro* culture of ESCs as EBs affords opportunities to mechanistically study early differentiation events of 3D assemblies of pluripotent cells. One advantage of *in vitro* differentiation studies is that genetic manipulation of ES cells can be studied for gene mutations or knockouts that prove to be lethal during normal embryonic development *in vivo*[18-20]. Although several phenotypic and functional differences between mouse and human ESCs have been determined[21-24], few studies have directly

6

examined differences between mouse and human EB differentiation. One such study, however, identified shared signaling pathways active during mouse and human EB differentiation, suggesting that mechanisms regulating differentiation may be conserved between the species[25]. EB differentiation begins with the formation of an aggregate of ESCs, the size of which is dependent on the number of cells which initially self-assemble via cell-cell adhesion receptors[26-28]. Following cell aggregation, the first indication of differentiation is the spontaneous formation of a layer of primitive endoderm (PE) on the exterior surface of the EBs (*23*). While the specific cues responsible for stimulating PE differentiation remain unknown, the formation of a PE layer on the exterior of EBs appears to be dependent on fibroblast growth factor (FGF) signaling mediated by the PI 3-kinase pathway [29, 30]. The PE cells exhibit an epithelial morphology on the EB surface, further differentiate into visceral and parietal endoderm, and deposit a basement membrane rich in laminin and collagen IV[18]. The basement membrane which separates the PE cell layer from the remaining mass of undifferentiated cells within the EB is generally thought to promote the survival of adjacent cells, whereas cells not in direct contact with the basement membrane undergo apoptosis, contributing to the formation of cystic cavities in most EBs[31-33].

As EB development progresses, differentiated cell phenotypes of all three germ lineages begin to arise[34]. For example, evidence of hematopoietic differentiation of EBs is supported by the appearance of yolk sac-like blood islands and spontaneously contractile foci of cells within EBs, indicative of cardiomyogenic differentiation, are readily apparent under low magnification[3, 35]. Upon plating onto an adherent substrate, elongated cell projections resembling neurite extensions emanate out from EBs

7

and morphological evidence of endothelial cells, fibroblasts and other cell types can be readily observed. Global DNA microarray analysis indicates that EBs temporally express genes in a manner that recapitulates the sequence of normal development from primitive ectoderm formation, to gastrulation, and eventual early cell specification prior to organogenesis[36]. Expression of phenotypic markers of endoderm (such as Foxa2, Sox17, GATA 4/6, α-fetoprotein, and albumin), mesoderm (such as Brachyury-T, Msp1/2, Isl-1, α-actin, ζ-globin, and Runx2), and ectoderm (such as Sox1, Nestin, Pax6, GFAP, Olig2, neurofilament, and βIII tubulin) definitively demonstrate the ability of EBs to generate cells from all three germ layers[37]. However, the typical heterogeneous differentiation of EBs is a significant challenge for the efficient production of defined cell types and can be influenced by EB formation and culture methods.

Embryoid body culture methods

The term 'embryoid body' has been broadly applied to describe pluripotent cell aggregates induced to differentiate using a variety of different formation and culture methods. Generally speaking, an aggregate of pluripotent stem cells, cultured in suspension, and capable of forming derivatives of all three germ lineages is regarded as an EB. Although no universally accepted benchmarks currently exist for EB formation, characteristics such as EB size, shape and homogeneity are typically used as points of reference for comparison. Common EB culture practices, such as hanging drop and static suspension culture were adopted from *in vitro* differentiation methods originally used for embryonic carcinoma (EC) cells, pluripotent precursors to the ESCs themselves[38]. A

8

comprehensive review describing several of the most common EB culture methods has recently been published[39].

The hanging drop method of EB formation produces homogeneous cell aggregates by dispensing a defined number of ESCs in physically separated droplets of media suspended from the lid of a Petri dish[40, 41]. Individual EBs form within each drop via gravity-induced aggregation of the cells and although EBs created by the hanging drop method can be subsequently introduced to suspension batch culture, the technique is not easily amenable to scale up for production of large numbers of EBs. An additional limitation of hanging drop culture is the difficulty in exchanging or manipulating the small volume of medium (typically 10-20 µl) without disturbing the EBs, thus the composition of the media cannot be easily controlled or assayed during the period of hanging drop suspension.

In contrast to hanging drop methods, static suspension culture is performed by simply adding a suspension of ESCs to a bacteriological grade Petri dish or similar vessel that inhibits cell adhesion (i.e. agar- or other hydrophilic polymer-coated substrate), thereby allowing the cells to spontaneously aggregate via cell-cell adhesions[3, 42, 43]. Static suspension cultures produce a large number of EBs rather simply, but the size and shape of the resulting EBs are highly variable due to the tendency of EBs in static suspension to agglomerate after initial formation, often producing large, irregularly shaped masses of cells. Often times, depending on the surface chemistry of the culture vessel, EBs may prematurely attach to the substrate, leading to greater heterogeneity and loss of EBs from suspension culture.

9

Entrapment of a single cell suspension or small clusters of ESCs in hydrogels, such as methylcellulose[35, 44, 45], fibrin[46] or hyaluronic acid[47], represents a compromise between hanging drop and static suspension approaches to attain physically separated EBs in a bulk semi-solid suspension media. Entrapment in methylcellulose, a temperature sensitive hydrogel, yields EBs of clonal origin, thereby improving the overall synchrony and reproducibility of EB differentiation; however, the efficiency of EB formation from individual ESCs can be rather low and soluble factor treatments and retrieval of differentiated cells may be complicated by the presence of the hydrogel material[44].

Alternative techniques for EB formation and culture have also been recently developed using multi-well and microfabrication technologies, as well as stirred and mixed suspension culture systems. Centrifugation of ESCs within round-bottomed 96-well plates induces aggregation more rapidly than hanging drops, but still requires individual processing and manipulation of the resulting EBs[48]. Microwells fabricated by lithographic techniques yield EBs in parallel at a much higher density than other physical separation methods and the ability to form EBs within microwells in a continuous volume of medium permits batch processing, therefore significantly improving the throughput of EB formation[49-51]. Likewise, batches of EBs can be formed in microfluidic chambers, separated from the flowing culture medium by a semi-permeable membrane, which allows for temporal control of the molecular makeup of the medium[52].

Formation of EBs in hydrodynamic conditions created by rotary orbital culture, stirred/ rotating culture vessels, or spinner flasks generally enhances ESC aggregation,

10

forming EBs faster and more uniformly than static bulk cultures[26, 53-58]. Hence, hydrodynamic conditions can generate large populations of EBs at a relatively high density, while at the same time, controlling the extent of EB agglomeration and subsequent differentiation of the cells[54, 56, 58, 59]. The mixing environment also distributes media components more homogenously throughout the culture volume so that the population of EBs is continuously exposed to a more uniform concentration of soluble factors and environmental conditions (i.e. pH, oxygen, etc.).

An inherent trade-off in most of the current systems available for EB formation is that batch-based suspension methods produce large numbers of EBs rather simply, but generally lack the fidelity of physical separation methods (hanging drop, microwell), thus yielding more heterogeneous populations of EBs. On the other hand, physical separation methods capable of generating homogeneous EB populations are often not capable of being directly scaled up to produce the yields of ESC derivatives thought to be necessary for therapeutic or diagnostic applications.

Engineering embryoid body cues

Differentiation of cells within EBs is directed by morphogenic cues comprising the intercellular and surrounding extracellular microenvironment, including exogenously administered molecules and endogenous factors produced by the ESCs. Individual aspects of the microenvironment can be studied rather simply in planar culture formats, but similar to a developing embryo, the 3D organization of an EB is inherently comprised of a complex milieu of integrated signals that synergistically affect cell differentiation. Although the 3D assembly of cells to form EBs presents unique challenges for regulating

11

the homogeneity of stem cell differentiation, attempts to control EB size, soluble factor delivery, extracellular matrix (ECM) interactions and cell-cell adhesions within EBs may influence differentiated cell phenotypes (Figure 2.1).
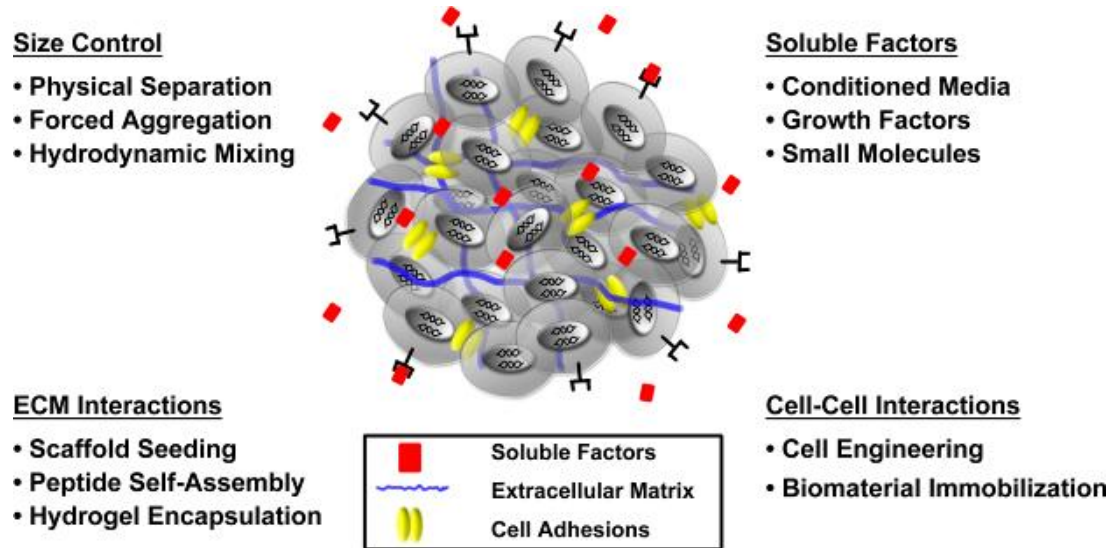
Figure 2.1. Environmental factors influencing EB differentiation. Embryoid body differentiation is influenced by a variety of factors comprising the intercellular microenvironment. The size of the EB, soluble factor signaling, ECM interactions and cell-cell interactions can all influence ESC commitment. General strategies to control the different elements of the EB microenvironment are listed for each.

Size control

The size of EBs, typically in the range of 100-400 μm, is thought to be a simple, yet important physical parameter capable of influencing the proportion of cells differentiating toward different lineages. EB size, which is primarily a function of the number of ESCs constituting each cell aggregate, impacts other environmental parameters affecting differentiation, such as the diffusion of soluble molecules and the extent of ECM-cell and cell-cell adhesive interactions. Recent developments in EB

12

formation techniques have enabled more controlled systems capable of modulating EB size in order to begin to determine the effects on subsequent differentiation of the cells.

As described above, forced aggregation of ESCs using multi-well round-bottomed plates or microtechnologies provides a very direct manner to precisely control the number of cells in individual cell aggregates. For example, the number of cells used to form hanging drops can influence the chondrogenic differentiation potential of EBs[60]. Likewise, forced centrifugation studies examining hematopoietic differentiation of human ESCs of varying sizes indicated that a minimum EB starting size (500 cells/EB) was required for myeloid differentiation to occur in over 90% of EBs and that an intermediate size range (1000 cells/EB) promoted erythroid cell differentiation[48]. The initial size of EBs can also be controlled through the geometric size of microwell or micropattern features in order to spatially define the number of ESCs within individual aggregates[50, 51, 61]. Micropatterned control of ESC colonies can dictate both the size of EBs and the phenotype(s) of the starting cell population used to form EBs, which can affect the differentiation of the cells to particular germ lineages[61]. Recently, microfabricated cell culture inserts compatible with standard multi-well culture plates were reported which significantly enhance the yield of EBs formed using forced aggregation[49]. The size of the resulting EBs can be controlled by the concentration of the cells inoculated into the well and after 24 hours, EBs can be extracted from the microwells with gentle pipetting and transferred to suspension culture. Depending on the dimensions of the microwells, the poly(dimethylsiloxane) inserts contain between 10^4 to 10^6 microwells per 100 cm^2 of surface area - a dramatic increase over the capabilities of round-bottomed 96-well plates[49].

13

In addition to forced aggregation methods, hydrodynamic culture conditions can be used not only to prevent EB agglomeration, but also regulate the size of EBs formed from single cell suspensions[53-55]. For EBs in horizontal rotary culture and stirred bioreactor culture, an inverse relationship exists between mixing speed and EB size, with decreasing EB size achieved by faster mixing conditions; thus EB size in bulk suspension can be modulated by hydrodynamic mixing conditions [54, 58]. EB size can also be controlled by encapsulating suspensions of individual ESCs or primitive EBs into hydrogel microbeads of controlled volumes. For example, agarose[26], alginate[62-64], and dextran[65] have all been used successfully to encapsulate ESCs, either as single cells or small clumps of cells, to form EBs within microgels. The diameter of the microgels laden with ESCs can vary greatly from 100 μm agarose beads[26] to 2.3 mm diameter alginate beads[64]. One problem with increasing microgel size, however, is that encapsulated ESCs may have a tendency to form multiple EBs within individual beads, limiting the ability to accurately control EB size.

Depending on the different culture methods used, the kinetics of EB formation vary dramatically from minutes (forced aggregation) to hours (hydrodynamic mixing) to days (cell encapsulation),. Despite such differences, the consequences of the time scale for EB formation on cell fate and lineage determination has not been directly examined independently of EB size. In addition, although different methods to control initial EB size have been developed, the mechanisms regulating the causal relationship between the size of individual EBs and their propensity to differentiate into different cell phenotypes has yet to be fully elucidated.

<u>Soluble factors</u>

Controlling the molecular composition of culture media to direct ESC differentiation has been studied extensively in a variety of systems and the effects of specific soluble factors and signaling pathways on ESC differentiation have been thoroughly discussed previously[66-68]. Small molecules such as ascorbic acid[69], retinoic acid[70] and dexamethasone[71], as well as larger growth factors such as fibroblast growth factors, bone morphogenic proteins and transforming growth factors[67, 72], are examples of soluble factors which have been shown to affect ESC differentiation. Presentation of soluble signaling molecules to ESCs in monolayer culture has been the primary method to screen the ability of libraries of chemical compounds and biomolecules to induce ESC differentiation into specific cell types[15, 69, 73]. In lieu of direct co-culture, complex, yet poorly defined media conditioned by secondary cell types has been applied to stem cells in order to direct differentiation[74, 75]. On the other hand, defined soluble media comprised of known amounts of different factors has also been used successfully to generate relatively homogeneous populations of cells, particularly for neural progenitors or neurogenic cell fates[15, 76, 77].

In stark contrast to 2D planar culture formats, only the cells on the exterior of 3D EBs are in direct contact with soluble factors present in the culture medium. Soluble factors must diffuse through this multi-layered cell environment and barriers to transport, which likely vary as a function of stages of EB differentiation, contribute to the formation of concentration gradients which comprise the cell microenvironment. Even the diffusion of small molecules (<1000 Da), may have a limited ability to pass through the peripheral cells of EBs[78]. High-powered SEM microscopy analysis of EBs indicates that the

15

surface layer of epithelial-like cells (Figure 2.2A) exhibit tight cell-cell junctions (Figure 2.2B) and cross-sectional analysis of EBs (Figure 2.2C) indicates that EBs tend to form a relatively dense layer of ECM and cells at the periphery of EBs (Fig. 2.2D), compared to the rest of the interior cellular morphology. Therefore, steric barriers to diffusion posed by EB structure make it unlikely that homogenous concentrations of molecules can be attained uniformly throughout the interior of EBs and limit the efficacy of differentiation strategies relying solely on the addition of soluble factors to the culture medium.

16
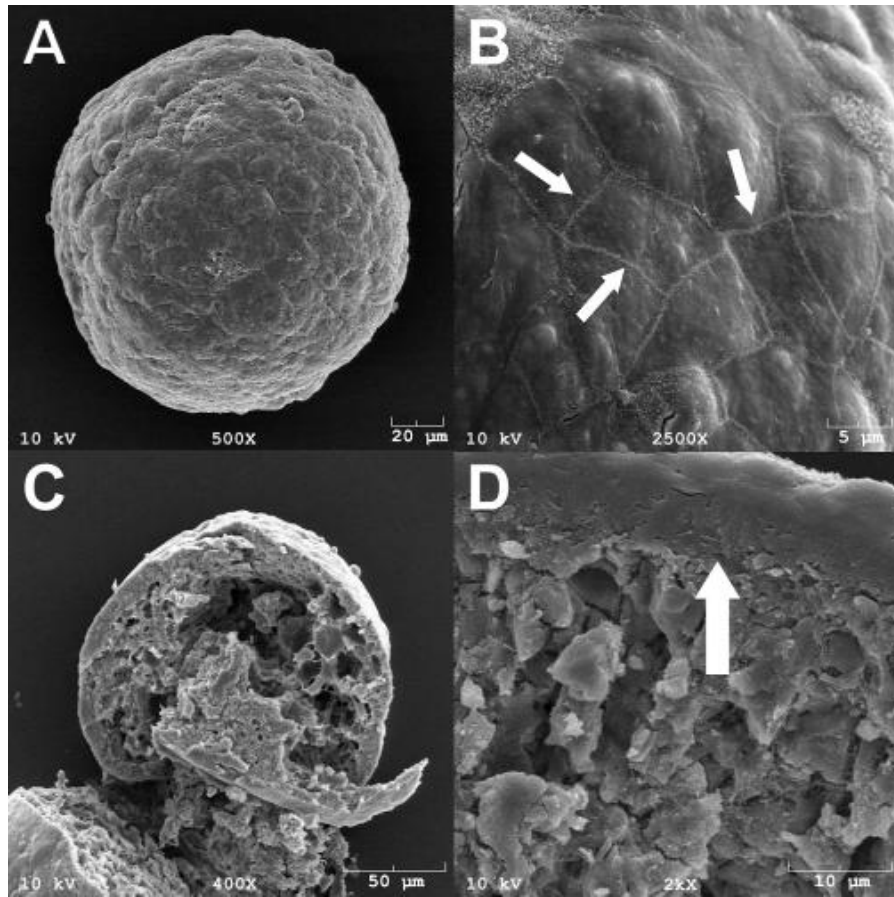
Figure 2.2. Embryoid body ultrastructure. Scanning electron microscopy analysis of EBs differentiated for 10 days in suspension culture. A) Endoderm layer on the EB exterior and B) tight junctions between cells on the surface (arrows), C) cross-sectional view of an EB showing the differences between the outer layer and the porous interior, D) the thick outer layer of cells and ECM that is formed on the exterior (arrows). Cell junctions and deposited ECM may limit homogeneous presentation of factors on the EB interior.

17

Members of the TGF-β superfamily have been shown to influence cell fate decisions during embryonic development, especially for cardiac and phenotypes. BMPs are large, dimeric secreted proteins shown to play important roles in embryonic development as well as adult physiology. BMPs interact with type I and type II serine/threonine protein kinase receptor subunits. The type II subunit contains a constitutively active kinase which phosphorylates the type I subunit upon ligand binding. Activated type I receptors then phosphorylate SMAD 1, 5, or 8, which heterodimerize with SMAD4, translocate to the nucleus and regulate gene expression. BMP-4 is expressed in the extraembryonic ectoderm in the post-implantation mouse embryo, and plays a role in regulating primitive streak formation[79]. BMP-4 is expressed in the visceral endoderm starting at E6.0, and appears to function in production of extraembryonic mesoderm as well as primordial germ cells. Mice deficient in BMP-4 exhibited defects in cardiac development, suggesting that BMP-4 secreted by the extraembryonic mesoderm plays a role in cardiogenesis[80]. Additionally, BMP-4 has been implicated in various roles of cardiac development and patterning[81-83]. *In vitro* and *in vivo* studies using embryonic stem cells (both mouse and human) have demonstrated that BMP-4 plays an inductive role in mesoderm formation, and specifically, cardiomyogenesis[84-87]. However, the role of BMPs in differentiation is context dependant, as BMP-4/4 has been implicated in maintaining the pluripotency of epiblast cells, and inhibition of BMP signaling results in neural induction [88]. Similarly, in mouse ESCs, BMP signaling has commonly been reported as an inhibitor of neural differentiation[89-92].

Extracellular matrix interactions

The ECM can be a potent mitigator of cell fate decisions by providing a complex assembly of morphogenic cues to stem cells. The ECM is a structural framework of secreted macromolecules consisting primarily of glycosaminoglycans and fibrous proteins which provide mechanical support, adhesive interactions and sequestration of growth factors. Native ECM components direct cell differentiation through integrin-mediated signaling events with adhesive proteins, as well as proteolytic release of affinity-bound growth factors during matrix remodeling[68, 93]. Integrin ligation and growth factor binding to receptors initiate intracellular signaling cascades that ultimately culminate in gene expression changes that modulate cell phenotype[94].

The effects of ECM molecules on EB differentiation have largely been examined by seeding ESCs or pre-formed EBs directly within natural ECM hydrogel materials[46, 47, 72, 95]. EBs differentiated in collagen scaffolds consisting of variable amounts of fibronectin and laminin demonstrated that varying the composition of the ECM could differentially direct EB differentiation. EBs in collagen scaffolds with high laminin content adopted a cardiomyocyte phenotype more frequently, whereas EBs were directed towards more epithelial and vascular cell fates in hydrogels with high fibronectin content, and EB cavitation and differentiation appeared to be inhibited in hydrogels with increasing collagen content[95]. ECM signaling peptides can also be incorporated into non-bioactive hydrogels used to encapsulate EBs, such as RGD modified dextran[65], to examine the effects of ECM on ESC differentiation. In addition to changes in the specific biochemical constituents of the ECM, differences in the elasticity of the ECM may also provide mechanotransductive cues capable of affecting stem cell differentiation[96].

19

Encapsulation of EBs within ECM matrices limits the interactions between ESCs and the ECM to the exterior surface of the ESC aggregates. Therefore, in an attempt to directly manipulate the composition of the ECM within the EB microenvironment, individual matrix molecules like collagen and laminin have been added solubly to suspensions of ESCs during EB formation[18, 97, 98]. Similarly, the addition of soluble complex, tissue-derived matrices, such as Matrigel or Cartigel, to EB culture media has been used to promote the formation of glandular and tubular-like structures or cartilage development, respectively[97]. Although soluble addition of ECM molecules to ESC suspensions may favor incorporation within EBs, soluble ECM molecules alone do not necessarily assemble to form a functional matrix. Self-assembling peptide-based matrices, on the other hand, can rapidly form within developing cell aggregates to form a hydrogel network of nanofibers presenting different signaling epitopes[99, 100]. Utilizing this strategy, neural progenitor cells encapsulated as neurospheres in a self-assembling IKVAV (laminin epitope) amphiphile solution differentiated rapidly into neurons, while astrocyte differentiation was attenuated[100]. Interestingly, the density of the peptide epitope within the cell microenvironment, a material characteristic which can be controlled by matrix formulation conditions, could modulate the differentiation of the cells. Applying a similar principle to EBs, self-assembling matrices could provide a novel route to control the composition and spatial distribution of extracellular signaling motifs present within aggregates of ESCs undergoing differentiation.

20

<u>Cell-Cell interactions</u>

EBs are initially formed via cell-cell adhesive interactions, but intercellular adhesions can also serve an important role in cell signaling throughout EB differentiation. Cell-cell interactions are mediated primarily by cadherins, a family of Ca^{2+} dependent transmembrane adhesion receptors that play important roles in cell differentiation during embryogenesis[101]. Homophilic cadherin receptor binding triggers intracellular signaling pathways mediated by cytoplasmic catenin proteins, such as β-catenin, which is linked to the Wnt pathway, a potent regulator of cell morphogenesis and differentiation[101]. Undifferentiated ESCs express epithelial-cadherin (E-cadherin), which is the primary molecular mediator of EB formation, but sustained E-cadherin expression can also be responsible for the agglomeration of EBs at later stages of differentiation[26]. Inhibition of E-cadherin mediated adhesion, either by the use of E-cadherin binding antibodies or E-cadherin null ESCs, prevents normal EB formation and subsequent differentiation[26, 27, 55]. Differential cadherin expression, associated with different cell phenotypes, is temporally regulated during the course of EB differentiation and can directly influence cell fate specification. For example, ESCs constitutively expressing E-cadherin are prone to more epithelial differentiation, while ESCs constitutively expressing N-cadherin differentiate more readily into cartilage and neuroepithelium[28]. Although it has not been systematically investigated, the use of cadherin signaling to control EB differentiation either through integration of a genetically modified cell line over-expressing a particular cadherin or through the presentation of cadherins on biomaterial surfaces integrated within EBs to mimic cell-cell interactions is a promising area for control of EB differentiation.

21

Strategies to control other types of cell-cell interactions, including transmembrane receptors and ligands not anchored to the cytoskeleton, have also been explored in stem cells. For example, the Notch pathway is involved in a variety of cell fate decision processes through development and adult tissue morphogenesis[102, 103]. ESCs can express multiple Notch receptors and Notch signaling has been implicated both in stem cell self-renewal and differentiation towards different phenotypes, such as neuronal cells[104-106]. In general, Notch signaling requires immobilized ligand presentation from a surface or cell membrane in order to achieve optimal bioactivity[107]. Jagged-1, a Notch ligand, immobilized to polystyrene or polyHEMA surfaces promoted early and late stage differentiation of cultured epithelial stem cells[108]. Comparable methods of presenting Notch ligands to cells uniformly within EBs would require that engineered biomaterials be integrated directly within the interior of the ESC aggregate.

Strategies for biomaterial control of the 3D microenvironment

As introduced above, adhesive protein biomaterials (i.e. Matrigel and gelatin) have been used as culture substrates for stem cell maintenance culture in 2-D. Biomaterials can also be integrated within 3D stem cell environments in order to control the increased complexity of the microenvironment. Strategies to control stem cell behavior using biomaterials have largely aimed to deconstruct elements of native biological complexity and integrate defined components into controlled systems to present molecular cues to stem cells.

Parameters such as hydrophobicity, porosity, degradation kinetics and surface coating can be engineered to create the desired material properties. The ability to

22

engineer biomaterial surface properties can be utilized to present insoluble factors to mimic cell-cell or extracellular matrix interactions. Stem cells and biomaterials can be combined as scaffolds in the classic tissue engineering paradigm, wherein a spongy or fibrous scaffold provides mechanical support for attachment and migration guidance initially and then degrades as the cells produce their own natural scaffolding. In addition to scaffolds, which have been used extensively with other cell types, single cell suspensions or EBs are often completely encapsulated in either a natural ECM matrix or in a polymer designed to provide differentiation cues. Encapsulation typically occurs in the form of small spherical beads (hundreds of microns in diameter) grown in suspension culture whereas scaffolds are much larger and are grown in static or perfused cultures. Another approach is to integrate biomaterials within stem cell spheroids, either using microcarriers or microparticles, to control the microenvironment from the 'inside-out.' Strategies utilizing scaffolds, encapsulation and microcarrier/microparticles for control of the stem cell microenvironment are depicted in Figure 1 and are discussed in further detail below.

Scaffolds

The application of polymeric scaffolds to support somatic cells was one of the original tenets of tissue engineering strategies[109]. Polymer scaffolds were originally designed primarily as carriers for cell transplantation which provided temporary structural support until cells could adequately synthesize their own matrix to replace the biodegradable synthetic material. However, advancements in the field of biomaterials have led to the development of more sophisticated scaffolds in various forms (e.g.

23

porous, fibrous), capable of responding to environmental changes (e.g. temperature, pH, electrical stimulation, proteases) and directly incorporating biomolecular cues to mediate cell attachment, proliferation and differentiation. Recently, pluripotent and multipotent stem cells have been seeded onto polymer scaffolds as a means to examine self-renewal and differentiation properties in 3D.

Scaffolds have been studied in combination with mesenchymal stem cells (MSCs) for a wide variety of applications including bone and cartilage regeneration. The ability of MSCs, derived from bone marrow or other tissues (e.g. adipose tissue), to differentiate into a variety of cell types, including osteo-, chondro-, and adipogenic lineages, has made MSCs the most common cell source for musculoskeletal tissue engineering strategies. A variety of synthetic and natural polymers have been utilized for both osteogenesis and chondrogenesis of MSCs, including nanofibrous electrospun poly(caprolactone) (PCL)[110-112], PLGA[113-117], and silk[118-121]. The ability of multiple scaffold types with a wide range of chemical and physical properties to support MSC proliferation and differentiation makes this a promising and active area of stem cell research.

Pluripotent stem cells can likewise be cultured on or within scaffolds, and much of the knowledge gained from previous studies with MSCs can be applied to ESC culture. As discussed above, culture of undifferentiated ESCs is typically performed in monolayer, with cells grown on either an inactivated MEF feeder layer or Matrigel. However, the use of synthetic scaffolds for self-renewal culture may circumvent the issues of xenogenic contact and scale-up feasibility associated with MEF and Matrigel substrates. The culture of hESCs on an artificial matrix composed of semi-interpenetrating polymer networks (sIPN) supported short-term maintenance of

24

pluripotency[122]. The sIPN hydrogels were functionalized with the arginine-glycine-aspartic acid (RGD) peptide sequence, and RGD concentration, as well as the mechanical properties of the hydrogel, were varied independently to identify conditions which promoted self-renewal of hESCs. Artificial extracellular matrices for stem cell renewal can be used as a xeno-free alternative to defined media.

Additionally, ESCs have been cultured on nanofibrillar polyamide matrices known as Ultra-Web under self-renewal conditions[123]. ESCs grown on Ultra-Web displayed higher alkaline phosphatase activity, indicative of pluripotency, as well as enhanced proliferation, relative to gelatin-coated glass coverslips. Activation of Rac, a small GTPase, was also enhanced in cells cultured on Ultra-Web, as was activation of the PI3K pathway and Nanog expression. These data indicate that the 3D architecture on which cells are cultured may play an important role in cell fate determination and must be taken into account in future design of cell culture systems for ESC self-renewal.

Synthetic scaffolds have also been applied to differentiation approaches for ESCs. Porous scaffolds composed of PLGA/PLLA have been investigated as substrates for hESC adhesion and differentiation, with the intent of forming complex tissue architectures to be used in transplantation therapies[124]. The combination of seeding human ESCs on porous scaffolds and media supplementation with growth factors was found to induce differentiation into various cell types that expressed markers of neural, chondrogenic and hepatic lineages. Cells remained viable on the scaffolds following implantation in severely immune compromised mice, and continued differentiation and reorganization was observed. Studies focusing specifically on neural differentiation of hESCs seeded onto PLGA scaffolds were performed, with the effect of various media

25

supplements reported[125]. The addition of nerve growth factor and neurotrophin 3 to the scaffold cultures enhanced differentiation to nestin and βIII tubulin positive cells, indicative of neural progenitors and neurons, respectively. However, formation of functional, higher-ordered tissues will likely require greater sophistication in scaffold architecture and differentiation-cue presentation to ESCs.

Scaffolds composed of biomimetic and natural polymers have been used in scaffold fabrication in order to present instructive microenvironments to pluripotent cells. ESCs cultured on the biomimetic material Cytomatrix formed 3D structures similar to EBs, but displayed enhanced ECM production as well as increased efficiency in differentiation to hematopoetic precursor cells[126]. Genes associated with ECM production as well as proliferation and differentiation were found to be enhanced relative to traditional EBs[127]. Incorporation of ESCs into porous alginate scaffolds resulted in efficient, homogeneous EB formation, with EBs spatially restricted within the pores. Agglomeration of EBs appeared to be inhibited, resulting in efficient cell proliferation and differentiation[56].

Fibrin scaffolds have also been investigated for use in directed ESC differentiation to neural cell types[128]. Cells from both dissociated and intact EBs were seeded within fibrin scaffolds, and conditions including cell density and fibrinogen and thrombin concentration were optimized for cell proliferation and differentiation. After 14 days, successful differentiation of ESCs into neurons and astrocytes was observed. In an independent study, cells were seeded onto fibrin scaffolds as well as PEGylated fibrin scaffolds, and proliferation and differentiation were assessed relative to traditional EBs as well as EBs grown in semi-solid methylcellulose[46]. Proliferation in both types of fibrin

scaffolds was enhanced relative to EBs and methylcellulose EBs. Culture in non-PEGylated fibrin resulted in differentiation similar to that observed in traditional EBs, with down-regulation of OCT4 and expression of VE-Cadherin, while ESCs growth in PEGylated fibrin were more similar to methylcellulose controls.

Semi-interpenetrating polymer networks composed of the natural polymers collagen, fibronectin and laminin were examined as scaffolds for ESC differentiation[95]. Differentiation was found to be a function of both network composition and concentration, as high collagen concentration inhibited EB cavitation, fibronectin appeared to enhance endothelial differentiation, and laminin enhanced cardiomyogenesis. Use of the self-assembling nanofibrillar peptide scaffold PuraMatrix was investigated for osteogenic differentiation of ESCs[99]. EB-derived cells were seeded onto PuraMatrix scaffolds after 8 days of differentiation, and cells plated onto tissue culture polystyrene served as a 2-D control. Both PuraMatrix and 2-D substrates supported osteogenic differentiation, although maintenance of OCT4 positive cells was more prevalent in 3D. Scaffolds can be used to control physiochemical elements of the microenvironment, however, their use for large scale production of homogeneous cells may be limited due to diffusional limitations of nutrients in large constructs lacking vasculature.

Encapsulation

Encapsulation of stem cells into hydrogels represents a scalable way to present factors locally to cells. Unlike scaffolds, large numbers of capsules can be cultured in suspension culture. Encapsulation of stem cells can affect diffusion, control aggregate size and prevent agglomeration as well as provide an instructive environment depending

27

on the properties of the material chosen for encapsulation. From a bioprocessing perspective, encapsulation provides a method to grow anchorage dependent cells in suspension thereby increasing the surface area to volume ratio and scale up potential. MSCs are difficult to maintain as aggregates in suspension[129] and for this reason they are often studied using encapsulation. In addition to bioprocessing advantages, the creation of an artificial matrix aids in study of cellular response to specific elements of native ECM. Elements such as material stiffness or peptide density can be varied independent of other factors.

Single cell suspensions or cell spheroids can be encapsulated several ways depending on the material properties. Thermosetting hydrogels such as agarose can be used to encapsulate cells by emulsifying a mixture of agarose, cells and oil. Agarose capsules containing EBs are formed in the oil phase after emulsification and can be gelled by lowering the temperature below the gelation point of agarose[26]. Materials such as alginate are useful for encapsulation because gelation occurs in the presence of Ca^{2+} ions and does not require oil phase emulsion or temperature change that can lower cell viability. Precisely sized droplets of alginate and cells can be created and gelled in $CaCl_2$ baths and cells can be retrieved at later time points after transfer to a medium without Ca^{2+}[62, 130-132]. Artificial polymers such as poly(NiPAAm-co-AAC)[133], poly(ethylene glycol) (PEG)[134], and PEG derivatives such as PEG diacrylate[135, 136] and oligo(poly(ethylene glycol)) fumerate[137] have been utilized as well.

Encapsulation also provides a method to investigate interactions between cells and specific signaling sequences in an artificial ECM environment in which the ligand density can be precisely controlled. For example, alginate can be modified to present

28

small peptide sequences such as arginine-glycine-aspartic acid (RGD) [132], found on ECM proteins such as fibronectin, fibrin and vitronectin. Increasing RGD density in alginate gels resulted in dose dependent decrease in encapsulated MSC response to TGF-B1 and dexamethasone, components of chondrogenic media. It was hypothesized that integrin mediated signaling may be responsible for inhibition of chondrogenesis in the cells and control of integrin signaling may be a useful target for directed differentiation strategies. Mimicking ECM interactions using small peptide sequences can aid in understanding the mechanisms by which ECM components contribute to the cellular microenvironment.

In regards to ESCs, encapsulation originated as a method to control the homogeneity of differentiation culture. ESCs express high levels of E-cadherin, a homotypic cell-cell adhesion molecule, which has been shown to be primarily responsible for EB formation in suspension culture[26, 55]. High levels of E-cadherin also can lead to agglomeration which is particularly problematic in static cultures. Agglomeration leads to heterogeneity in EB culture and is contributes to the heterogeneity of the resultant differentiated cell population. In addition, the size of the initial ESC aggregate has been implicated in the trajectory of subsequent differentiation, and therefore precise size control of EB formation is considered advantageous[48, 60, 61]. In addition, EBs formed using other methods can be later be encapsulated with one EB/capsule to prevent agglomeration and to shield EBs from shear forces experienced in a stirred bioreactor. ESCs can be encapsulated as a single-cell suspension and depending on the material used and the size of the capsule formed, the result can be single EBs or small individual clumps of cells.

ESCs can be encapsulated in natural polymers such as hyaluronic acid[47] or alginate[138] to maintain a pluripotent state useful for production of large amounts of cells. Cells can then either be retrieved from the gels or switched to differentiation conditions for further culture. Retrieval from hyaluronic acid encapsulation requires that the capsules be incubated in hyaluronidase, while alginate capsules can be depolymerized through the removal of divalent cations. Encapsulation can be further used to promote differentiation into hepatocytes[62], chondrocytes[139], cardiomyocytes[140], and definitive endoderm[141]. In some cases, encapsulation is used as a method to support differentiation of ESCs, however, directed differentiation techniques, such as the addition of soluble factors, can also be combined with encapsulation to promote specific directed differentiation.

Material design can be based on knowledge of biological processes which occur naturally to direct stem cell behavior, such as the presentation the RGD peptide to promote adhesion, however, another strategy is to screen biomaterials with different surface chemistries to discover new non-physiological interactions which can be useful in directing cell differentiation. Using this strategy, the gene expression of stem cells on different surfaces can be analyzed on an array set-up with high-throughput analysis and materials that promote the desired differentiation can be further analyzed in 3D culture. PEG hydrogels functionalized with small side functional groups of varying charge and hydrophilicity illicit different gene expression profiles of encapsulated hMSCs[142].

Microcarriers

Encapsulation of ESCs and other stem cell types is a method to introduce biomaterial control of differentiation cues; however, this method is an "outside-in"

30

strategy. Biomaterial interaction with the microenvironment is directly imparted on cells of the surface of encapsulated aggregates whereas interior cells are not directly affected. Alternative strategies have similarly focused on incorporating biomaterials with cells cultured in suspension; however, they rely either on culture of cells on microcarriers or the incorporation of microparticles within stem cell aggregates.

Microcarriers are spherical beads, normally 150-500 microns in diameter, and can be made of a variety of materials such as polystyrene, dextran and glass. Cells can be grown on the surface of microcarriers to increase the available growing surface area per unit volume and have been used to scale up culture of anchorage dependent cells. Microcarriers have been reported to support maintenance culture of human ESCs[143-145], mouse ESCs[55, 146, 147] and MSCs[148, 149] and importantly, population doubling times remain comparable to 2D culture standards. Dextran beads coated in collagen are most often used for ESC attachment. These cells can then be differentiated while adhered to the bead or they can be separated from the beads for use in other differentiation protocols. The choice of coating is important to the cell yield and in the case of polystyrene beads cells can adhere without a coating through electrostatic interactions. Cell collection from uncoated polystyrene is difficult and results in decreased cell viability, whereas with gelatin coated dextran, trypsin can digest the collagen layer and cells can be recovered with high yield. Matrigel has also been successfully used as a dextran bead coating as it is known that Matrigel will support undifferentiated growth of ESCs[143, 145].

In contrast to scaffold-based approaches, the material properties of microcarriers have not been extensively studied in regards to directed differentiation or

31

microenvironmental control. Microcarrier materials are evaluated on their ability to expand large amounts of undifferentiated cells. This is in part due to the fact that microcarrier culture is analogous to 2D culture where media manipulation using growth factors or small molecules is a potent regulator of cell behavior. Limitations remain with microcarrier culture including agglomeration and low cell viability after collection procedures. Stirred suspension bioreactors are commonly utilized to agitate the culture and prevent agglomeration and a balance must be reached between shear forces experienced by cells and agglomeration at lower agitation rates.
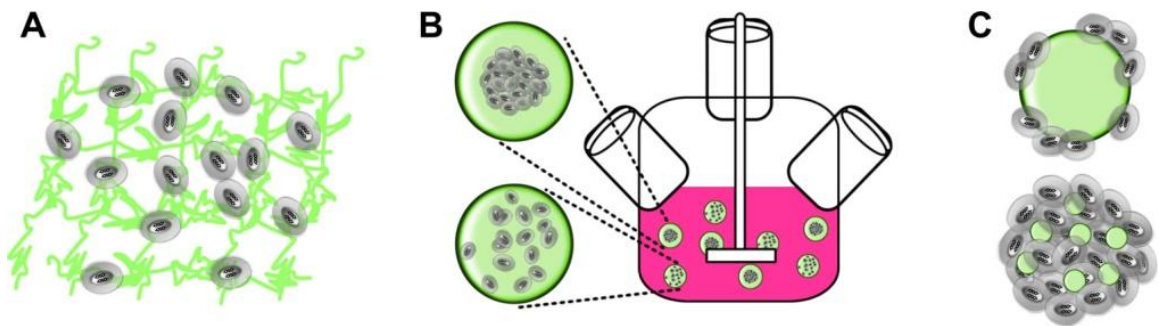
Figure 2.3. Biomaterials can be incorporated within 3D stem cell microenvironments to direct cell behavior. Cells can be cultured on or within polymeric scaffolds (A) which provide physiochemical cues. Encapsulation of cell aggregates or single cells (B) can be used to increase the surface area to volume ratio for scalable culture and to provide an artificial matrix. "Inside-out" approaches to direct the microenvironment include culture of cells on microcarriers (C, Top) and the incorporation of microparticles within stem cell aggregates (C, Bottom).

While microcarriers are used to scale up the culture monolayers of cells, smaller-sized particles, ranging from 250 nm to 10 um in diameter, can be incorporated within larger cell spheroids to take advantage of increased cell-cell contacts and 3D ECM contact. The incorporation of materials within stem cell aggregates is a relatively new approach of "inside-out" engineering that can be used to place cells on the interior of the

32

aggregate in direct contact with the biomaterials. Biomaterial microparticles have been widely used in the field of drug delivery as vehicles for controlled release of encapsulated molecules, and their surface can be functionalized with cell specific adhesion ligands for cell-targeted delivery, especially useful in cancer therapies. In addition, microparticle surfaces can be modified to mimic cell-cell interactions, loaded with soluble morphogens for controlled release or can be used to introduce ECM proteins for control of matrix properties[150]. The surfaces of materials such as polystyrene and poly(2-hydroxyethel methacrylate) have previously been modified in 2D cultures to present LIF to prevent differentiation or Jagged-1 to mimic cell-cell signaling[108, 151]. Microparticles can be combined with other techniques discussed previously to add further control of soluble factor release. Microparticles incorporated in scaffolds[152, 153] can continually release encapsulated factors throughout the construct and this could similarly be used in capsules of encapsulated cells.

Microparticles incorporated within progenitor cell spheroids was first used to improve post-transplantation cell viability of neural cells[154]. Fetal rat brain cells were mixed with poly(lactic-co-glycolic acid) (PLGA) microparticles which released nerve growth factor (NGF) to increase cell viability after transplantation. This concept has also been applied to synthetic microenvironments for ESCs for the purpose of directed differentiation[155, 156]. As introduced in the beginning of the chapter, ESC spheroids present barriers to diffusion and therefore cells in the interior are not completely accessible to molecules in the media as is the case with 2D culture. Cell-cell contacts and deposited ECM can limit the diffusion of even small molecules and the formation of gradients is likely to contribute to the heterogeneous nature of EB differentiation.

33

Incorporation of biomaterials within EBs circumvents the diffusion barriers to cells on the EB periphery and microparticles can act as point sources continuously releasing morphogen within the EB (Figure 2.4). In this way, gradients of molecules can be minimized to create a more homogeneous environment for the cells within EBs. An example of microparticle-mediated control of the EB microenvironment is the incorporation of PLGA microparticles within mouse EBs[155]. The microparticles were loaded with retinoic acid (RA), a small, hydrophobic morphogen, and were designed to continually release RA throughout EB culture. The resulting EBs upregulated gene expression of genes characteristic of epiblast stage embryos and uniform cavitation was observed in large populations of EBs. This effect could not be matched through any soluble addition of RA to the EB medium, suggesting that the controlled release of the RA by the particles inside the EBs was needed to provide the appropriate microenvironment for epiblast-like EB formation. Evidence that this effect was widespread throughout the entire culture indicates that this strategy could be used to direct differentiation of ESCs in a scalable manner. Controlled release of morphogens is also desired to conserve growth factor for large scale experiments. Biomaterials can preserve the bioactivity of encapsulated growth factor by maintaining the molecule in a bound state and preventing degradation. Soluble addition of growth factors must be replenished as determined by the half-life of the molecule in order to maintain the desired concentration for cell signaling.
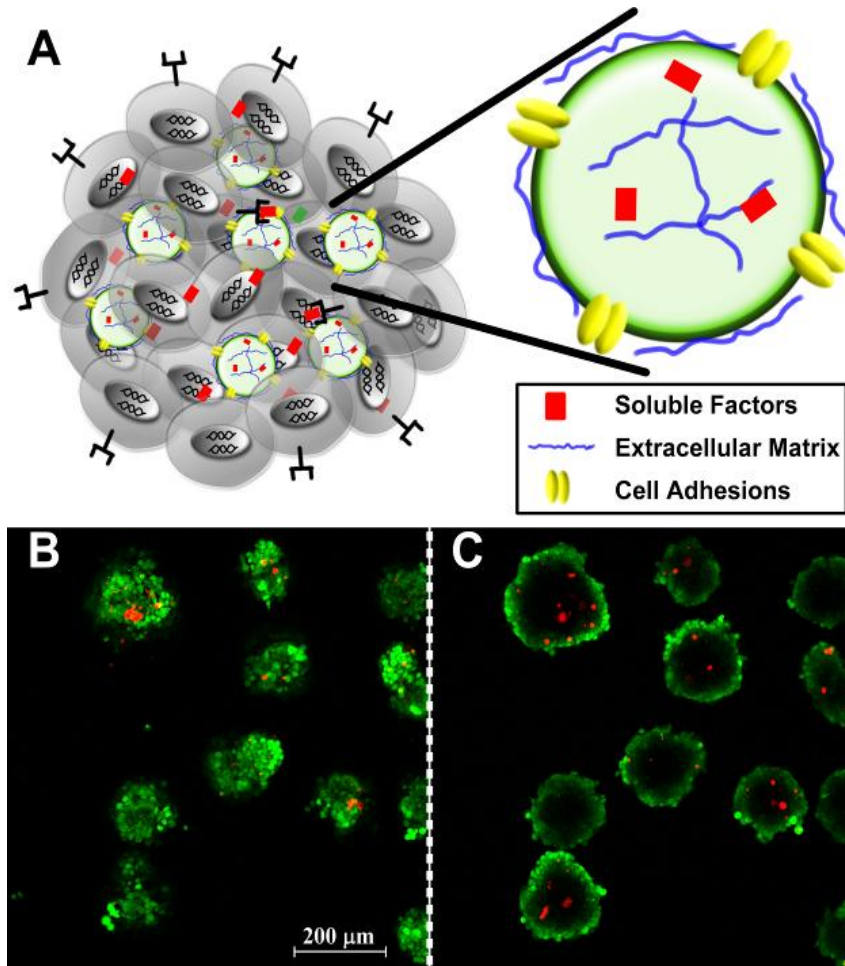
Figure 2.4. Biomaterial incorporation within EBs. Integrated biomaterials can be used to present ECM molecules, release soluble factors and mimic cell-cell interactions in a precisely controlled manner. A) Biomaterial microparticles integrated within the EB. Particles can be engineered with immobilized cell adhesion mediating receptors, ECM and incorporated soluble factor for delivery within the EB. B,C) Confocal microscopy demonstrates fluorescently-labeled microparticles (CellTracker™ Red) are distributed throughout the interior of the EBs. EBs were also counter-stained with CellTracker™ Green, which only labeled the cells on the exterior of the EBs, demonstrating the diffusive limitation of small molecules into 3D EBs. Separate optical sections (denoted by dashed white line) were imaged 45um apart.

35

CHAPTER 3

BIOMATERIAL EFFECTS ON PLURIPOTENT STEM CELL

AGGREGATE DIFFERENTIATION[†]

Introduction

Pluripotent stem cells (PSCs), including embryonic stem cells (ESCs) and induced pluripotent cells, provide a powerful model system for the study of morphogenic differentiation and represent a potent cell source for regenerative medicine therapies. Maintenance of pluripotency or differentiation of PSCs is dependent on extracellular cues such as autocrine and paracrine signaling, cell-cell and extracellular matrix interactions[157]. Appropriate culture conditions have been developed for the derivation and maintenance of pluripotent mouse[3] and human cells[7] and likewise, manipulation of the stem cell microenvironment can be used to promote lineage specific differentiation[150]. Although simple addition of soluble factors to cell culture medium is a commonly used method for directed differentiation protocols, it represents only a portion of the complex extracellular milieu which directs morphogenesis in the developing embryo.

In order to enhance the efficiency of many differentiation protocols, biomaterials are increasingly being used to engineer the biochemical and biophysical properties of the

---

36

stem cell microenvironment[158]. Relevant properties of biomaterials such as degradation kinetics, molecular compatibility, porosity, etc., can be engineered to enable spatial-temporal control of extracellular cues presented to stem cells, thereby allowing for the customization needed for the differentiation to a variety of cell types. Studies of biomaterial-stem cell interactions have demonstrated that materials may influence stem cell differentiation even in the absence of delivered biomolecules. Though the exact mechanisms remain the subject of ongoing studies, material properties such as surface chemistry[142, 159] and elasticity[96] have been reported to promote lineage specific differentiation of stem cells. For the most part, stem cell-biomaterial interactions have been examined by introducing stem cells into artificial environments, such as 2D cell culture on biomaterial surfaces[159, 160], encapsulation of cell suspensions within hydrogel materials[26, 142], or cell seeding on 3D polymeric scaffolds[124]. In contrast, incorporation of materials directly within 3D stem cell environments, such as cell spheroids, permits control over the amount and spatial presentation of materials enabling systematic examination of the effects of biomaterials on stem cell differentiation and morphogenesis.

Recent studies have demonstrated the efficacy of morphogen delivery within stem cell spheroids via incorporated biomaterials[155, 156, 161]. ESCs mixed with poly(lactic-co-glycolic) acid (PLGA) MPs loaded with retinoic acid (RA) resulted in the homogeneous and organized differentiation of ESC-derived spheroids, referred to as embryoid bodies (EBs)[155]. The observed biological response could not be duplicated by simple soluble application of RA suggesting the importance of spatial presentation of morphogens in the context of EB differentiation. PLGA MPs are well suited for the

37

encapsulation and release of small, hydrophobic molecules, such as RA; however, organic solvents used in fabrication of MPs can adversely affect the bioactivity and efficiency of encapsulation of larger biomolecules such as growth factors[162, 163]. As an alternative, growth factors can be loaded into hydrogel materials, such as agarose[164] or gelatin[165, 166], under aqueous conditions without substantially compromising subsequent bioactivity. Stem cell differentiation protocols utilize a wide variety of molecules delivered with distinct temporal profiles, accordingly, it is advantageous for biomaterials-based strategies to be compatible with a variety of materials so the appropriate molecular compatibility and release kinetics can be engineered for the desired application. As previous studies have been limited to PLGA, the aims of this study were first to develop a method for robust incorporation of various biomaterials within PSC aggregates, and second to characterize the effects of biomaterial incorporation on stem cell differentiation.

Here we examined the incorporation of equal-sized microparticles (MPs) fabricated from different materials (agarose, PLGA and gelatin) within aggregates of PSCs. A forced aggregation technique, previously developed for formation of populations of homogeneously sized EBs[49], was used to coalesce MPs and cells and compared to simple mixing during formation under dynamic culture. The quantities of MPs incorporated within cell aggregates were assessed as a function of the seed ratio of MPs to cells used to form the biomaterial/cell hybrid constructs. The morphology, gene and protein expression patterns of aggregates with different types of incorporated MPs were evaluated to determine the effects of the materials on PSC differentiation. Overall, the controlled incorporation of microparticles within stem cell aggregates represents a

38

new approach to systematically investigate the effects of biomaterials on stem cell phenotypes in 3D.

Methods

ESC culture and aggregate formation

Undifferentiated D3 ESCs were maintained on gelatin-coated tissue culture dishes in DMEM media supplemented with 15% fetal bovine serum and 10^3 U/ml leukemia inhibitory factor (LIF) (Millipore, Billerica, MA). ESCs were trypsinized into a single cell suspension and aggregates were formed by forced aggregation in AggreWell™ 400 inserts (Stem Cell Technologies, Vancouver, CA)[49] or by rotary orbital culture[167]. Briefly, 1.2 x 10^6 cells in 0.5 mL of medium were inoculated into AggreWell™ inserts, containing approximately 1200 wells per insert, and centrifuged at 200 x g for 5 minutes to cluster cells in the wells. After 24 hours of culture, cell aggregates were removed from the wells using a wide-bore pipette and transferred to suspension culture on a rotary orbital shaker (40 RPM) to maintain the homogeneity of the population. In order to investigate material incorporation, a second centrifugation of 200 μL of a MP solution at 200 x g for 5 minutes was performed immediately after cell centrifugation. Rotary orbital culture was used for aggregate formation with and without MPs by modifying a method previously described[155]. Uncoated MPs and cells were mixed together in a suspension-culture Petri dish and cultured on a rotary orbital shaker at 40 RPM. Following initial formation, cultures were re-fed with fresh differentiation media (without LIF) every 2 days.

39

Microparticle fabrication and size characterization

Agarose MPs were fabricated using a water-in-oil single emulsion similar to previously described methods[168]. A 3% w/w solution (2 mL) of Ultra-low melt SeaPrep Agarose (Lonza, Rockland, ME) was prepared in deionized (dI) water at 60°C and added drop-wise to 60 mL of corn oil (Sigma Aldrich St. Louis, MO) containing 1 mL Tween 20 (Sigma Aldrich, St. Louis, MO). An emulsion was created by homogenizing at 5000 RPM for 5 minutes using a PT3100 (Kinematica, Switzerland). The emulsion was cooled at 4°C for 20 minutes, agarose MPs were retrieved through centrifugation at 200 x g and rinsed a minimum of 3 times with 25 mL of dI H_2O to remove residual oil. Agarose MPs were conjugated to AlexaFluor 488-labeled bovine serum albumin (BSA) using the hetero-bifunctional, photochemical crosslinker Sulfo-Sanpah, *N*-Sulfosuccinimidyl-6-(4'-azido-2'-nitrophenylamino) hexanoate (Pierce Biotechnology, Rockford, IL), using a modification of a previously described method[169]. A Sulfo-SANPAH solution, 6 mg in 24 μL dimethyl sulfoxide, was mixed into 2 mL 3% w/w agarose solution. The solution was treated with 365nm longwave UV light using a Blak-Ray B-100AP light source (UVP, Upland, CA) for 30 minutes, at a distance of 10 cm, to conjugate the Sulfo-Sanpah to the agarose. Subsequently, a 50 mg/mL solution of AlexaFluor 488 succinimidyl ester (Invitrogen, Carlsbad, CA) labeled BSA was added to the agarose solution and allowed to react overnight. The agarose MPs were rinsed 3 times in 20 mL of dI H_2O to remove unbound BSA.

Gelatin MPs were fabricated using a modification of a previously published protocol[165]. Briefly, 2 mL of a 10% w/w solution of gelatin B (Sigma Aldrich) in dI H_2O was heated to 55°C, added drop-wise to 60 mL of corn oil, and homogenized at

40

5000 RPM for 5 minutes to create a water-in-oil emulsion. The emulsion was cooled at 4°C for 10 minutes without mixing, before adding 35 mL of cold acetone to the solution and sonicating the emulsion continuously at 12 W for 1 minute (Sonicator 3000, Misonix, Inc, Farmingdale, NY). The solution was cooled at 4°C for 10 minutes and the MPs were retrieved through centrifugation at 200 x g followed by 3 washes in 25 mL of acetone. The MPs were then crosslinked at room temperature with a 5 mM glutaraldehyde, 0.1% w/w Tween 20 solution in dI H_2O under stirred conditions. After 15 hours of crosslinking, the MPs were retrieved by centrifugation and treated with 25mL of 25 mM glycine in dI H_2O to block residual aldehyde groups. MPs were washed 3 times in 25 mL dI H_2O and labeled either with AlexaFluor 488 or 546 succinimidyl ester in a 0.1 M sodium bicarbonate solution at a pH of 8.3 for 1 hour at room temperature. Fluorescently labeled MPs were washed 3 times in 25 mL of diH_2O to remove un-conjugated dye.

PLGA (50:50, Absorbable Polymers International) MPs were fabricated using an oil-in-water single emulsion[155]. PLGA was dissolved in dichloromethane (DCM) (20mg/mL), added to 0.3% PVA, and homogenized at 3000 RPM. The DCM was evaporated for 4 hours at room temperature in a fume hood and MPs were collected by centrifugation at 200 x g. Prior to homogenization, PLGA MPs were fluorescently labeled by adding 50 mg of CellTracker[TM] Red (Molecular Probes, Invitrogen, Carlsbad, CA) to the DCM solution. For all materials, MPs were suspended in a small volume of diH2O and frozen at -80°C before lyophilization and storage.

The average size of the MP populations was assayed using a Multisizer 3 Coulter Counter (Beckman Coulter, Fullerton, CA) equipped with a 100 µm aperture with a lower

41

detection limit of 2 μm. MPs were suspended in Isoton II diluent (Beckman Coulter) at a dilution which resulted in the counting of at least 2000 events in a sample size of 0.5 mL.

Scanning electron microscopy

Samples were dehydrated in graded acetone dilutions and critically point dried using a Polaron E3000 critical point dryer (Quorum Technologies Inc., Guelph, ON, Canada). MPs were sputter coated for 120 seconds at 2.2 kV using a Polaron SC7640 sputter coater and imaged using a Hitachi S-800 scanning electron microscope (Hitachi High Technologies, Pleasanton, CA).

Microparticle incorporation analysis

After 24 hours of formation, aggregates were removed from the microwells and washed several times in media to separate unincorporated MPs. In order to quantify MP incorporation, volumes chosen to contain on the order of 40-60 aggregates from each experimental condition were sampled and the precise number of aggregates were counted prior to lysing the cells in a 5% SDS solution. MPs were then retrieved from the lysate and quantified using a hemocytometer and normalized to the number of lysed aggregates. Incorporation levels of MPs were assayed in triplicate over 3 separate experiments (n = 9 total for each ratio and condition examined).

The spatial location of fluorescently-labeled MPs within spheroids was analyzed using a LSM 510 microscope (Carl Zeiss, Inc). Cells were labeled with Hoechst dye (1:100) for 15 minutes followed by 3 washes in PBS prior to imaging. Images were obtained at a minimum depth of 30 μm (significantly greater than microparticle

42

diameters) into spheroids for each experimental condition in order to examine the distribution of particles throughout the cell aggregates.

Cell viability

PSC spheroids were formed as described above, and after 2 and 10 days of differentiation, cell viability was assessed using LIVE/DEAD staining (Invitrogen). Samples were incubated in serum-free, phenol red-free medium containing 1 μM calcein AM and 2 μM ethidium homodimer I at room temperature for 30 minutes. Spheroids were then washed three times with PBS and immediately imaged using confocal microscopy.

Gene expression analysis

RNA was extracted from spheroids at various time points for up to 14 days of differentiation with the RNeasy Mini kit (Qiagen Inc, Valencia, CA). Samples analyzed using the Mouse Embryonic Stem Cell array (PAMM-081, SA Biosciences, Frederick, MD) were converted to complimentary DNA using the RT^2 First Strand Kit (Qiagen Inc), loaded in the pre-fabricated 96-well array plates and analyzed using real time PCR (MyIQ cycler, BioRad). Genesis software version 1.7.5 (http://genome.tugraz.at/genesisclient/genesisclient_ download.shtml) was used to construct a heat map of log2 transformed PCR array data[170]. Hierarchical clustering was performed using Euclidean distance and average linkage clustering.

For all other gene expression analysis, RNA was converted to complimentary DNA using the iScript cDNA synthesis kit (Bio-Rad, Hercules, CA) and analyzed using

43

real time PCR (MyIQ cycler, BioRad). Forward and reverse primers for Oct-4, MLC-2V, Pax6, AFP, and glyceraldehyde-3-phosphate dehydrogenase (GAPDH) were designed with Beacon Designer software (sequences and conditions are given in Table 1) and purchased from Invitrogen. Oct-4 gene expression was calculated with respect to undifferentiated ESC expression levels using the Pfaffl method[171]. Pax6, MLC-2V, and AFP expression in treated samples were normalized to GAPDH expression levels and compared to untreated spheroid expression.

Histology and immunostaining

PSC spheroids were collected, fixed in 10% formalin, embedded in Histogel (Thermo Scientific), processed and paraffin embedded. Sections of 5 µm in thickness were deparaffinized before staining with hematoxylin and eosin (H&E). Histological samples were imaged using a Nikon 80i upright microscope and a SPOT Flex camera (15.2 64MP Shifting Pixel, Diagnostic Instruments). For whole-mount immunofluorescent staining, spheroids were permeabilized in a 1.5% Triton X-100 BSA solution for 30 minutes, incubated with primary antibody in 2% BSA solution overnight at 4°C, rinsed with PBS and incubated with a secondary antibody for 4 hours. Antibodies and concentrations used were: mouse monoclonal, anti-α-sarcomeric actin (5c5, Sigma, St. Louis, MO) (1:500) with an AlexaFluor 488 conjugated, goat–anti-mouse secondary (Invitrogen) (1:200), and rabbit polyclonal anti-human alpha-fetoprotein (AFP) (Dako, Glostrup, Denmark) (1:200) with a goat–anti-rabbit, FITC-conjugated secondary (Invitrogen) (1:200). Spheroids were counterstained with Hoechst (1:100), washed 3 times in PBS and imaged using a Zeiss LSM 510 confocal microscope (Carl Zeiss Inc.).

44

Experimental values are reported as mean ± standard deviation (n≥3). Statistical analysis was determined using one or two way ANOVA coupled with Tukey's post hoc analysis using Systat (v12, Systat Software Inc.). P-values < 0.05 were considered statistically significant.

Results

Microparticle formation

SEM micrographs indicated that MPs from each of the materials exhibited similar round shapes and smooth topological surface morphologies. The hydrogel MPs are likely to appear smaller when analyzed by SEM due to the necessary dehydration of the samples, prior to imaging, thus the diameter of the different MPs was analyzed using a Coulter Counter in an aqueous buffer in order to obtain more accurate size measurements. The average diameters of the PLGA, agarose and gelatin MPs were determined to be 5.2 ± 2.8, 4.5 ± 1.7 and 5.1 ± 2.9 µm, respectively (Figure 3.1).
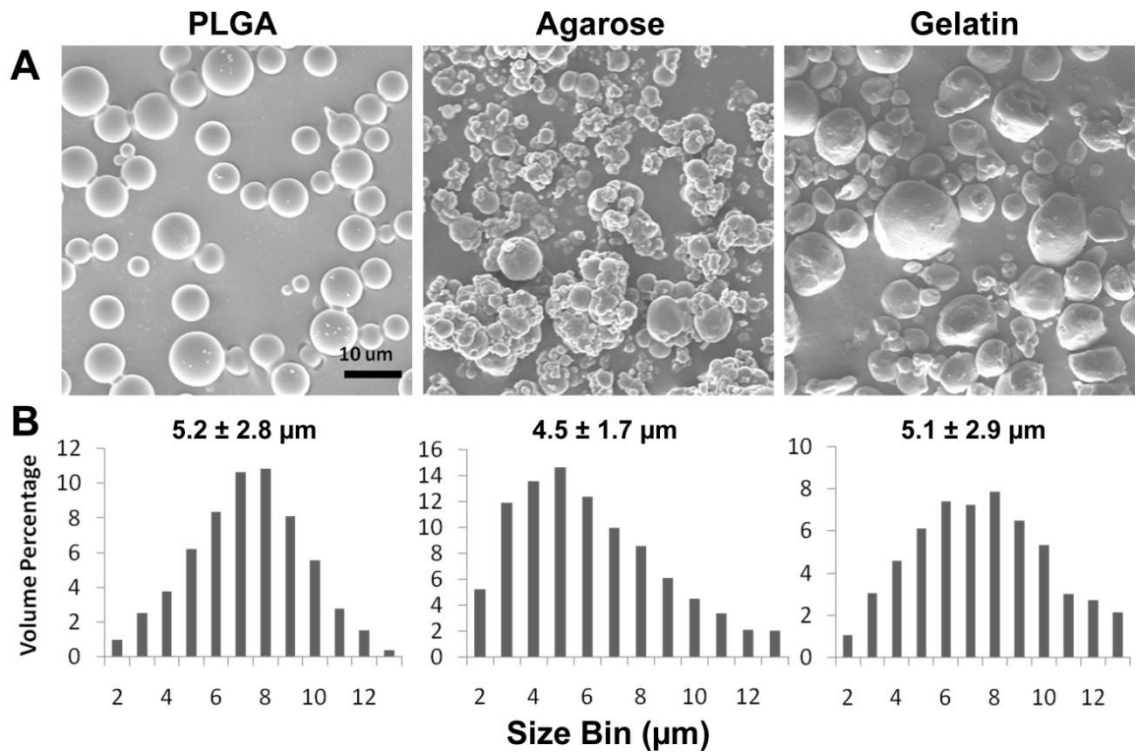
Figure 3.1. MP characterization. PLGA, agarose and gelatin MPs were fabricated using a single oil-in-water or water-in-oil emulsion to create similarly sized MPs. MPs were generally round with smooth surfaces as indicated by scanning electron microscope images. Coulter counter size analysis of MPs in aqueous conditions revealed average diameters of the MPs to be between 4.5 - 5.2 µm. Scale bar = 10 µm.

Microparticle incorporation using forced aggregation

Simple mixing of MPs and PSCs did not result in efficient incorporation of the various materials assayed; therefore forced aggregation of MPs and PSCs in microwells was investigated as an alternative means to incorporate materials within aggregates.

Material incorporation using rotary orbital culture

Rotary spheroid formation has been used previously by our lab as a method to control the incorporation of ECM-coated PLGA MPs within EBs[155, 161], and was therefore tested initially as a method to incorporate various uncoated MPs within the aggregates. However, simple mixing of ESCs with uncoated PLGA or agarose MPs using rotary culture resulted in limited incorporation of the materials within aggregates (Figure 3.2). Out of nearly 150 aggregates analyzed, 57% did not contain any PLGA MPs, 42% contained 1 to 5 PLGA MPs, and only a single aggregate contained more than 5 PLGA MPs. Agarose MP incorporation within aggregates was even lower, with no aggregates containing more than one MP and <5% containing a single agarose MP. In contrast, rotary orbital mixing of ESCs with gelatin MPs resulted in 100% of the aggregates examined containing 10+ gelatin MPs each; however, the extent of incorporation was rather heterogeneous and large (~1mm diameter) gelatin MP-cell aggregates were frequently observed.
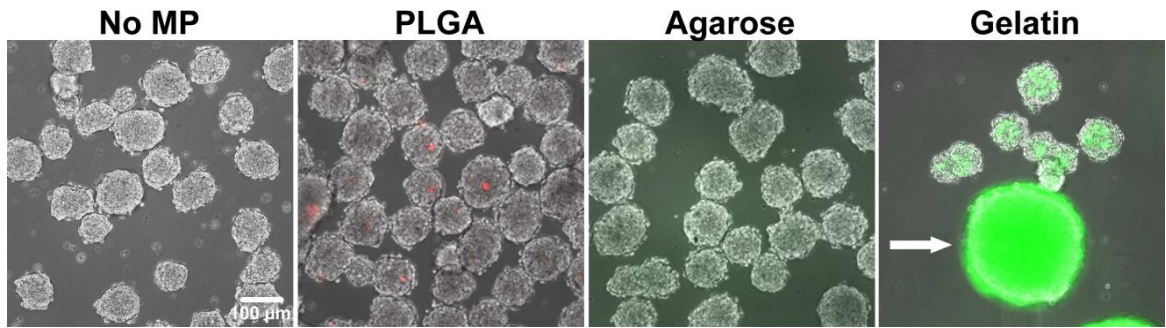
Figure 3.2. Rotary culture results in variable MP incorporation within EBs. Fluorescently labeled MPs (CellTracker[TM] Red incorporated or AlexaFluor® 488 succinimidyl ester conjugated) were mixed with ESCs at a ratio of 2:1 and cultured on a rotary orbital shaker at 40 rpm for 48 hours to promote aggregate formation. Non-adhesive materials (PLGA and agarose) were not efficiently incorporated as demonstrated by a lack of punctuate fluorescent particles. Gelatin, an adhesive material, was incorporated efficiently within the aggregates, however, the formation of large masses of MPs and cells (arrow) were observed along with smaller sized aggregates. Scale bar = 100 μm.
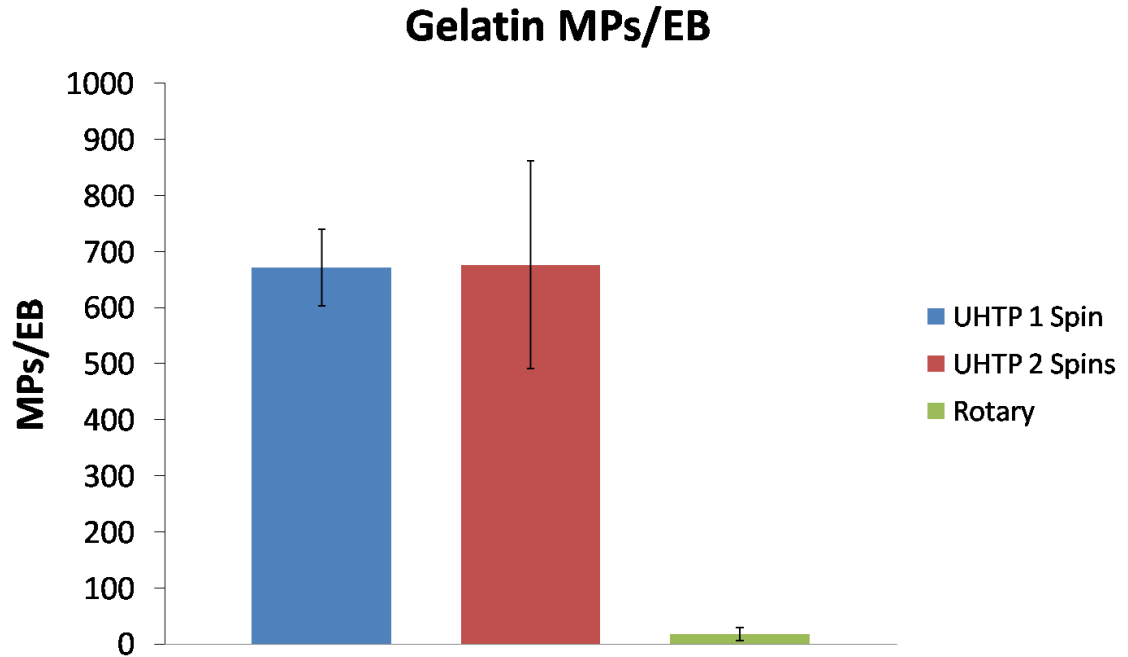
Figure 3.3. Rotary and forced aggregation incorporation of gelatin microparticles. Gelatin microparticles were incorporated within ESC spheroids either through rotary mixing at 40 RPM or by forced aggregation. In each case, microparticles were added to ESCs at a 2:1 MP:cell ratio. Forced aggregation resulted in ~10 fold higher incorporation (33% vs. 3.5%) compared to rotary incorporation.
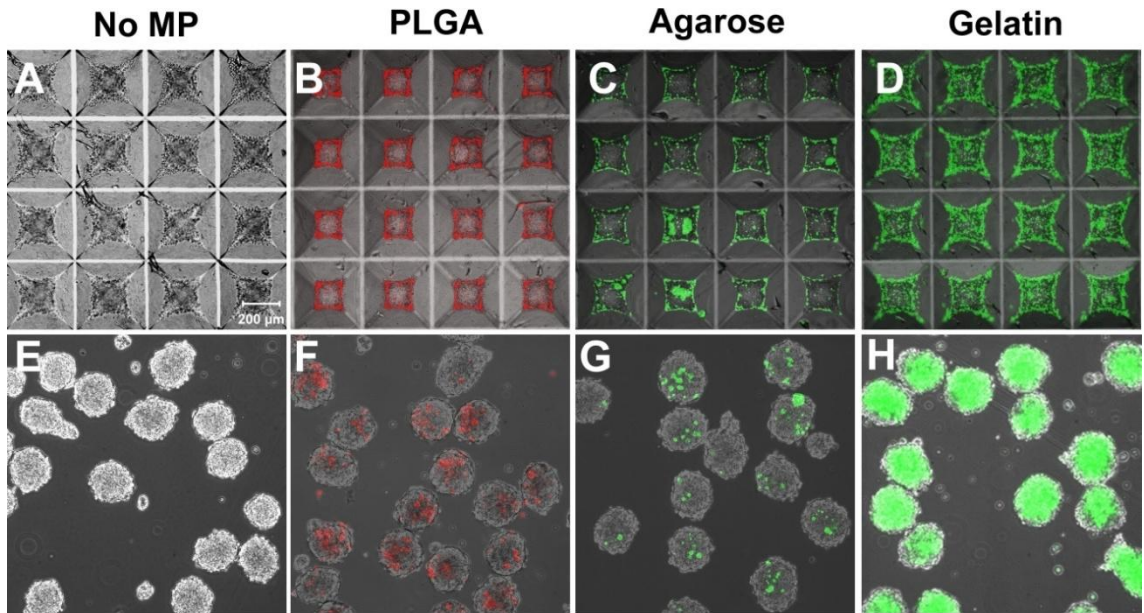
Figure 3.4. Forced aggregation of PSCs and MPs results in uniform material incorporation within spheroids. ESCs centrifuged alone (A), or with fluorescently labeled MPs (B-D) in microwells formed spheroids after 24 hours of culture. Spheroids were removed from the wells and thereafter maintained in rotary orbital suspension culture at 40 rpm (bottom row). Uniform incorporation of materials within populations of PSC aggregates was observed (E-H). Scale bar = 200 μm.

Using the same 2:1 ratio of MPs to cells as used in rotary formation, increased incorporation of each material in homogeneously sized aggregates was observed when the materials were either centrifuged with the cells (1 spin) or centrifuged on top of the cells (2 Spins) (Figure 3.3). Two centrifugations, however, were observed to be necessary for materials which do not contain integrin binding sequences such as agarose. Agarose MPs were only observed to be incorporated when centrifuged on top of the cell layer.

Analysis of the fluorescent signal within aggregates indicated that gelatin MP-treated aggregates contained the most incorporated MPs and agarose MP-treated aggregates contained the fewest MPs per aggregate. In contrast to rotary culture, all aggregates formed through forced aggregation contained more than one MP for each

material investigated. Because the efficiency of incorporation was noticeably different across material groups, the average number of MPs incorporated per aggregate was analyzed as a function of the seed ratio of MPs to cells for a range of MP values with a fixed number of 1.2×10^6 cells/insert (1000 ESCs/microwell) (Figure 3.4A). The incorporation of non-adhesive materials (PLGA and agarose) was characterized by a gradual increase allowing for incorporation of up to approximately 125 MPs per aggregate over the range of seed ratios examined, whereas gelatin MPs were incorporated with much greater efficiency. In order to determine if incorporation was dependent on the adhesivity of the material surface, the incorporation of gelatin-coated PLGA MPs was also analyzed. The profile of gelatin-coated PLGA MP incorporation resembled that of gelatin MPs and was greater than uncoated PLGA MPs. Optical sectioning of aggregates indicated that MPs were incorporated throughout the aggregate and not simply localized to the surface of the aggregates (Figure 3.4B). In PLGA and gelatin-treated samples, some aggregation of MPs was observed within spheroids, whereas aggregation of incorporated agarose MPs was not observed. In order to test the method with other cell types, gelatin MPs were incorporated within another mouse ESC line, R1, and also within a human induced pluripotent stem cell line derived from IMR-90 fibroblasts (Figure 3.5). Together these results indicate that forced aggregation can be used to control the extent of incorporation and distribution of adhesive and non-adhesive biomaterial MPs within PSC aggregates.

51
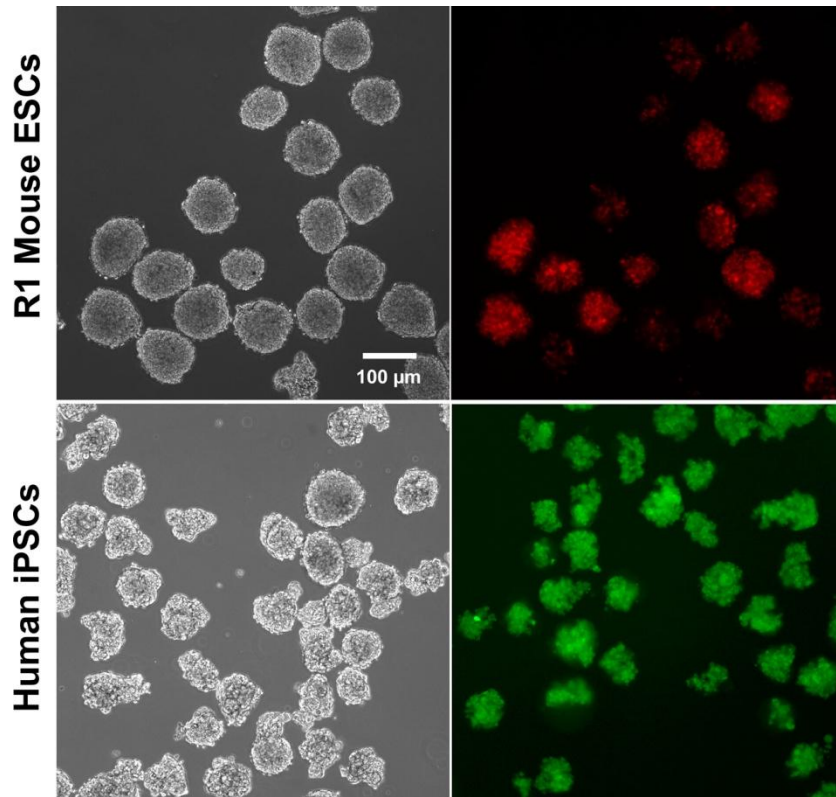
Figure 3.5 Forced aggregation can be used to incorporate biomaterial microparticles in various stem cell lines. In order to demonstrate the applicability of forced aggregation to incorporate biomaterial MPs within pluripotent stem cell lines, another mouse line, R1, and also a human induced pluripotent stem cell line were used to incorporate gelatin MPs. MPs were labeled with AlexaFluor 488 (R1s) or with AlexaFluor 546 (human iPSCs).

Gelatin microparticle degradation within EBs.

        The gelatin MPs are essentially denatured collagen, cross-linked to provide stability in aqueous solutions. As the gelatin MPs were fluorescently labeled to visualize incorporation the degradation of the particles could also be tracked by fluorescence microscopy (Figure 3.6). Punctate fluorescence was observed at early time points (day 4-10) indicative of intact particles. As culture time increased, the fluorescence became more diffuse, indicative of degradation. At the higher loading ratio, intact particles were still observed after 14 days of EB culture.
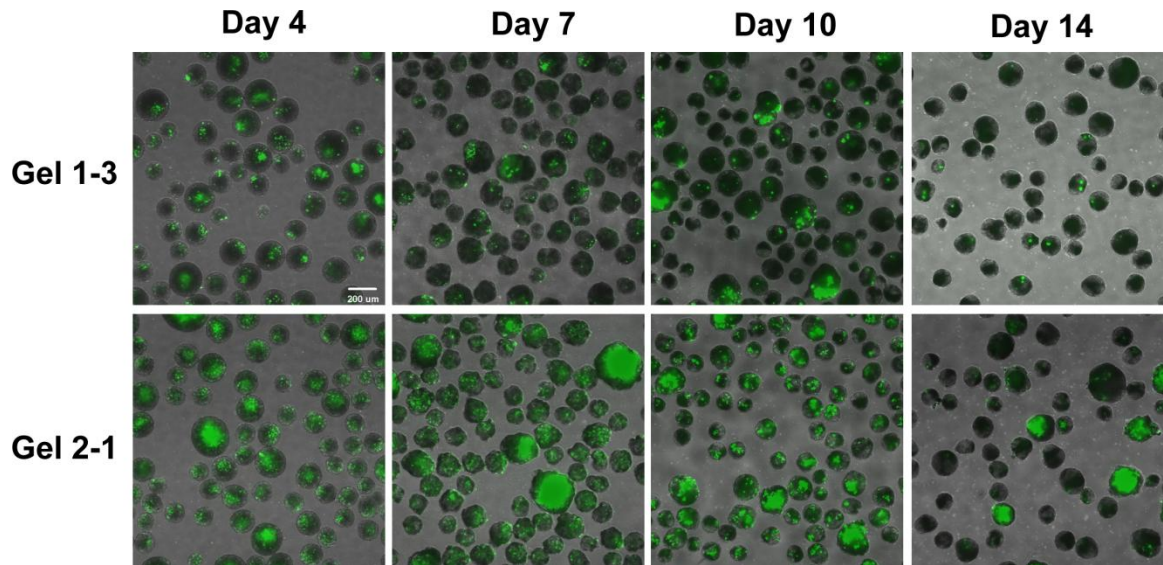
Figure 3.6 Degradation of gelatin MPs within mouse EBs. Gelatin MPs were fluorescently labeled and incorporated within D3 EBs using forced aggregation at seeding ratios of 1:3 and 2:1 (MPs : cells). Fluorescence is punctate at early time points indicative of intact MPs and diffuse at later time points indicative of MP degradation. In both cases the number of punctuate particles decreases; however, with higher MP loading individual MPs are still observed at day 14 of culture.

Microparticle effects on viability and differentiation

        The effects of MP incorporation on PSC viability and differentiation were examined for aggregates containing approximately equal amounts of different types of

53
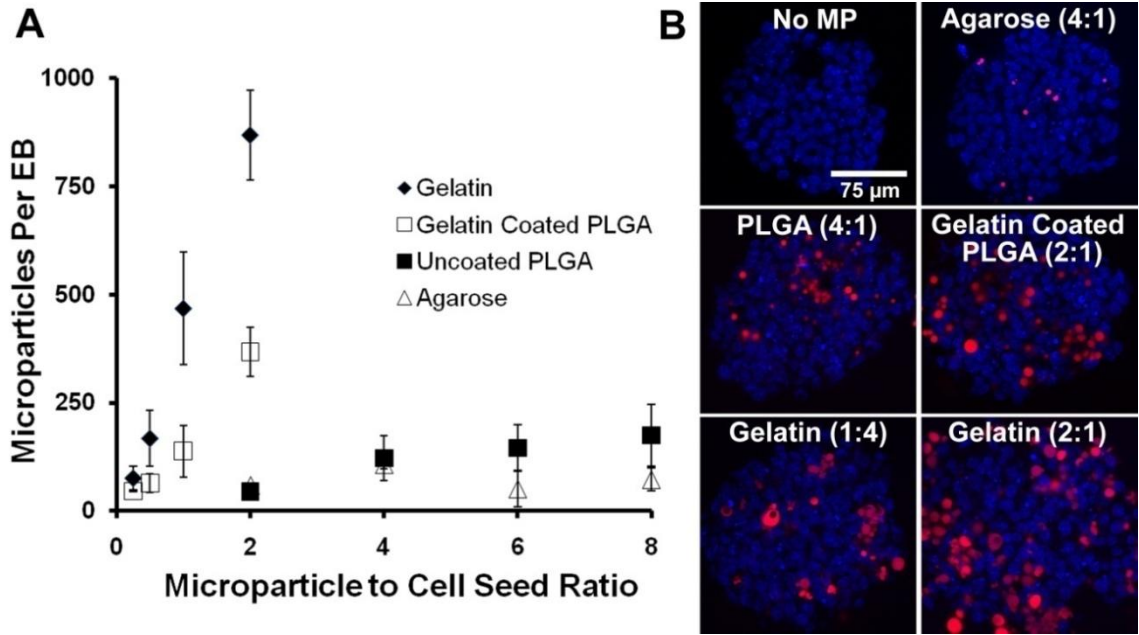
Figure 3.7. MP incorporation is controlled in a dose-dependent manner. Incorporation was analyzed as a function of MP to cell seed ratio (A). Adhesive materials (gelatin and gelatin-coated PLGA) were incorporated more efficiently than non-adhesive materials (agarose and PLGA). The presence of fluorescently labeled particles throughout the spheroids was confirmed by confocal microscopy (shown at a depth of 30 µm) (B). Scale bar = 75 µm.

MPs. Formation conditions which resulted in ~125 MPs per spheroid (1 MP for every 8 cells) were chosen for subsequent studies and corresponded to the following MP to cell seed ratios: agarose 4:1, PLGA 4:1, and gelatin 1:4 (as indicated in Figure 3.7). In addition, in order to investigate the effects of increased MP incorporation, the increased dynamic range of gelatin incorporation was exploited to include a fourth MP experimental group of 2:1 gelatin, which resulted in an average incorporation of ~800 MPs per spheroid (4 MP for every 5 cells).

PSC aggregates cultured with materials were collected at days 2 and 10 of differentiation and stained for live and dead cells (Figure 3.8). At both time points, spheroids contained few dead cells and no differences were observed across any of the experimental conditions suggesting that the presence of materials did not negatively affect cell viability at early or later stages of culture.

55
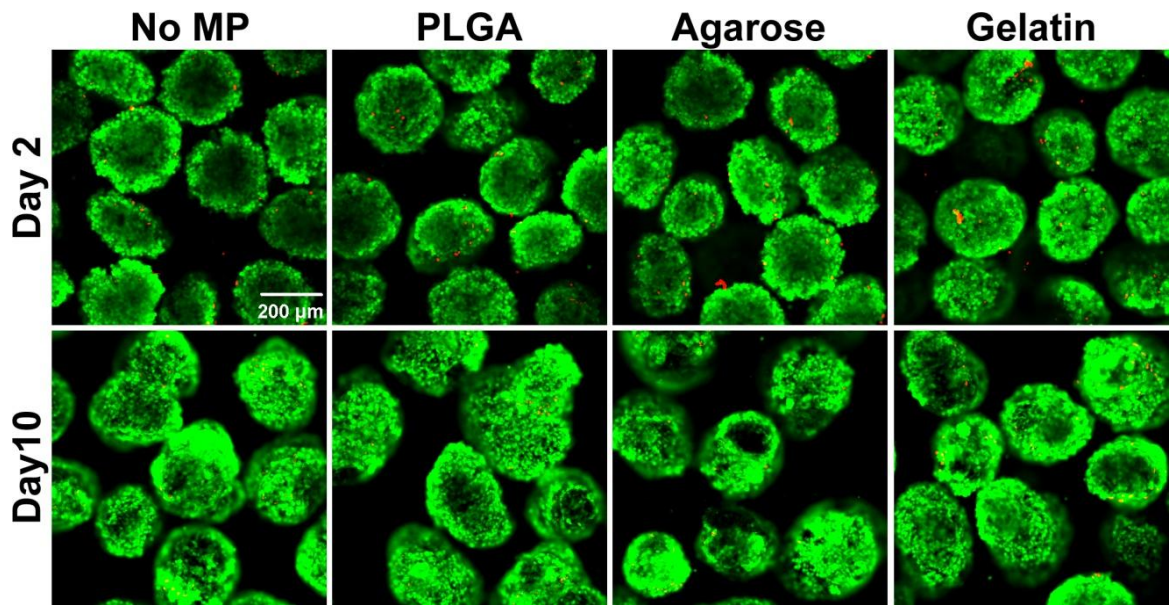
Figure 3.8. Cell viability is not adversely affected by MP incorporation. Cell viability was assayed after 2 (top row) and 10 (bottom row) days of differentiation using LIVE/DEAD® stain. Live cells were labeled with calcein AM (green) and dead cells were labeled with ethidium homodimer (red). Few dead cells were observed in any of the groups at either of the time points examined.

Gene expression analysis of PSC aggregates after 10 days of suspension culture was performed for 84 distinct genes initially using PCR SuperArrays (Figure 3.9A). Overall, relatively modest differences were observed for the majority of genes examined within any of the experimental groups compared to spheroids that lacked MP incorporation. Interestingly, hierarchical clustering of the resulting data indicated that each of the replicate samples grouped most closely together, reflecting a common gene expression profile among spheroids treated with the same type of material. Significant differences ($p \leq 0.05$) in the expression of 34 of the genes assayed (40%) were noted in at least one of the MP-treated groups compared to untreated spheroids; this level of significance corresponds to a probability of no more than 2 falsely identified genes. The majority of the genes affected by incorporation of different MPs were associated with endoderm (AFP, Gata-6, Serpina1a, Glucagon, and Ptf1a) or mesoderm (Hemoglobin Y,

56

VE-Cadherin, CD34 antigen, Hemoglobin X) differentiation, whereas few differences in pluripotent or ectoderm lineage markers were observed. Thus, the gene expression profile of PSC aggregates is sensitive to the incorporation of different materials even after normalization of MP size and number are taken into account.

Temporal gene expression analysis of the pluripotent marker Oct-4 (Figure 3.9B), as well as several germ lineage markers (AFP, Myosin light-chain 2 ventricle (MLC-2V), Pax6, Figure 3.9C) was performed using qRT-PCR over 14 days of culture. In all of the conditions examined, Oct-4 expression decreased significantly after 4 days of differentiation and no significant differences were observed between any of the experimental groups. Pax-6 expression was not affected by the presence of materials; however, consistent with PCR array data, significant differences in mesoderm and endoderm marker expression were detected. MLC-2V expression was significantly ($p <$ 0.05) increased by 4.5 fold in gelatin 2:1 spheroids at day 14 compared to untreated spheroids. Agarose and PLGA spheroids expressed 1.7 and 3.2 fold less AFP at day 10, respectively, while gelatin 2:1 spheroids expressed AFP at a 1.6 fold higher level than untreated controls (Figure 3.9C).
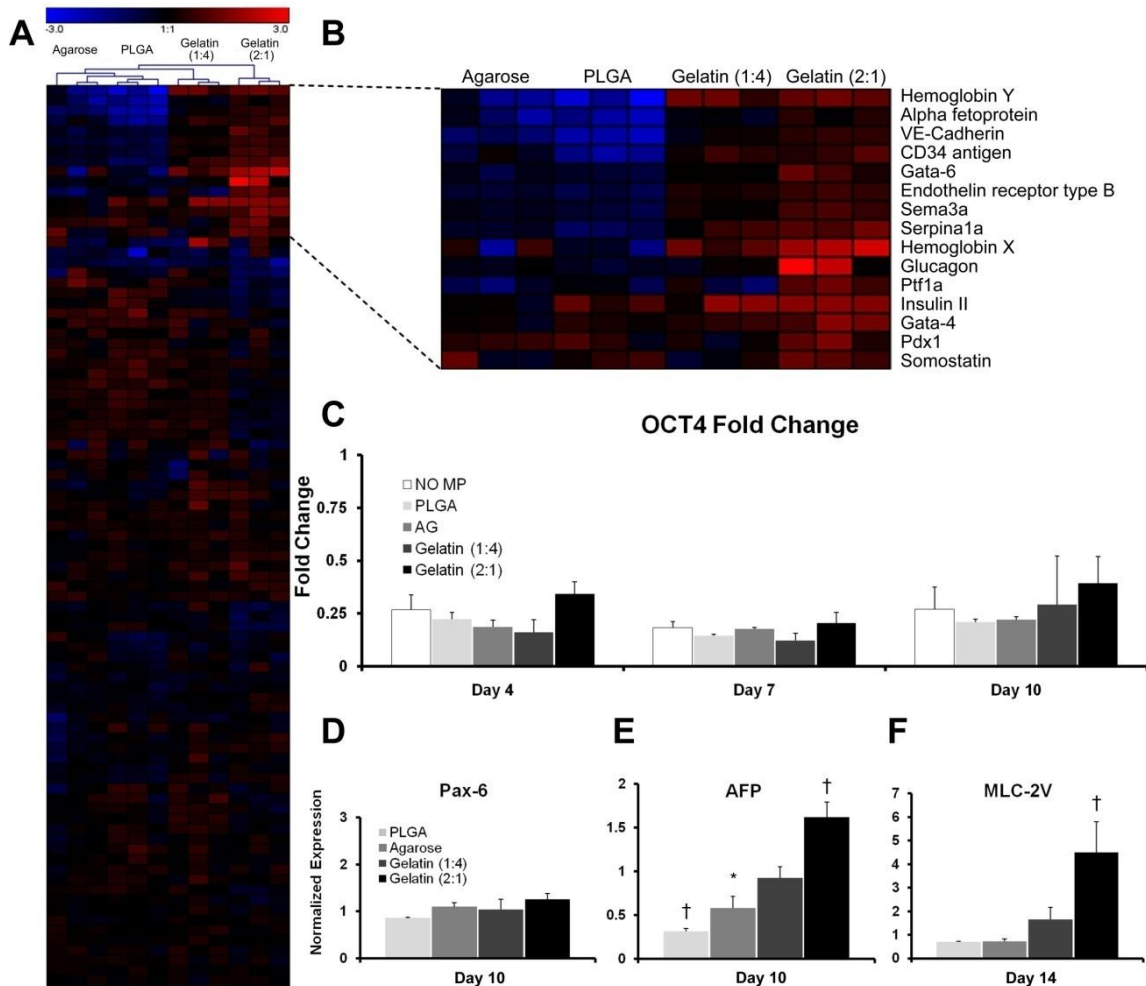
Figure 3.9. Gene expression is modulated by the presence of different materials. SuperArray analysis (A) at day 10 of differentiation demonstrated that the presence of different materials within PSC aggregates significantly ($p<.05$) modulated the gene expression of 40% (34/84) of the genes examined. Magnified view of heat map (B) results displayed the top 15 genes with the greatest fold changes relative to aggregates that lacked MPs. Oct-4 gene expression (C) was not significantly different between any of the experimental groups at any of the time points examined (days 4, 7 and 10). Pax-6 gene expression was not significantly altered, whereas AFP (E) and myosin light chain 2-ventricle (MLC-2V) (F) were modulated by the presence of different materials at days 10 and 14, respectively. n=3 for all experiments. * = $p \leq 0.05$, † = $p \leq 0.005$.

58

Incorporation of MPs did not appear to have any gross effects on aggregate formation or morphology through 14 days of differentiation in suspension culture. Immunostaining of the spatial distribution of phenotypic markers was assessed within the aggregates to further characterize differentiation as hematoxylin and eosin staining of cross-sections of spheroids revealed no observable differences in morphology (Figure 3.10, day 7 shown). Whole-mount immunofluorescent staining was performed on alpha-sarcomeric actin (cardiac mesoderm) and AFP since gene expression differences were almost exclusively found in mesoderm and endoderm markers. The observed spatial distributions of mesoderm-like and endoderm-like phenotypes were altered within the different treated groups. In untreated spheroids, positive expression of alpha-sarcomeric actin, a cardiac muscle actin, was localized to small, concentrated regions on the spheroid exterior, and similar expression patterns were observed in spheroids with agarose MPs. In contrast, alpha-sarcomeric actin staining was not observed in PLGA and gelatin 2:1 spheroids at the same time point (14 days), whereas gelatin 1:4 spheroids displayed positive expression in larger sections including the interior sections. In day 14 spheroids, AFP expression was localized to the outer layer of cells for most of the experimental groups, in agreement with previous literature reports that endoderm differentiation is primarily localized to the periphery of EBs by this stage of differentiation[29, 30]. However, in gelatin 2:1 spheroids, more homogeneous AFP expression was observed throughout and was not limited to the cells at the periphery. Altogether the gene and phenotypic marker expression data demonstrate that materials incorporated within PSC aggregates during formation influence differentiation through 14 days of culture.
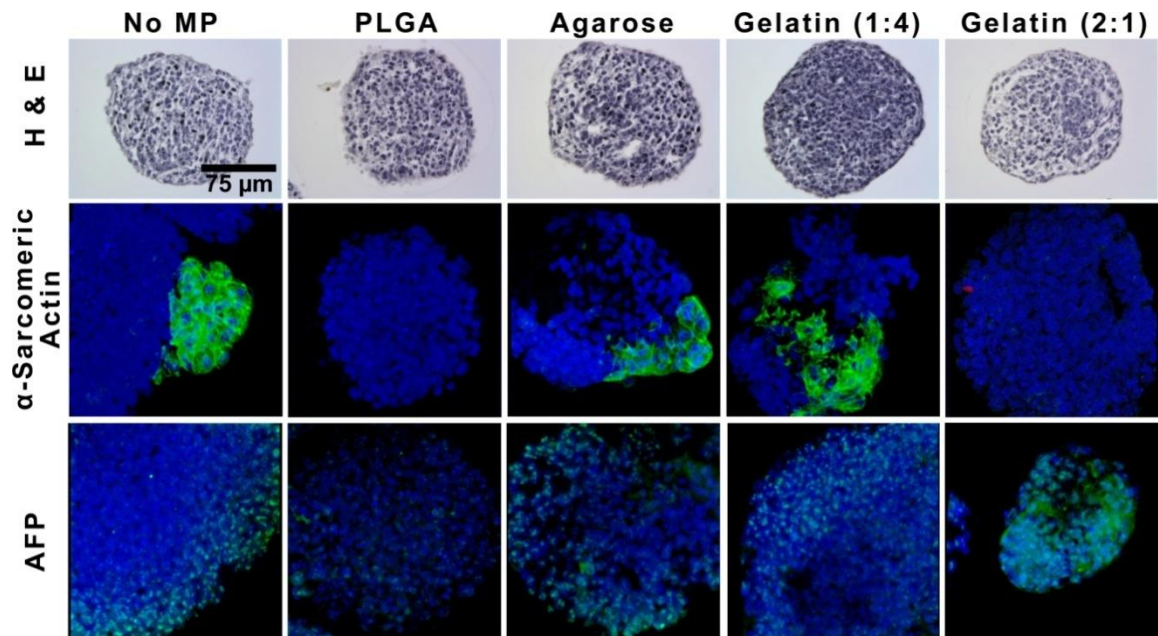
Figure 3.10. Spatial distribution of cell phenotypes is altered by the presence of materials. Hematoxylin and eosin staining of day 7 PSC spheroids with or without different MPs did not exhibit gross differences in morphology (top row). At day 14 of differentiation, the spatial distribution of α-sarcomeric actin and AFP within EBs was assessed. α-sarcomeric actin expression in gelatin (1:4) aggregates was observed throughout, while positive expression was localized to the periphery in untreated and agarose-treated spheroids and no positive expression was observed in PLGA- and gelatin 2:1-treated spheroids. AFP expression was localized to the periphery of all experimental groups with the exception of gelatin 2:1 spheroids, where expression was detected throughout the cell aggregates. Scale bar = 75 μm.

Discussion

In this study, the effects of PLGA, agarose and gelatin MPs (of equal size) incorporated within pluripotent stem cell aggregates were directly examined and compared. Rotary aggregate formation, previously used to incorporate gelatin-coated PLGA MPs, was not sufficient to homogeneously incorporate the three materials equally and therefore we developed a forced aggregation technique that enabled dose-dependent control of MP incorporation for each of the materials. The incorporation efficiency of the materials varied according to their relative adhesivity and therefore, the appropriate aggregate formation conditions for each material were determined empirically in order to normalize for equivalent numbers of MPs/spheroid to make fair evaluations of material effects. No differences were observed in the formation of aggregates or cell viability in any of the experimental groups compared to cell aggregates alone, although gene and protein expression of phenotypic markers indicated that even at low incorporation levels (~1 MP/8 cells) the differentiation of PSCs to mesoderm and endoderm lineages was affected. Interestingly, none of the genes assayed were uniformly up-regulated or down-regulated by MP-treated spheroids, suggesting that the differences in gene expression were related to specific material characteristics and not simply the presence of foreign particles. While the gross morphology of the MP-treated aggregates was not distinguishable from untreated aggregates, the spatial distribution of certain differentiated phenotypes was altered, suggesting that the biomaterials themselves influence the extracellular microenvironment. The adhesive and elastic properties of the biomaterials examined, both of which have been linked to stem cell fate determination[96, 172], vary widely between PLGA, agarose and gelatin. Overall, the results of this study indicate

61

that PSC differentiation within spheroids is sensitive to various types of biomaterials and that forced aggregation can be used as a platform for direct study of stem cell-biomaterial interactions in 3D culture.

Previous studies of stem cell-biomaterial interactions have been performed using monolayer culture or cell encapsulation[142, 159]. Stem cells cultured on spotted biomaterial arrays can be used for high-throughput screening of various surfaces and in this manner materials may be identified for further study in more complex 3D systems. Monolayer culture has been used previously to identify polymer combinations which supported the growth and differentiation of human ESCs[159]. Encapsulation of cells within biomaterials is low-throughput in comparison to monolayer arrays, but allows for study of the biomaterial effects on stem cell differentiation in a 3D suspension-culture. Mesenchymal stem cell differentiation, for example, can be influenced by the chemical moiety presented in the hydrogel in which they are encapsulated[142]. Encapsulation works particularly well with single cell suspensions, where each cell is surrounded by the biomaterial, however; with respect to spheroid culture, encapsulation presents the material surface only to the cells on the aggregate exterior. The distinction of MP-based strategies is that the material can be incorporated in a controlled manner throughout cell spheroids allowing for the study of biomaterials directly within a 3D stem cell aggregate environment. Although the forced aggregation approach detailed in this study was originally developed for the production of homogeneous EBs, it has recently been successfully applied to form spheroids of mesenchymal stem cells (MSCs) as well[173]. Thus, the method of controlled incorporation of biomaterials within cell aggregates described herein could be applied to other cell types cultured as spheroids, such as MSCs,

62

neural stem cells or tumor cells[174], for studies of directed differentiation or the influence of microenvironment on cell fate.

The materials examined in this study were chosen to represent different classes of biomaterials that have been used in conjunction with stem cells either as molecular or cellular delivery vehicles. PLGA is a hydrolytically-degradable, synthetic copolymer, commonly used for controlled release of small, hydrophobic molecules. Agarose is a polysaccharide thermo-sensitive hydrogel material that is largely considered non-adhesive and is not degraded by mammalian cells, however it can be functionalized in a variety of manners for controlled presentation of biomolecules, such as growth factors[175, 176] and short peptide sequences[177]. Gelatin is an enzymatically degradable hydrogel material formulated from denatured collagen that is dually capable of growth factor delivery and direct binding to cells via integrin receptor ligation. The three materials can be used alone or in combination to deliver a variety of morphogens or growth factors with different kinetics, yet it is notable that even in the absence of loading with exogenous molecules, the results presented within this study indicate that naïve materials themselves can influence the relative differentiation of PSC aggregates.

PLGA is composed of acidic monomers, consequently, the hydrolytic degradation of the polymer can result in acidification of the local environment[178]. Although the effects of pH on ESC differentiation have not been extensively studied, it has been reported that below pH 7.0, mouse ESC proliferation is decreased and at a pH of 6.7 Oct-4 expression is reduced[179]. PLGA MP treatment at the levels studied here did not result in any differences in cell viability nor in relative changes to Oct-4 expression (Figure 6B), suggesting that the local pH levels may not be decreased significantly within

63

the spheroids during the culture period examined. This is supported by previous studies of the degradation kinetics of 50:50 PLGA, which have reported that degradation is limited to between 10 and 15% of the original mass during the first 2 weeks of degradation[180, 181]. Longer-term studies using PLGA for stem cell cultures may need to take into account acidification of the stem cell microenvironment.

Integrins are known to play critical roles in cellular differentiation, migration and proliferation[182]. Likewise, growth of ESCs on extracellular matrix proteins such as laminin has been used to direct neural differentiation of human ESCs mediated through $\alpha_6\beta_1$ integrin signaling[183]. In addition to integrin signaling effects, it is possible that the addition of adhesive materials within the spheroids can affect the mobility of cells. Time lapse microscopy and cell tracking have demonstrated that cells are very mobile within early stage embryos[184] as well as EBs[185], a characteristic which may be modulated by the presence of adhesive MPs within PSC aggregates. Tracking of Disabled-2 (Dab2) positive, primitive endoderm cells suggests that endoderm differentiation may occur throughout aggregates during the earliest stages of differentiation and as cells are passively migrating throughout the spheroid, Dab2 mediated polarization enables primitive endoderm cells to create a non-adherent apical interface and remain preferentially at the exterior surface of EBs throughout differentiation[185]. We observed endoderm, identified as AFP[+], cells on the exterior of untreated, PLGA and agarose-treated spheroids. However, in aggregates containing an increased concentration of gelatin MPs, positive AFP expression was observed throughout. In aggregates with a high adhesive MP to cell ratio, more cells are exposed to adhesive biomaterial surface within the spheroid and it is possible that cell adhesion to

64

the biomaterial could restrict movement and disrupt the normal migration patterns of PSCs undergoing differentiation. In future studies, incorporation of adhesive ECM-derived MPs within PSC aggregates could be used to specifically examine the effects of cell movement on early differentiation events, such as endoderm formation, primitive streak development and the resulting spatial distributions of differentiated cell phenotypes.

Conclusions

We have developed a forced aggregation technique to control the incorporation of biomaterials within PSC aggregates, without the need for surface modification of the materials. This advance allows for direct study of stem cell-biomaterial interactions in a 3D model system of PSC differentiation. The results of this study demonstrate that PSC differentiation is sensitive to the presence of biomaterials in the extracellular microenvironment, suggesting that biomaterials incorporated within stem cell spheroids can be used in conjunction with other methods (i.e. soluble molecule delivery, mechanical forces) to direct the differentiation of stem cells for tissue engineering and regenerative medicine applications.

CHAPTER 4

HEPARIN-MODIFIED GELATIN MICROPARTICLE INCORPORATION WITHIN EMBRYOID BODIES

Introduction

The fate of embryonic stem cells (ESCs) is influenced by microenvironmental factors including soluble factors, extracellular matrix composition and cell-cell interactions[150, 157]. In 3D culture, the effects of cell-cell interactions and extracellular matrix interactions can be investigated through the use of genetically engineered cells or biomimetic materials engineered to present integrin binding sequences or cell-adhesion molecules. Supplementation of soluble factors to the culture medium; however, remains the most heavily utilized method for directed cell differentiation due to ease of use and efficacy. Additionally, ESCs can also be cultured in conditioned media (CM) as growth factors secreted by somatic cell types can provide instructive cues for differentiation, though more current research has favored defined, xeno-free media for maintenance of pluripotency and differentiation.

Stem cells are also known to secrete their own factors into their surroundings *in vitro* and when transplanted *in vivo*[186, 187]. Study of the secretome of both mesenchymal stem cells (MSCs) and ESCs has increased recently as it is believed that that benefits observed after transplantation of stem cells in models of disease and wound healing are due to the release of paracrine factors by the transplanted cells rather than engraftment and subsequent stem cell differentiation, as was first hypothesized to be the case[187, 188]. Not surprisingly, the profile of secreted molecules is dynamic and

depends on the state of cell differentiation[189], [Ngangan and Nair et al., Unpublished data]. Research from our lab and others has aimed to collect factors secreted from stem cells *in vitro* in biomaterials which could then be used in cell-free application of stem cell-produced molecules for regenerative medicine[190-193]. It is notable that many of the molecules identified in secretome studies are also molecules, such as bone morphogenetic protein-4 (BMP-4) and vascular endothelial growth factor (VEGF), that are added to ESCs for directed differentiation protocols[194-196]. For example, BMP-4 has been shown to induce and mesoderm differentiation in ESCs[195, 197, 198], VEGF promotes angiogenesis during early embryonic development[197, 199], and insulin-like growth factor 2 (IGF-2) promotes growth in mouse embryos[200]. It is likely that what is generally referred to as "spontaneous" differentiation observed within EBs is due in some part to the secreted molecules from neighboring cells. One possible hypothesis for why incorporation of unloaded MPs within EBs modulated differentiation[201] is that the materials themselves are capable of interacting with secreted molecules and can alter growth factor concentration or availability for cell signaling.

Recent reports have utilized heparin-modified materials or materials containing heparin binding peptides, to direct cellular interaction with endogenous growth factors[202, 203]. The aim of this study was to utilize this strategy within 3D stem cell aggregates by incorporating hydrogel microparticles capable of interacting with secreted growth factors within EBs and then to investigate growth factor secretion and differentiation of the ESCs.

67

Methods

ESC culture and aggregate formation

Undifferentiated D3 ESCs were maintained on gelatin-coated tissue culture dishes in DMEM media supplemented with 15% fetal bovine serum and 10^3 U/ml leukemia inhibitory factor (LIF) (Millipore, Billerica, MA). ESCs were trypsinized into a single cell suspension and aggregates were formed by forced aggregation in AggreWell^{TM} 400 inserts (Stem Cell Technologies, Vancouver, CA)[49]. Briefly, 1.2 x 10^6 cells in 0.5 mL of medium were inoculated into AggreWell^{TM} inserts, containing approximately 1200 wells per insert, and centrifuged at 200 x g for 5 minutes to cluster cells in the wells. For EB culture, the media was switched to ESGRO complete basal media (Millipore) supplemented only with penicillin and antimycotic. After 24 hours of culture, cell aggregates were removed from the wells using a wide-bore pipette and transferred to suspension culture on a rotary orbital shaker (40 RPM) to maintain the homogeneity of the population. In order to investigate material incorporation, a second centrifugation of 200 µL of a MP solution at 200 x g for 5 minutes was performed immediately after cell centrifugation.

Fabrication of gelatin microparticles

Gelatin MPs were fabricated using a modification of a previously published protocol[165]. Briefly, 2 mL of a 10% w/w solution of gelatin B (Sigma Aldrich) in dI H$_2$O was heated to 55°C, added drop-wise to 60 mL of corn oil, and homogenized at 5000 RPM for 5 minutes to create a water-in-oil emulsion. The emulsion was cooled at 4°C for 10 minutes without mixing, before adding 35 mL of cold acetone to the solution

and sonicating the emulsion continuously at 12 W for 1 minute (Sonicator 3000, Misonix, Inc, Farmingdale, NY). The solution was cooled at 4°C for 10 minutes and the MPs were retrieved through centrifugation at 200 x g followed by 3 washes in 25 mL of acetone. The MPs were then crosslinked at room temperature with a 5 mM glutaraldehyde, 0.1% w/w Tween 20 solution in dI H_2O under stirred conditions. After 15 hours of crosslinking, the MPs were retrieved by centrifugation and treated with 25mL of 25 mM glycine in dI H_2O to block residual aldehyde groups. MPs were washed 3 times in 25 mL dI H_2O and labeled either with AlexaFluor 488 or 546 succinimidyl ester in a 0.1 M sodium bicarbonate solution at a pH of 8.3 for 1 hour at room temperature. Fluorescently labeled MPs were washed 3 times in 25 mL of diH_2O to remove un-conjugated dye.

<u>Heparin modification of gelatin MPs</u>

Heparin was conjugated to the gelatin microparticles using 1-ethyl-3-(3-dimethylaminopropyl)-carbodiimide (EDC) and Sulfo-N-hydroxysuccinimide (S-NHS) chemistry. Heparin was first activated using a 1:10 molar ratio of Heparin to EDC and combined with 2:5 ratio of EDC to S-NHS in a 0.1M MES, 0.5M NaCl buffer for 15 minutes at 37°C with agitation. The reaction was quenched by addition of 20mM 2-mercaptoethanol solution. The solution was then added at desired molar ratio (1:10, 1:1, 5:1, or 10:1) of heparin to gelatin microparticles and allowed to react for 4 hours on a tube shaker at 37°C.

Following conjugation of heparin to the gelatin MPs, free heparin was removed by washing the MPs 3x in ddH2O with 30 minutes of rotation between each wash. The amount of heparin per mg of microparticles was then determined using a toluidine blue

assay. Toluidine blue forms a color-shifted crystal when reacted with heparin. Free toluidine can then be removed by centrifugation and the precipitant can be solubilized measured using a spectrophotometer. Toluidine blue (500 µL of 0.4mg/ml toluidine blue and 4 mg/ml sodium chloride in 0.1M Hydrochloric Acid) was added to approximately 3 mg of gelatin MPs and heparin-gelatin MPs in 300 µl of ddH20 and agitated on a tube shaker at 2000 RPM for 4 hours. Free dye was removed by washing the MPs 3x after centrifugation at 6000 RPM for 10 minutes. The precipitant was then dissolved in 1 mL dissolving buffer (1:4 solution of 1 M sodium hydroxide to 95% ethanol) and the resulting solution was read on a spectrophotometer at 595 nm and compared to a set of standards of known heparin concentration.

Collection and analysis of spent media

After formation in AggreWells^{TM}, (Stem Cell Technologies, Vancouver, CA) the EBs were transferred to 100 mm suspension culture dishes and further cultured on a rotary orbital shaker at 40 RPM[54]. Every 48 hours following transfer to rotary culture, the EBs were transferred to 15 mL conical tubes and allowed to sediment to the bottom of the tube. The media was then removed and stored for analysis of growth factor content and fresh medium was added to the EBs and then the solution was transferred back to the culture dish for further culture. At each collection point the EBs were cultured in the media for 48 hours. The spent media was then analyzed using ELISA (R&D Systems, Minneapolis, MN) based assays to determine growth factor concentration. For all samples, ESGRO media supplemented only with penicillin and antimycotic was used both for culture and for standard dilution in the ELISA.

70

The growth factor binding capacity of the MPs was determined for the following growth factors: BMP-4, IGF-II, and VEGF. Lyophilized microparticles (1 mg) were suspended in 0.5 mL of day 9 spent media from untreated EBs. The solution was then allowed to equilibrate with gentle agitation 24 hours at 4°C. After 24 hours the sample was centrifuged at 4000 x g for 5 minutes and the supernatant was sampled for growth factor content analysis using the appropriate ELISA (R&D Systems) for each respective growth factor. A sample of spent media with no MPs was handled in parallel with MP treated samples and was used as the reference point to determine the starting concentration of growth factor.

Gene expression analysis

RNA was extracted from spheroids at various time points for up to 11 days of differentiation with the RNeasy Mini kit (Qiagen Inc, Valencia, CA). Samples to be analyzed using a custom designed PCR array (SA Biosciences, Frederick, MD) were converted to complimentary DNA using the RT^2 First Strand Kit (Qiagen Inc), loaded in the pre-fabricated 96-well array plates and analyzed using real time PCR (MyIQ cycler, BioRad).

For all other gene expression analysis, RNA was converted to complimentary DNA using the iScript cDNA synthesis kit (Bio-Rad, Hercules, CA) and analyzed using real time PCR (MyIQ cycler, BioRad). Forward and reverse primers for Oct-4, MLC-2V, Pax6, AFP, and glyceraldehyde-3-phosphate dehydrogenase (GAPDH) were designed with Beacon Designer software and purchased from Invitrogen. Oct-4 gene expression

71

was calculated with respect to undifferentiated ESC expression levels using the Pfaffl method[171]. Pax6, MLC-2V, and AFP expression in treated samples were normalized to GAPDH expression levels and compared to untreated spheroid expression.

Histology analysis and immunostaining

Spheroids were collected, fixed in 10% formalin, embedded in Histogel (Thermo Scientific), processed and paraffin embedded. Sections of 5 μm in thickness were deparaffinized before staining with hematoxylin and eosin (H&E). Histological samples were imaged using a Nikon 80i upright microscope and a SPOT Flex camera (15.2 64MP Shifting Pixel, Diagnostic Instruments). For whole-mount immunofluorescent staining, spheroids were permeabilized in a 1.5% Triton X-100 BSA solution for 30 minutes, incubated with primary antibody in 2% BSA solution overnight at 4°C, rinsed with PBS and incubated with a secondary antibody for 4 hours. Antibodies and concentrations used were: mouse monoclonal, anti-α-sarcomeric actin (5c5, Sigma, St. Louis, MO) (1:500) with an AlexaFluor 488 conjugated, goat–anti-mouse secondary (Invitrogen) (1:200), and rabbit polyclonal anti-human alpha-fetoprotein (AFP) (Dako, Glostrup, Denmark) (1:200) with a goat–anti-rabbit, FITC-conjugated secondary (Invitrogen) (1:200). Spheroids were counterstained with Hoechst (1:100), washed 3 times in PBS and imaged using a Zeiss LSM 510 confocal microscope (Carl Zeiss Inc.). Sections of 5 μm were stained using Safranin-O (Sigma-Aldrich) for GAG detection, Fast Green (Sigma-Aldrich) for cytoplasm, and Weigert's hematoxylin (Sigma-Aldrich) for cell nuclei and imaged using a brightfield microscope (Nikon Eclipse 80i).

Results

Microparticle fabrication and heparin modification

Heparin was conjugated to gelatin MPs using EDC / S-NHS chemistry at a range of molar ratios (heparin : gelatin) from 1:10 to 10:1. Agitation at high speeds (>1500 RPM) was required to prevent aggregation of the MPs during the heparin conjugation phase presumably because the EDC / S-NHS can also crosslink MPs to other MPs. The amount of heparin that was conjugated to the gelatin MPs was then assayed using a toluidine blue stain, which is a commonly used histological stain to identify GAGs (Figure 4.1A). Heparin content increased with increasing heparin:gelatin ratio from 1:10 (no increase from unmodified gelatin) to 5:1 (5.53 ± 1.3 μg / mg MP). Conjugation performed at a 10:1 ratio of heparin:gelatin did not result in significantly ($p < 0.05$) more heparin present (7.48 ± 1.32 μg / mg MP) compared to 5:1, and therefore a 5:1 conjugation ratio was used for all further analysis. In addition to heparin quantification, the toluidine stain could be visualized using a phase microscope (Figure 4.1B,C). Heparin-gelatin MPs were stained with toluidine blue, while unmodified gelatin MPs treated with toluidine blue demonstrated some low-level background staining on phase images, which necessitated subtracting baseline values of unmodified gelatin MPs from heparin-gelatin values for more accurate heparin quantification analysis in the plate reader assay.

73
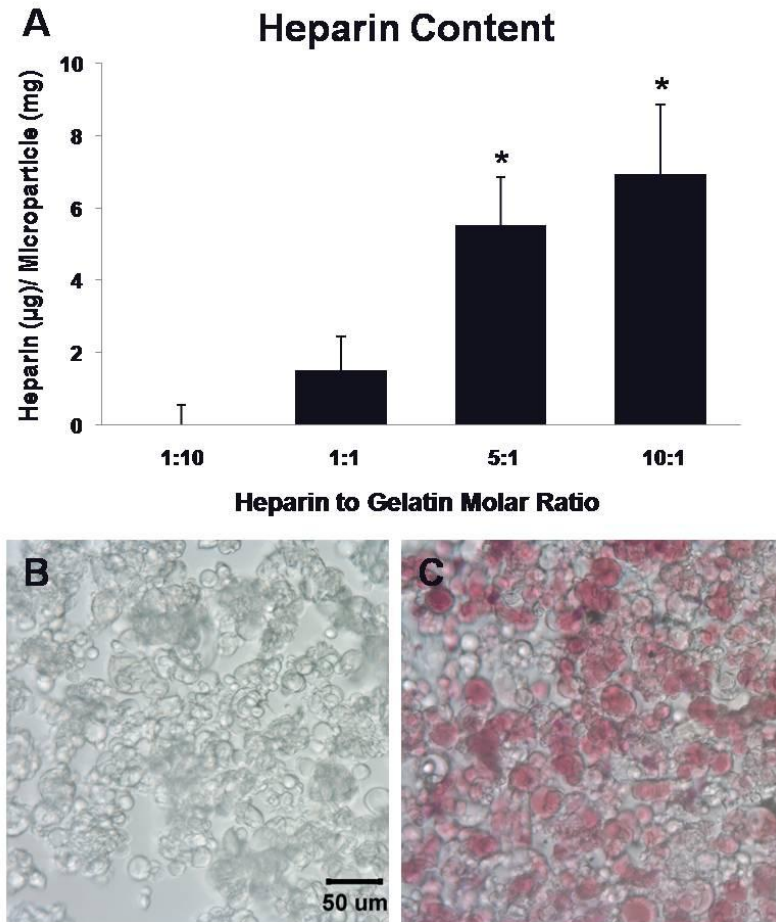
Figure 4.1. Gelatin MPs can be modified with varying amounts of heparin. The molar ratio of heparin to gelatin was varied in the conjugation phase in order to characterize total amount of heparin which could be conjugated to the gelatin MPs (A). Molar ratios of 5:1 and 10:1 (heparin:gelatin) resulted in significantly higher heparin content ($p < 0.05$) compared to both 1:1 and 1:10 molar ratios (n = 3). The heparin content between the 5:1 and 10:1 ratios were not significantly different suggesting 5:1 could be used to obtain heparin content of approximately 4-7 µg heparin per mg of gelatin MPs. The conjugated heparin was evenly distributed across the population of MPs. Both gelatin (B) and heparin-gelatin (C) MPs were treated with toluidine blue in liquid form which forms purple crystals upon reaction with heparin. Gross examination demonstrated a small baseline of color in unmodified gelatin MPs but a noticeably darker stain was observed distributed throughout the heparin modified gelatin MPs. Scale bar = 50 µms.

74

Both gelatin and heparin-gelatin MPs were incorporated within EBs using forced aggregation. In order to visualize the MPs within the aggregates using fluorescent microscopy, amine-reactive AlexaFluor 546^{TM} was conjugated to both groups of MPs. EBs formed within 24 hours in the microwells as reported in chapter 3. After transfer to suspension culture, EBs appeared as previously described and no gross differences were observed in phase images of EBs with gelatin or heparin-gelatin MPs (Figure 4.2). One noted change in the EB culture was that the EBs from all groups grew to a much larger size (~0.5-1mm) in the defined medium compared to medium supplemented with 15% fetal bovine serum.

Analysis of spent media and growth factor binding capacity

EBs are known to secrete BMP-4, IGF-II and VEGF into the surrounding medium as differentiation progresses, therefore the concentration of these three growth factors was assayed in spent medium at days 5, 7, and 9 of culture to begin to assess material effects (Figure 4.3). The detected levels of IGF-II decreased as differentiation progressed in control EBs, while both MP-treated EB conditions remained relatively constant except for heparin-gelatin MP EBs which contained significantly ($p < 0.05$) lower amounts of IGF-II in the medium at day 9. In contrast to IGF-II levels, VEGF was present in increasing levels as differentiation progressed in all samples and was significantly higher in heparin-gelatin MPs compared to untreated EBs at all days assayed. The only significant difference in BMP-4 samples was observed in day 9 spent medium, where levels were below the detectable range (15 pg/mL)

As differences were observed between treatment groups in the amount of secreted protein, it was necessary to confirm the ability of the MPs to sequester the individual growth factors from a complex media. Spent medium was chosen over pure preparations of recombinant factors to characterize the ability of both MP formulations to bind and sequester growth factors for more relevant analysis of binding capacity in presence of other molecules capable of competing for binding (Figure 4.4). Interestingly, though IGF-II levels were decreased in heparin-gelatin MP EB groups, the heparin modified MPs did not sequester any detectable amount of IGF-II,; however, unmodified particles captured approximately 50 pg IGF-II per mg MPs. The amount of VEGF captured from heparin-gelatin MPs was not different compared to unmodified particles. The affinity of BMP-4 for heparin is highest among the growth factors tested, therefore it was expected that heparin modification would result in increased capture of BMP-4 from the spent media compared to unmodified particles. In fact, capture of BMP-4 by heparin-gelatin MPs (15 ng per mg MP) was over 5x higher than that of unmodified MPs.
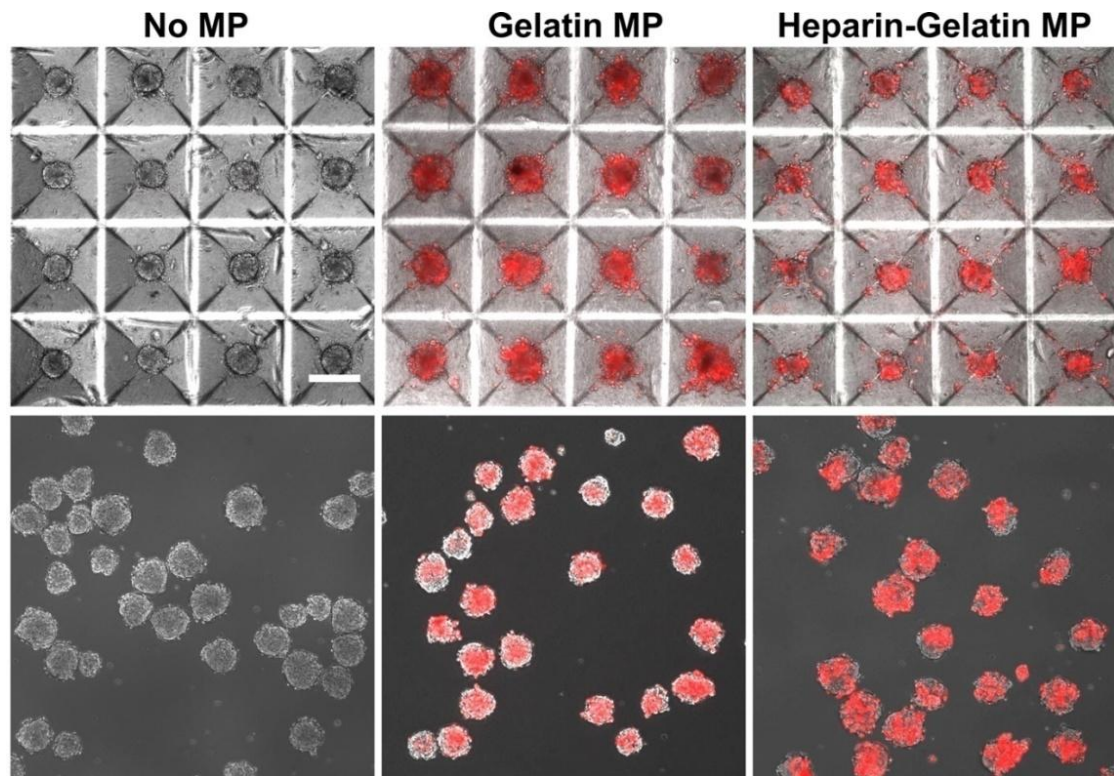
Figure 4.2. Fluorescently labeled MPs are incorporated within EBs using forced aggregation. EBs were formed with 1000 cells per well and MPs were seeded at a ratio of 1:3 cell:MPs. No differences were observed across groups during formation (top row, 24 hours of culture) or after immediately after transfer to suspension culture (bottom row). Scale bar = 200 μm.
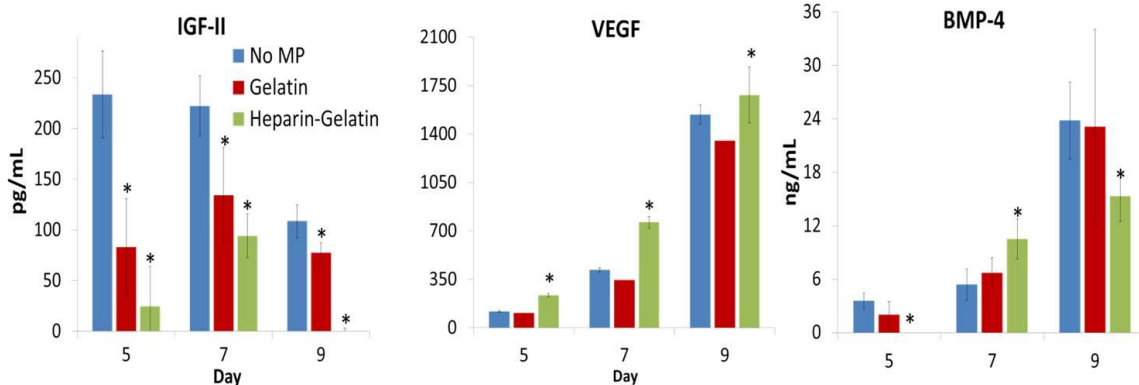
Figure 4.3 Growth factor concentration in spent media. IGF-II concentration decreased with differentiation in all groups and for days 5 and 7, both microparticle groups demonstrated significantly ($p < 0.05$) lower levels than untreated control. On day 9, levels of IGF-II were undetectable in the heparin-gelatin MP group, which was significantly lower than gelatin MP EBs and untreated EBs. BMP4 and VEGF levels increased with differentiation time and heparin-gelatin MPs had higher levels than the other groups. *= Significant difference compared to No MP ($p<0.05$) †=significant difference compared to gelatin MPs ($p<0.05$)
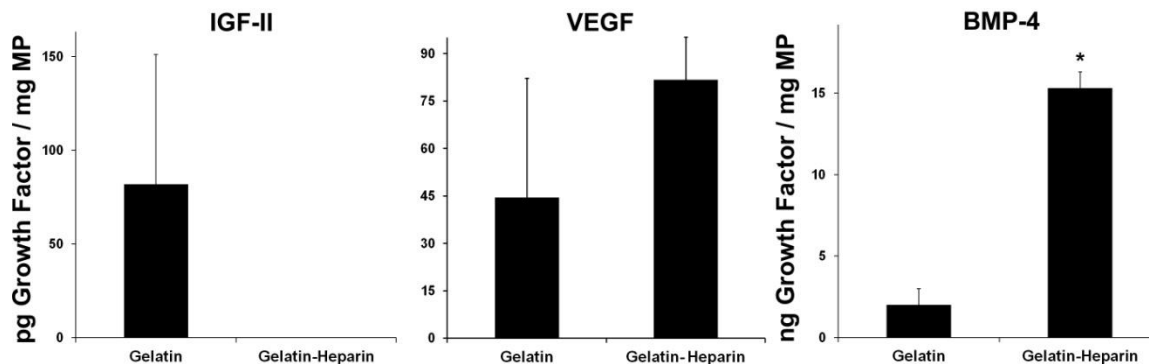
Figure 4.4 Analysis of growth factor content in the medium before and after MP addition. Gelatin MPs were able to sequester ~50 pg/mg IGF-II per mg MPs while the heparin-gelatin MPs did not sequester any detectable amount. The opposite was true with BMP-4, where the heparin-gelatin MPs were able to sequester significantly more growth factor compared to unmodified gelatin. VEGF was captured at similar levels by both types of MPs.

78

<u>Effects of MP incorporation on EB differentiation</u>

Having demonstrated that the gelatin and gelatin-heparin particles are capable of sequestering growth factors produced by EBs and that growth factors are secreted in different concentrations into the surrounding media, the particular effects of MP incorporation on differentiation were first analyzed using a custom PCR array containing 24 genes of interest including markers for pluripotency and for each of the three germ layers (Figures 4.5 and 4.6). Expression of 20 out of the 24 markers was down regulated in both microparticle groups on day 7 of culture. Of the remaining 4 markers, Brachyury-T, Pax6, Flt1 and Sox4, only expression of Pax6 was significantly different ($p < 0.05$) from No MP expression levels. Of the genes significantly decreased, Gata4 (endoderm, -4.94 fold), Nkx 2.5 (cardiac mesoderm, -5.47 fold) and desmin (mesoderm, -6.42 fold) decreased the most in heparin-gelatin treated EBs.

79
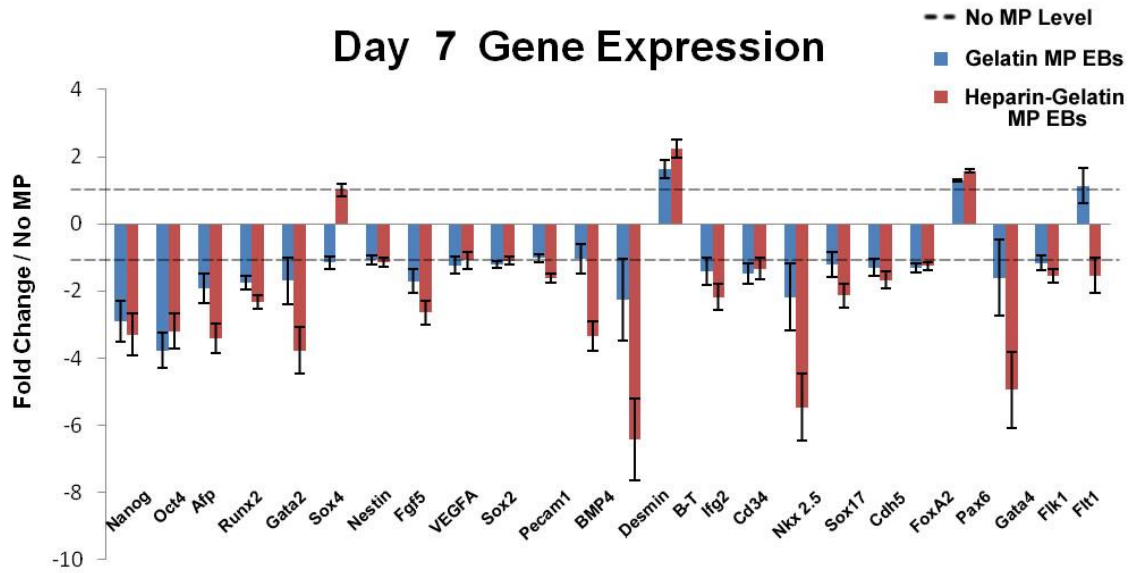
Figure 4.5. Gene expression analysis of day 7 EBs with gelatin and heparin-gelatin MPs normalized to untreated EB expression levels. 20 out of 24 genes analyzed were down regulated in both MP groups compared to untreated EBs.
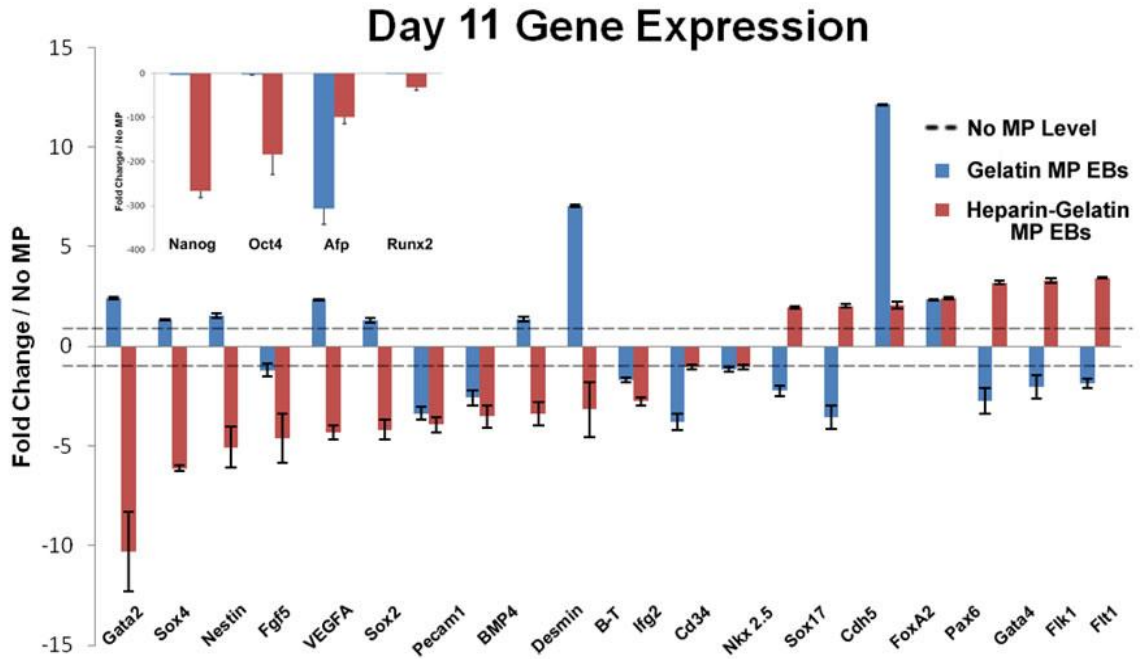
Figure 4.6 Gene expression analysis of day 11 EBs with gelatin and heparin-gelatin MPs normalized to untreated EB expression levels. For heparin-gelatin MP EBs, all but 4 of the 24 genes assayed were significantly altered. Unmodified gelatin MPs had less of an effect both in the magnitude of gene shifts and also the number of significantly affected genes (11 out of 24) (p < 0.05).

Day 11 gene expression data demonstrated increased differences between the treated groups (Figure 4.6). As with day 7 gene expression, a majority of the genes were down regulated in the presence of both types of MPs, and similarly, heparin MP treatment resulted in larger changes compared to unmodified gelatin MP treatment.

Pluripotent marker expression was significantly down-regulated in the presence of heparin MPs (Nanog down 265 fold, Oct4 down 183 fold and sox2 down 4 fold). Several markers showed up-regulation in the presence of heparin including both Flk1 and Flt1, both encoding for receptors of VEGF. This is notable because the amount of VEGF in the medium of heparin-gelatin EBs was also increased, suggesting that the cells were responding to the increased presence of VEGF even though VEGF was down-regulated by almost 5 fold at the gene level in heparin-gelatin MP EBs. Also of interest are genes that were up-regulated in the presence of one type of particle and down-regulated in the presence of the other particle and vice versa. Genes up-regulated in heparin-gelatin MP EBs but not gelatin MP EBs include the VEGF receptors, Gata4, Cdh5 and Sox17. Similarly, genes up-regulated in gelatin MP EBs but not heparin-gelatin MP EBs were Gata2, Sox4, Nestin, VEGFA and Brachyury-T.

EB morphology and safranin-O staining

EB morphology was next examined in paraffin processed 5 µm sections. Morphological differences were observed in Day 11 EBs containing gelatin or heparin-gelatin MPs. (Figure 4.7). For example, the cross-sectional area of EBs with MPs appeared to be larger even though large amounts of MPs were not visible in any single section of a particular EB. The appearance of organized, oval-shaped cell organization,

82

morphologically similar to gut-like structures identified in teratoma assays[204], (Figure 4.7, arrows) was noted in each of the conditions. Untreated EBs contained 1-2 of the gut-like areas, whereas gelatin MP EBs contained 3-5 and heparin-gelatin MP EBs contained 5-15 per EB. The presence of these structures was transient as they were not observed at later time points. Safrinin-O staining was performed to identify areas of proteoglycans and glycosaminoglycans. It was hypothesized that Safranin-O stain would identify regions of heparin; however, areas of positive stain were observed in all groups possibly indicative of heparan sulfate which is expressed on the cell surface.
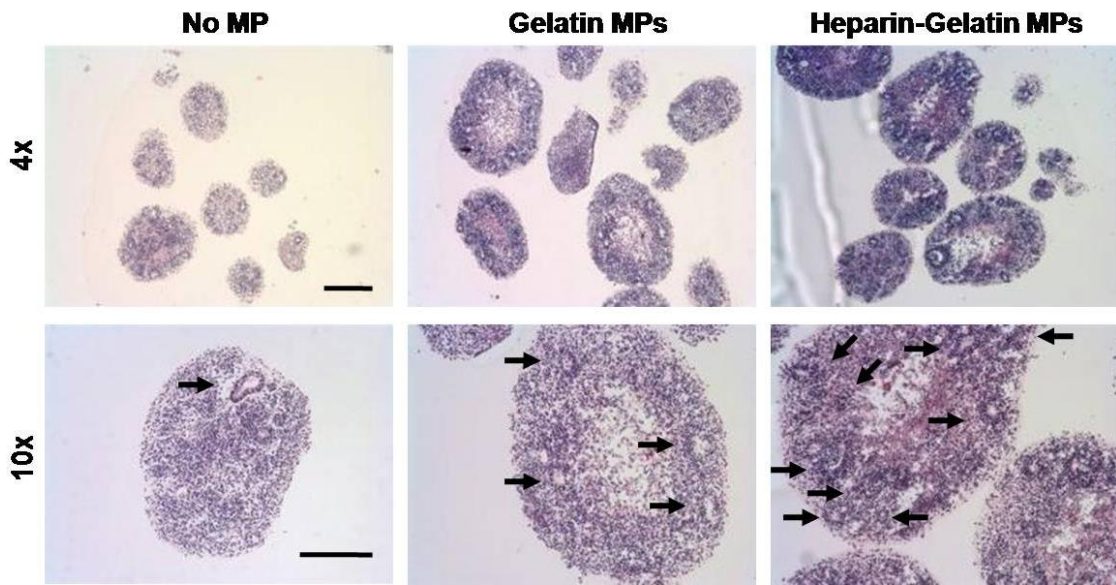
Figure 4.7. MP incorporation results in distinct morphological differences in EB structure. H&E staining of day 11 EBs revealed the presence of organized structures resembling the formation of gut like structures identified in teratoma assays[204]. The oval-shaped structures (indicated by arrows in 10x images) contained an outer cell layer of organized cells with void space in the center. Scale bars = 250 μms.
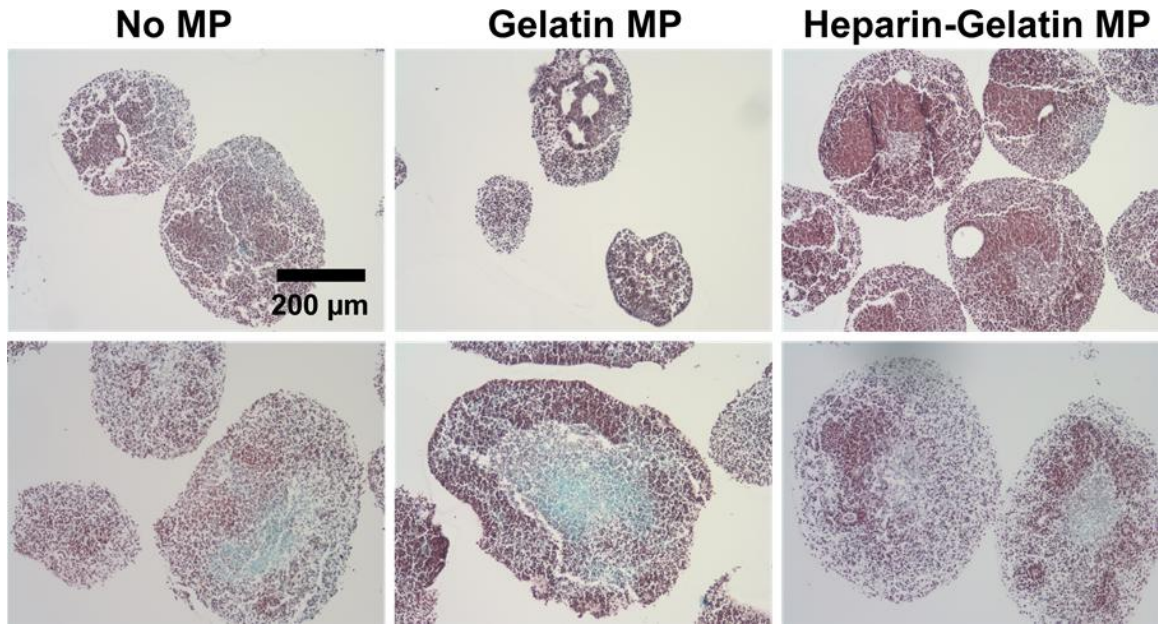
Figure 4.8. Safranin-O stain of day 7 and 11 EBs. Safranin-O stain was performed to identify areas of proteoglycans and glycosaminoglycans. It was hypothesized that Safranin-O stain would identify regions of heparin; however, areas of positive stain were observed in all groups possibly indicative of heparan sulfate which is expressed on the cell surface.

VE-Cadherin Localization

Immunostaining of vascular endothelial cadherin (VE-cadherin) was next performed to investigate the effects of MPs on spatial patterning of differentiation. VE-cadherin is expressed on the surface of endothelial cells at an early stage of differentiation[205] and is encoded by the cadherin-5 (cdh5) gene which was significantly up-regulated at day 11 (2 fold) compared to untreated EBs at day 11 of differentiation. Additionally, because VEGF is used as a supplement in endothelial differentiation protocols and both VEGF receptor gene expression and VEGF content in spent media were increased in heparin-gelatin MP samples, VE-cadherin expression was investigated. Positive VE-cadherin staining was observed in all three groups at days 7 and 11 of culture. In day 7 samples, both heparin-gelatin MP EBs and EBs without MPs

84

displayed greater amounts of positive VE-cadherin expression than EBs with gelatin MPs. Interestingly, VE-cadherin expression was observed in the area directly adjacent to the heparin-gelatin MPs (Figure 4.9). This phenomenon was not observed in the EBs containing unmodified gelatin MPs or in heparin-gelatin MPs at day 11 (Figure 4.10), indicating that the positive stain was not an artifact due to antibody interaction with the gelatin or with the heparin. Immunostaining of day 11 revealed that the organization of positive staining was no longer related to the MPs, even in the case of the heparin-gelatin MPs. This may suggest that the heparin specific effects have been attenuated by day 11 possibly due to degradation of the particles or redistribution or degradation of the heparin.
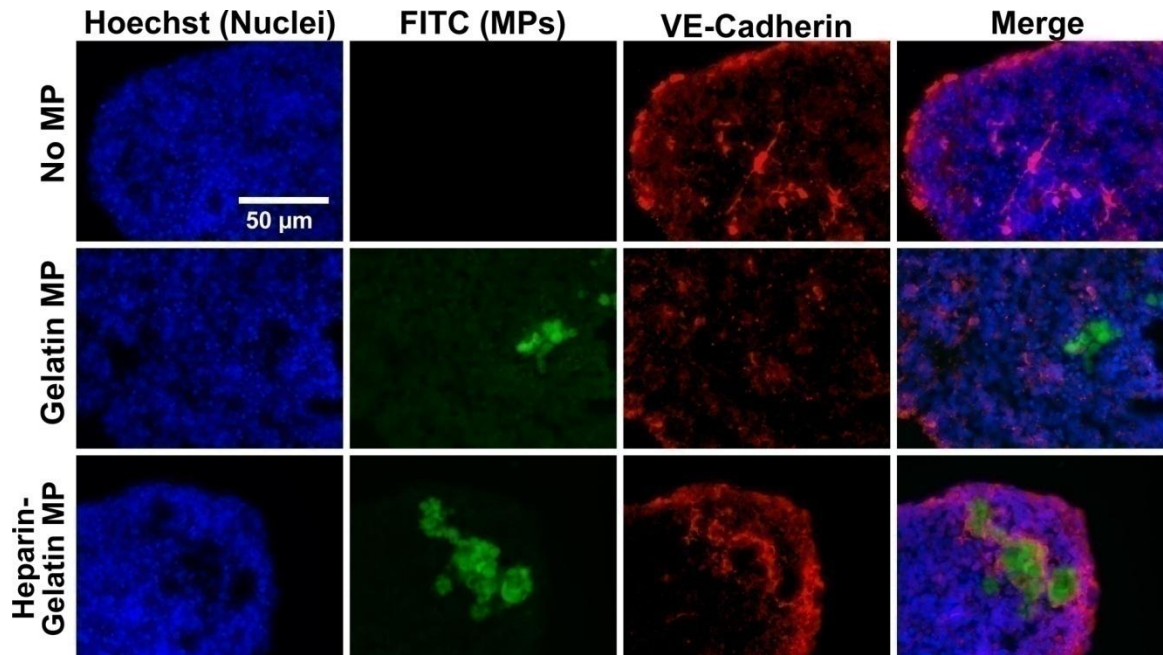
Figure 4.9 VE-Cadherin immunostaining of day 7 EBs. Immunostaining for VE-cadherin was performed on day 7 EBs. Positive expression was observed in each of the samples analyzed. Differences in the samples were noted in the special localization of VE-cadherin signaling in that almost uniformly, positive signal was immediately adjacent to heparin modified MPs but not in unmodified MPs. Scale bar = 50 μm.

86
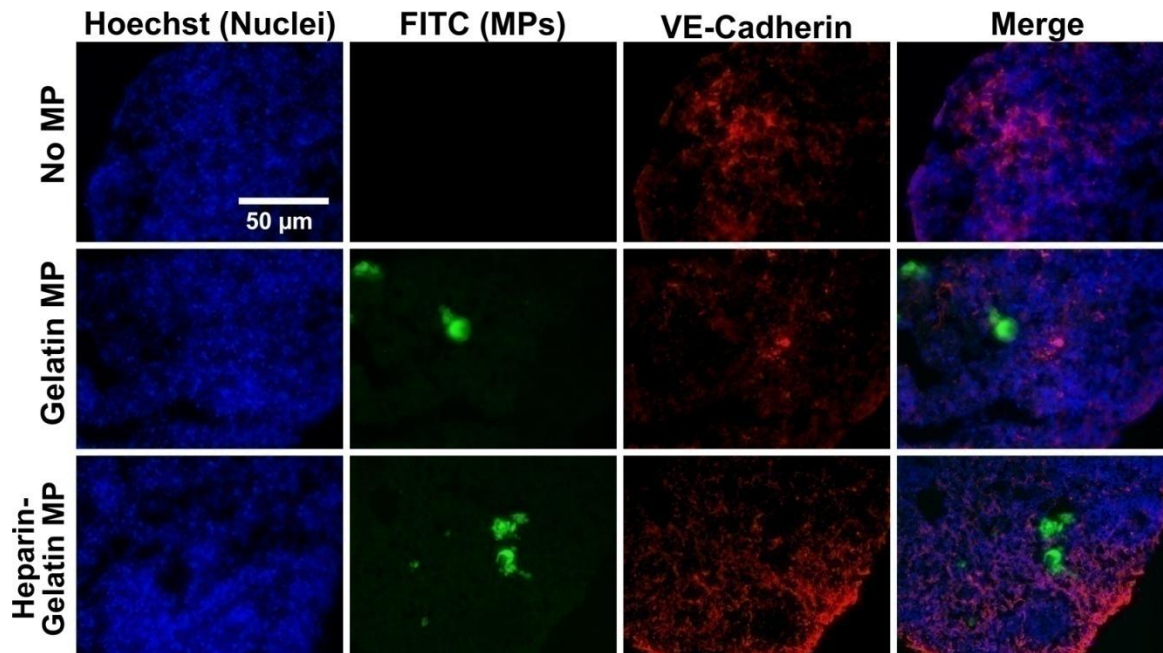
Figure 4.10 VE-Cadherin immunostaining of day 11 EBs. Positive expression was observed in each of the samples analyzed. Though the spatial patterning observed in day 7 samples was not observed in day 11 samples, positive expression was increased compared to day 7. Scale bar = 50 µm.

87

Discussion

The data presented here demonstrate that incorporation of heparin-modified gelatin MPs alters growth factor production and patterns of differentiation within EBs. Previous studies investigating the effect of microparticle incorporation within EBs used a medium supplemented with 15% fetal bovine serum[155, 161, 201]. The study in this chapter was the first to use a defined medium with no serum to incorporate biomaterials within EBs. Serum is an undefined mixture of proteins and growth factors but is known to contain BMPs which can promote mesoderm and endoderm differentiation and inhibit ectoderm differentiation. This was confirmed at the gene level where EBs cultured in defined medium expressed higher levels of Pax-6, a marker for ectoderm, compared to EBs in serum which never expressed Pax-6 at levels higher than ESCs, suggesting ectoderm differentiation was inhibited[201]. The basal media is designed to allow spontaneous differentiation to occur with a minimal level of signals which could influence differentiation. A low baseline of environment may be a better suited for investigation of material specific effects, which otherwise could be overwhelmed by soluble signals from serum. The addition of basic fibroblast growth factor (bFGF) to ESC media can be used to direct ESCs towards an ectoderm phenotype[15, 42, 67, 75]. Spent media in this study were analyzed for bFGF secretion, but no significant levels were detected (data not shown). It is still possible that heparin-gelatin MPs are capturing, concentrating or enhancing the local signaling of even small amounts of bFGF that are secreted due to the known ability of heparin to bind bFGF[206] Concentration of growth factor signaling may even be enhanced in part because the EBs were cultured under

88

hydrodynamic conditions where factors otherwise washed away into the surrounding medium could be locally retained by their affinity to the heparin on the gelatin MPs.

Changes in growth factor concentration in spent media do not necessarily indicate that the MPs were able to capture growth factor within the EB. Other factors can affect secreted growth factor content such as the state of differentiation of the cells as indicated by changes in the growth factor secretion profile with differentiation time in EBs which do not contain MPs. Analysis of the amount of growth factor within EBs would be helpful in combination with growth factor content in the spent media. Western blot analysis is required of EB lysates to determine the amount of growth factor retained.

Gene expression profiling of EBs cultured with or without incorporated MPs revealed that MP incorporation decreased a wide variety of genes associated with early lineage differentiation. Taken alone, the low expression levels of differentiated markers could suggest that the presence of particles inhibits differentiation; however, out of all the genes analyzed, the ones most decreased were Nanog, Sox2 and Oct4, genes expressed in undifferentiated cells. Additionally, the increased secretion of VEGF along with decreased secretion of IGF-2 as culture time progressed is consistent with what has been observed in differentiating EBs cultured in serum media [Ngangan et al. unpublished data]. Therefore, it is likely that the kinetics of differentiation are not suppressed, but altered in the presence of materials, especially with heparin-gelatin MPs. Further characterization of global gene expression by EBs with and without MPs would likely yield insights to the overall profile of differentiation.

Overall, the data presented for IGF-II may seem contradictory. IGF-II levels in the spent media of heparin-gelatin MP EBs was below the assay detection limits, yet

89

heparin-gelatin MPs did not demonstrate the ability to sequester any significant amount of IGF-II from spent media in the absence of EBs. Unmodified gelatin MPs were able to capture measurable amounts of IGF-II suggesting that the heparin conjugation not only does not promote capture of IGF-II from spent media, but may prevent passive absorption observed in the unmodified MPs. Altered levels of IGF-II secretion could be attributed either to altered differentiation in which cells responsible for IGF-II secretion were absent when treated with heparin-gel MPs, or the heparin on the MPs is not directly interacting with IGF-II, but instead with IGF binding proteins (IGFBPs)[207]. IGFBP-3,5,6 are known to contain a heparin binding sequence (B-B-B-X-X-B, where B is a basic residue[208]) and serve to regulate IGF protein interactions both with the extracellular matrix and with heparin-sulfate molecules on the cell surface. Indirect interactions of the heparin with proteins responsible for regulating growth factor signaling should also be considered in a holistic model of MP microenvironemental effects.

The spatial localization of VE-cadherin at day 7 indicated that the heparin-gelatin MPs can have local effects on the microenvironment which promote endothelial differentiation. Because gene expression is a population based assay, localized effects of the particles could be diluted out by the cells not in the local vicinity of the MPs. Further characterization of the phenotype of cells in direct contact with heparin-gelatin MPs may further elucidate the effects of heparin incorporation on differentiation. The spatial patterning of VE-cadherin was transient and not observed in day 11 samples. Analysis of the degradation of fluorescently-labeled gelatin MPs in chapter 3 demonstrated that the particles are degraded and are not detected after 14 days of culture in the case of 1:3 cell:MP seeding ratio, the same ratio used in this study. As the particles are degraded and

90

remodeled, the spatial organization of the heparin will also be degraded which could explain the loss of spatial organization at later time points. Maintenance of spatial control could be possible if the heparin molecule were instead conjugated to the surface of a non-degradable material such as agarose.

Conclusions

Molecular engineering of the MP surface can be performed by heparin conjugation to modulate interactions between the MPs and the microenvironment. Heparin modification resulted in differences in the amount of growth factors secreted by EBs into the surrounding medium and also altered the ability of the gelatin MPs to capture growth factors from EB spent medium. Gene expression analysis as well as VE-cadherin staining indicated that the addition of heparin to the gelatin MPs increased modulation of differentiation observed with unmodified gelatin MPs. Interestingly, VE-cadherin expression was localized to the area in the immediate vicinity of the heparin MPs suggesting alterations in the local microenvironment cause by heparin addition. The results of this study suggest that MPs can be used to introduce engineered extracelullar matrices to direct endogenous growth factor signaling. MPs capable of controlled interactions with endogenous growth factors could be used to locally direct differentiation within EBs or possibly to remove the need for exogenous delivery of growth factors to cell culture medium for directed differentiation protocols.

91

CHAPTER 5

EXOGENOUS GROWTH FACTOR DELIVERY FROM GELATIN MICROPARTICLES

Introduction

Pluripotent stem cells are a unique in their ability to differentiate to any cell type in the body. This plasticity, along with their theoretically infinite capacity for self-renewal, makes them an ideal source for therapeutic cell types. Their plasticity is also the major impediment to their use because efficient differentiation towards homogeneous populations of mature cell types is difficult. The difficulty is due, in part, to the sensitivity of the cells to their microenvironment where small perturbations in soluble signals along with cell-cell and cell-extracellular matrix interactions can provide cues for differentiation. This is especially relevant to the differentiation of ESCs as embryoid bodies (EBs) which are aggregates grown in suspension. The microenvironment of cells in the EB is complex and constantly changing as cells differentiate and produce autocrine and paracrine factors.

Soluble factors are commonly added to the surrounding medium of EBs in an attempt to promote lineage specific differentiation[150]. This method is limited by barriers to free diffusion of molecules which exist in EBs. These barriers are intensified with culture time as cell-cell contacts mature with outer-layer endoderm formation and also as cell produce their own ECM[78, 155]. Recently, incorporation of biomaterial microparticles (MPs) has been reported as a possible method to circumvent barriers to access of the interior microenvironment[150, 155, 156, 161, 201]. Poly(lactic-co-

92

glycolic acid) (PLGA) MPs loaded with growth factors or with retinoic acid have been used in an attempt to direct differentiation within EBs. Retinoic acid delivery from PLGA MPs in mouse EBs resulted in the formation of an epiblast-like aggregate which was comprised of two layers of well-organized cells, with OCT-4 positive cells found on the inner layer and FoxA2 positive cells lining the outside of the structure[155]. The effects could not be reproduced by soluble addition of retinoic acid at any of a wide range of concentrations, suggesting that the spatio-temporal control of morphogen delivery using MPs incorporated within the extracellular space may yield yet unknown insights to stem cell biology and may be useful for directed differentiation and tissue engineering applications.

Disadvantages exist to the use of PLGA MPs for growth factor encapsulation including low incorporation efficiency, batch to batch variability and decreased bioactivity[162, 163]. Therefore, a forced aggregation method of EB formation was adapted to allow for controlled incorporation of hydrogel MPs within EBs. Hydrogels are advantageous for growth factor delivery in part because bioactivity can be preserved during the loading phase by soaking of lyophilized MPs within a concentrated growth factor solution[209]. Gelatin has been used for growth factor delivery of molecules such as basic fibroblast growth factor (bFGF), bone morphogenetic proteins (BMPs) and vascular endothelial growth factor (VEGF)[165, 209]

Gelatin can be manufactured with differing properties depending on the method in which it is isolated. Type A gelatin is produced using acid curing of connective tissue which results in a gelatin material which has an isoelectric point between 7 and 9 with a net positive charge, whereas gelatin type B is produced from lime cured tissue and has an

93

isoelectric point ~5.6 making it net negatively charged. The isoelectric point of the protein to be delivered and the effects of polyion complexation should be taken into consideration when choosing the type of gelatin for MP fabrication[210].

Previously the effects of unloaded MPs on ESC differentiation were investigated and the goal of this study was to utilize gelatin MPs for delivery of BMP4, a growth factor known to induce mesoderm differentiation in ESCs[195, 197] and a BMP4 agonist, Noggin[211]. Growth factor release profiles were first characterized from gelatin MPs. Then the differentiation effects of incorporation of growth factor loaded MPs within EBs were investigated by gene expression and morphological analysis of adherent and suspension cultured EBs.

Materials and methods

Cell culture

Brachyury-GFP cells (E14.1, 129/Ola)[212] were maintained on 0.5 % gelatin coated flasks in a humidified 5 % CO_2 atmosphere, using the modified serum-free maintenance media and base differentiation media previously described[199]. Undifferentiated D3 ESCs were maintained on gelatin-coated tissue culture dishes in DMEM media supplemented with 15% fetal bovine serum and 10^3 U/ml leukemia inhibitory factor (LIF) (Millipore, Billerica, MA).

Aggregate formation

ESCs were trypsinized into a single cell suspension and aggregates were formed by forced aggregation in AggreWell^{TM} 400 inserts (Stem Cell Technologies, Vancouver,

94

CA)[49].   Briefly, 1.2 x 10^6 cells in 0.5 mL of medium were inoculated into AggreWell^{TM} inserts, containing approximately 1200 wells per insert, and centrifuged at 200 x g for 5 minutes to cluster cells in the wells.   For EB culture, the media was switched to ESGRO complete basal media (Millipore) supplemented only with penicillin and antimycotic.   After 24 hours of culture, cell aggregates were removed from the wells using a wide-bore pipette and transferred to suspension culture on a rotary orbital shaker (40 RPM) to maintain the homogeneity of the population.   In order to investigate material incorporation, a second centrifugation of 200 µL of a MP solution at 200 x g for 5 minutes was performed immediately after cell centrifugation.   In all cases the MP:cell seed ratio used was 1:3.

Fabrication and loading of gelatin microparticles

Microparticles of type A (G1890) or B (G9391, Sigma) gelatin were generated using a water-in-oil emulsion method and fluorescently labeled as previously described[201].   Expected electrostatic interactions between the gelatin types and proteins were examined using ExPASy's Compute pI/MWprogram (www.phosphosite.org/psrSearchAction.do)[213, 214].   Heparin sodium salt (CalBiochem, San Diego, CA) was conjugated to gelatin type A MPs after MP formulation in the following manner.   EDC and S-NHS (Thermo Scientific, Waltham, MA) were added to heparin at 10:1 and 25:1 molar ratios respectively, relative to heparin dissolved in 800 µL activation buffer (0.1M MES, 0.5M NaCl, pH 6.0) and reacted for 15 min at room temperature to modify the carboxyl groups of heparin to amine reactive S-NHS esters.   The EDC/NHS reaction was quenched with 20 mM 2-mercaptoethanol

95

and the activated heparin was added to 400 µL of particles in PBS at a 5:1 molar ratio of heparin to gelatin and allowed to react with agitation for 4 hours at 37 C. Prior to cell culture, MPs were treated in 70 % ethanol for a minimum of 30 min before washing 3x with ddH$_2$O. Each MP batch was lyophilized and stored at -20 C. Growth factors were added to MPs at 5 µL/mg and kept overnight at 4 C, MPs were resuspended in differentiation media ($\leq$ 500 µL) and counted on a hemocytometer to estimate the concentration (ng/MP).

Human BMP4 ELISA

A quantitative sandwich enzyme immunoassay technique was used to determine BMP4 concentration after release from MPs suspended in PBS, based on the manufacturer's protocol (R&D, DBP400). Briefly, 2-5 mg of MPs were suspended in 750 µL of a 0.1% solution of BSA in PBS at 37°C with rotation; at each sample time point 300 µL was removed following centrifugation of the microparticles and replaced with an equivalent volume.

Gene expression analysis

RNA was extracted from spheroids after 4 days of differentiation with the RNeasy Mini kit (Qiagen Inc, Valencia, CA). RNA was converted to complimentary DNA using the iScript cDNA synthesis kit (Bio-Rad, Hercules, CA) and analyzed using real time PCR (MyIQ cycler, BioRad). Forward and reverse primers for Oct-4, Brachyury-T, Pax6, Flk1, and glyceraldehyde-3-phosphate dehydrogenase (GAPDH) were designed with Beacon Designer software and purchased from Invitrogen. Gene expression was

calculated with respect to expression levels of EBs without MPs using the Pfaffl method[171].

Statistical Analysis

Unless otherwise indicated, data are reported as mean ± standard deviation of the mean. Statistical significance was assessed using one-way ANOVA with Tukey's post hoc analysis or student's t-test. P-values of less than 0.05 were considered significant ($n \geq 3$).

Results

Growth factor release from gelatin-based microparticles

Growth factor release kinetics from gelatin MPs were analyzed for VEGF (Figure 5.1). The release of VEGF displayed a burst phase in the first 24 hours where the majority of the VEGF was released from gelatin type B MPs. Gelatin type B was chosen for VEGF because the isoelectric point of VEGF is 9.22 indicating that VEGF has a net positive charge. Because VEGF has known affinity for heparin, heparin-modified gelatin type B MPs were also tested for release of VEGF in an attempt to limit burst release. The amount of VEGF released by the heparin-gelatin MPs was decreased in the burst phase; however, less VEGF was released over the entire time studied as well.

97
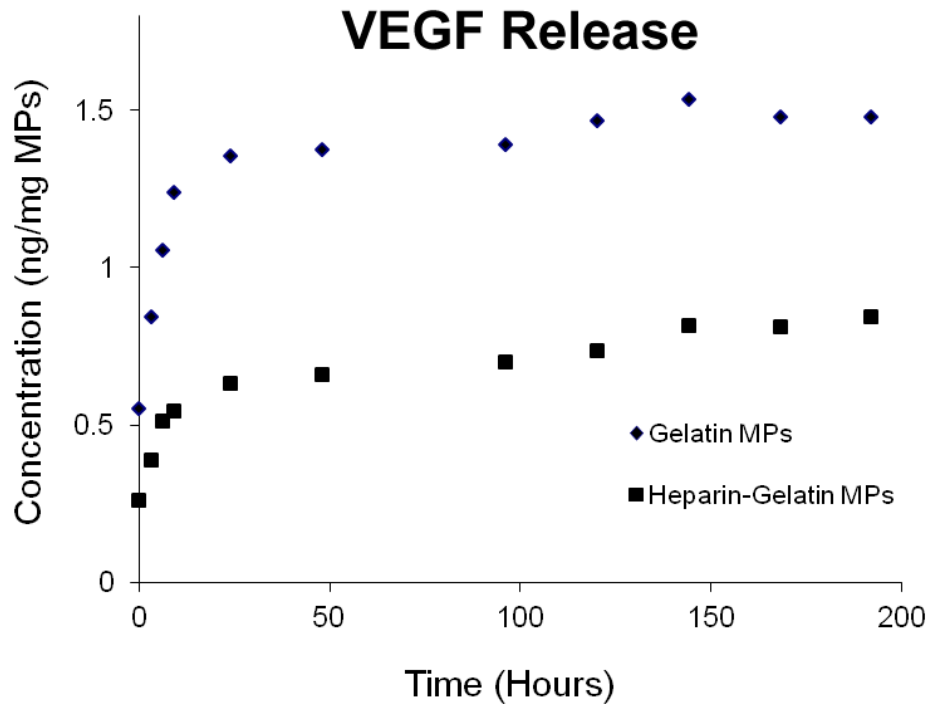
Figure 5.1 VEGF release from gelatin and heparin-gelatin MPs. VEGF release profiles appeared similar from both type of MP except unmodified gelatin MPs released a higher percentage of VEGF and released stopped after 24 hours compared to heparin-gelatin MPs which continued to release VEGF for several days.

BMP-4 release kinetics

BMP-4 release kinetics were next investigated from both gelatin type A and B. BMP-4 has a lower isoelectric point (8.97) compared to VEGF; therefore the positive formulation of gelatin (type A) was included. Release results from type A gelatin MPs revealed that almost 100% of the loaded BMP-4 is released by the particles after 24 hours. This is explained by the fact that gelatin type A and BMP-4 are both positively charged, meaning they lack electrostatic interactions to slow the release from the particles. Type A MPs were then modified with heparin in an attempt to increase the affinity of the MPs for BMP-4 and slow release. BMP-4 release from heparin-type A gelatin MPs was then analyzed along with release from unmodified gelatin type B MPs under various growth factor loading conditions. Heparin modification of gelatin type A

98

MPs resulted in decreased release of the BMP-4 molecule, whereas nearly all was released by type A MPs, only 40-70% of the incorporated BMP-4 was released by heparin-modified type A and gelatin type B MPs. Release from heparin-type A MPs and type B gelatin MPs was similar and individual replicates overlapped between groups. It was observed that a greater percentage of the loaded BMP-4 was released when more BMP-4 was loaded into the MPs. This suggests that there is a threshold level of BMP-4 which remains entrapped within the particle and that significant release of this portion of BMP-4 is not detected after 6 hours. When excess BMP-4 is loaded beyond this threshold, the time period of release is extended as demonstrated in the group loaded with a 25 µg/mL concentration of BMP-4.
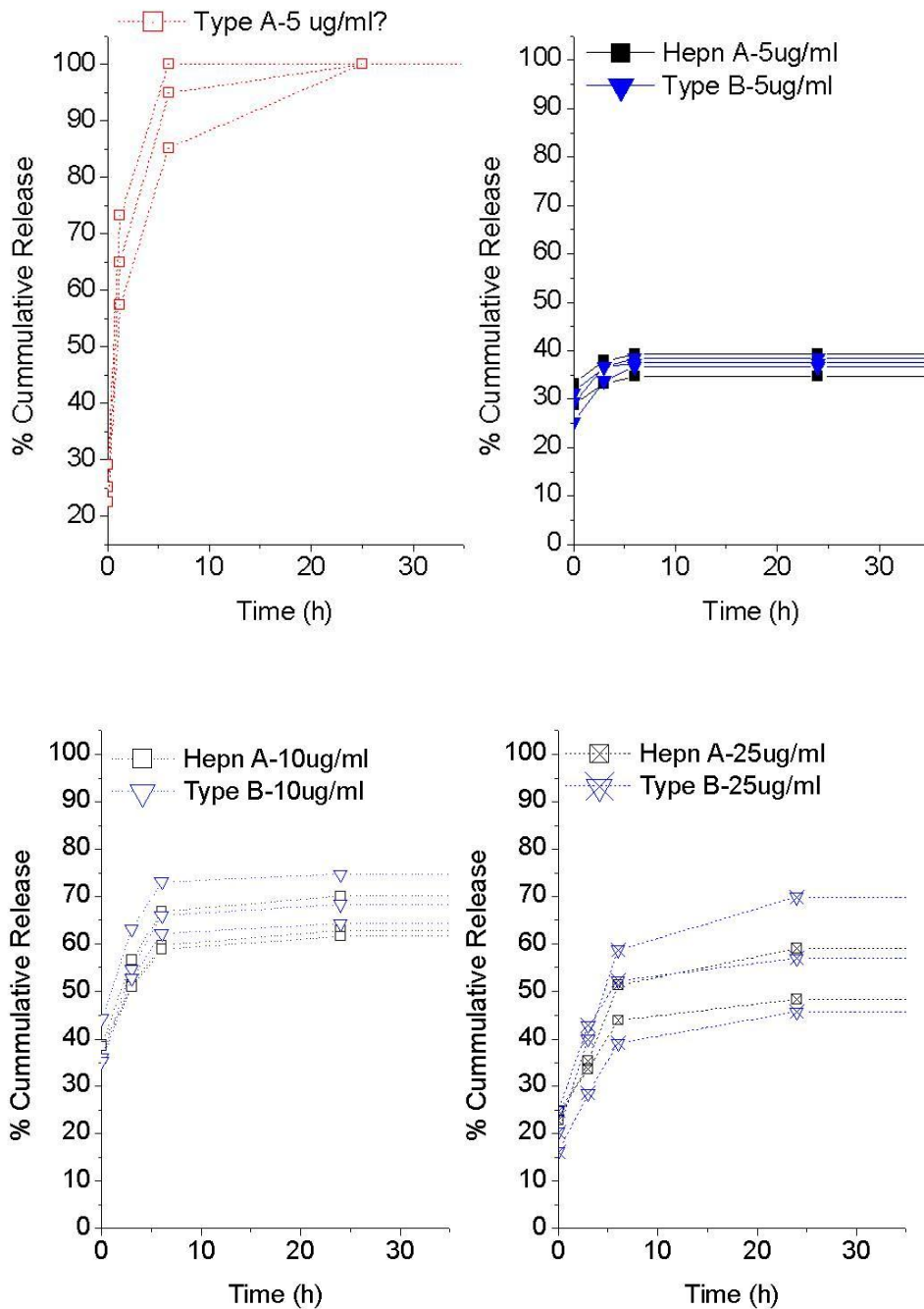
Figure 5.2 BMP-4 release from gelatin MPs. Analysis of BMP-4 release from various formulations of gelatin including type A, type B and also type A with heparin modification demonstrated that BMP-4 release was dependent on both the concentration of growth factor used when loading the MPs and also the affinity of the MP material for BMP-4. Each replicate was plotted as an individual point for each group analyzed.

100

<u>Fluorescently labeled BSA release within EBs</u>

Bovine serum albumin was first fluorescently labeled with AlexaFluor 488 and then incorporated within gelatin type B MPs for the purposes of visualization of molecule release within EBs. After EB formation the particles could be identified within the EBs using fluorescent microscopy. As culture time progressed, the fluorescent signature became more diffuse indicating the tagged BSA was being released from the particles. Release occurred over a period of 4-6 days and by day 7 no areas of punctuate fluorescence were identified in EBs. Fluorescent signal from the BSA could be distinguished from gelatin auto fluorescence by limiting exposure time to less than 30ms at which point unlabeled gelatin particles were no longer visible.
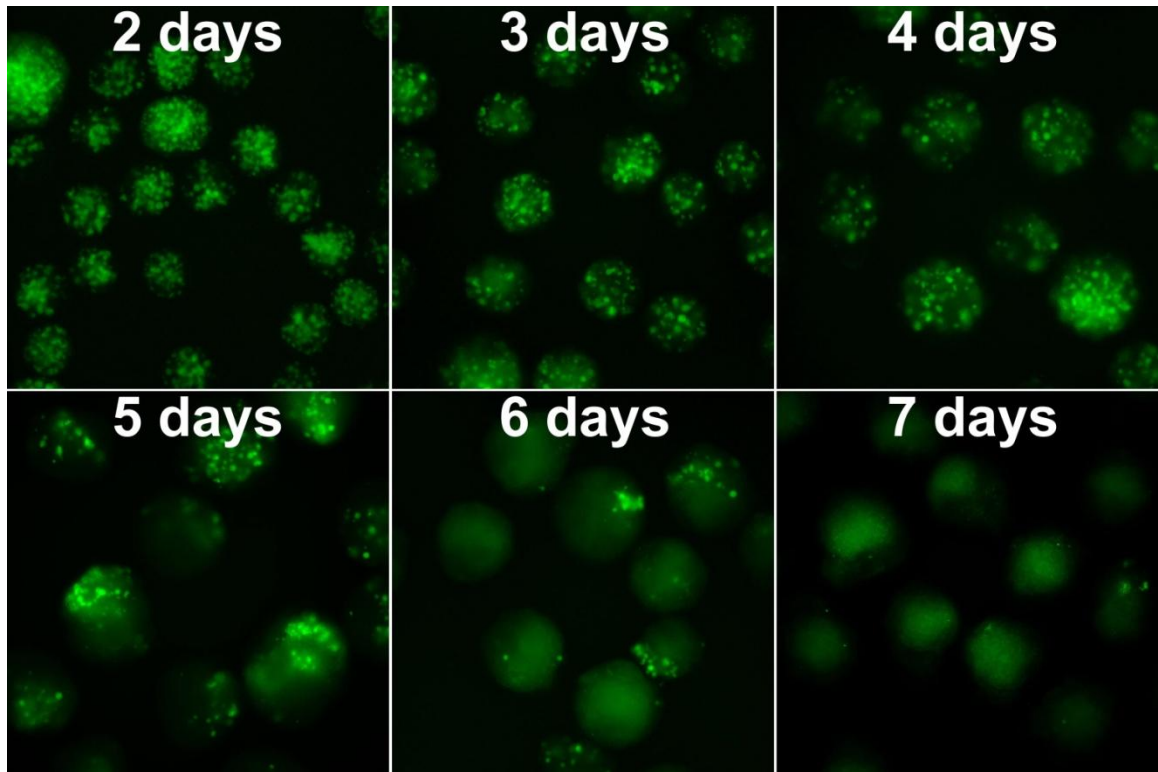
Figure 5.3. BSA release from gelatin microparticles. BSA fluorescently labeled with Alexa488 was incorporated within gelatin microparticles and then loaded within EBs. The fluorescence was punctuate at early time points (2-4 days) and gradually was replaced by a diffuse fluorescence indicating that BSA was released from the MPs within EBs for a period of 4-6 days.

<u>Brachyury-T expression</u>

R1 ESCs genetically engineered to express green fluorescent protein (GFP) on the Brachyury-T promoter were used to investigate induction of mesoderm differentiation either with BMP-4 delivered solubly to the media or delivered from MPs. GFP signal peaked day 4 of differentiation in BMP4 treated samples. At day 4 EBs were fixed and counterstained with Hoechst, a nuclear dye, and then imaged using a confocal microscope (Figure 5.4). Heparin-gelatin MPs were included in the experiment because it was hypothesized that affinity of BMP-4 for heparin would maintain a higher local concentration of BMP-4 immediately surrounding the MPs and therefore direct mesoderm differentiation only in the direct vicinity of the MPs. The data did not support this hypothesis as no spatial patterns were observed in BMP-4 MP EBs. BMP4 treated samples appeared similar but expression varied greatly from EB to EB. Noggin treated EBs (soluble and both types of MPs) demonstrated a similar level of GFP expression.

Brachyury-T expression was then quantified by flow cytometry measuring GFP positive cells in day 3 and 4 EBs. On day 3, expression was limited to 5% in any of the groups, with the exception of the BMP MP group in which an average of 17% of cells were GFP positive (Figure 5.6A). Day 4 expression increased in each of the groups, and it was revealed that Noggin treatment did not suppress Brachyury-T signaling compared to the untreated EB controls.

103
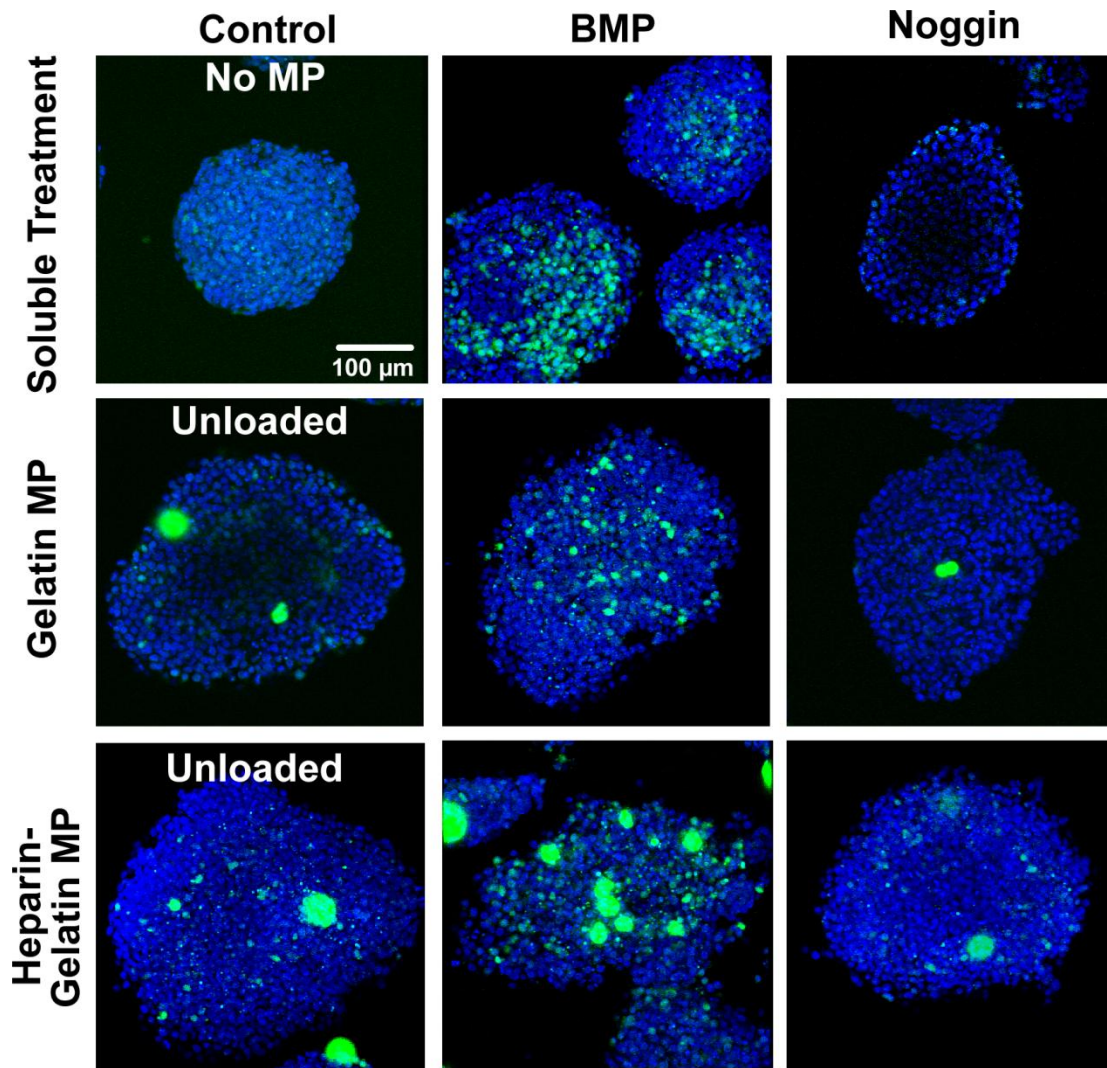
Figure 5.4 Brachyury expression of EBs at day 4 of culture. Brachyury-T expression was visualized by analysis of GFP signal. Very few GFP positive cells were observed in control EBs (no treatment or unloaded MPs) or in Noggin treated samples. The highest GFP signal was observed in EBs treated with soluble BMP-4; however, positive expression was also recorded in both BMP-4 MP treatment groups.

It was hypothesized that local presentation of growth factor would be more efficient compared to bulk, soluble delivery in directing differentiation. Because the relative levels of Brachyury-T positive cells were similar with MP delivery and soluble delivery, the total amount of growth factor used in each case is of interest. In the case of soluble delivery, BMP4 was added to the medium at a concentration of 10 ng/mL first during EB formation in the microwells, then to the medium after 24 hours of culture when EBs were transferred to suspension and then again at day 3 prior to analysis of differentiation at day 4 of culture. The total amount of BMP-4 added soluble was therefore 210 ng. In the case of MP based delivery, 125 ng of BMP-4 was added to each mg of MPs during loading. Each mg of MPs equates to approximately 3 million individual MPs. For each well of EBs formed 400k MPs (0.133 mg) were added. The amount of BMP4 originally loaded in this amount of MPs was 16.67ng. Therefore, the amount of BMP-4 delivered via MPs was 12 fold lower than the amount delivered by traditional soluble application.
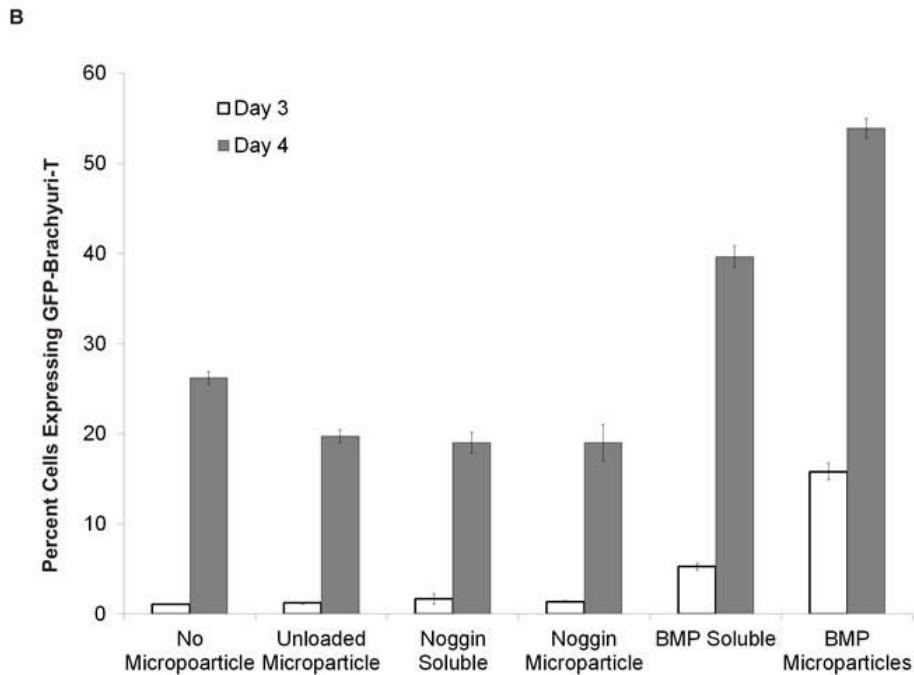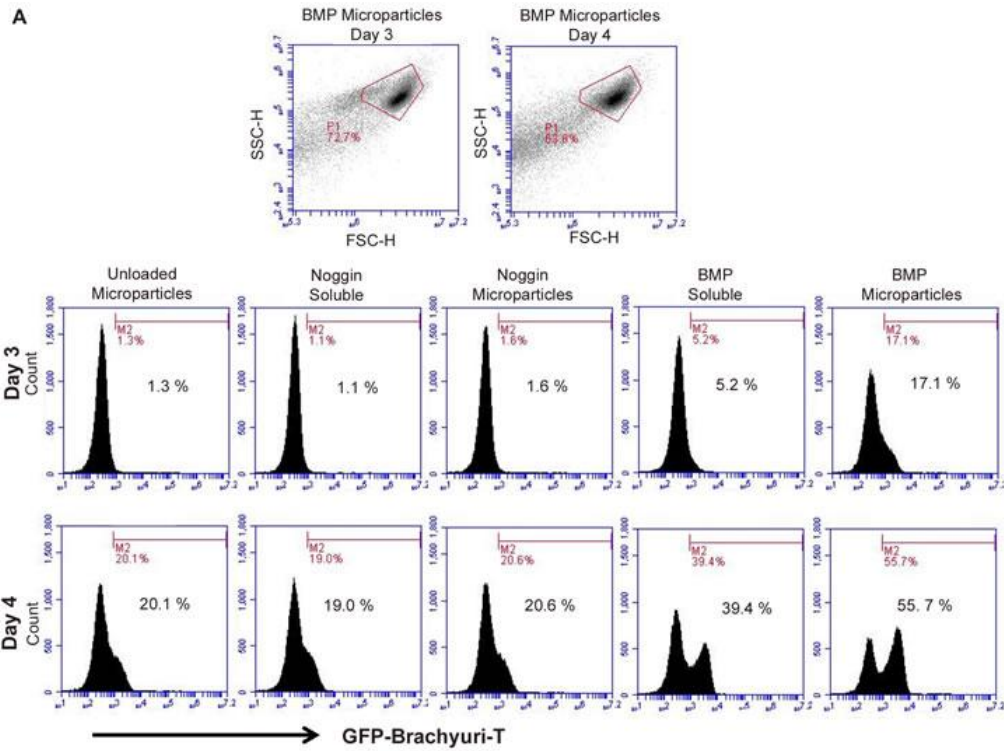
Figure 5.5 Quantification of Brachyury-T positive cells in day 3 and 4 EBs. Flow cytometry was performed on day 3 and 4 EBs and analyzed for GFP expression. Day 3 samples had low positive expression (<5%) except for BMP MP treated EB in which 17% of the cells were positive. At day 4, expression increased in all groups, up to a baseline level of 20% in untreated and noggin treated samples and 40% and 55% in BMP soluble and MP groups, respectively.

<u>Microparticle dose response</u>

Growth factor loading experiments demonstrated that release kinetics and the total amount of growth factor released can be modulated by the concentration of growth factor used to load the MPs. In order to identify whether or not this translated into dose responses in differentiation, gelatin MPs were loaded with 10 and 25 µg/mL solutions of BMP-4 and Noggin. This corresponded to addition of 50 and 125 ng of growth factor per mg of MPs. After loading, MPs were incorporated within EBs and differentiation was assessed using gene expression of Brachyury-T, Flk1 and Pax6 at day four of differentiation. Samples containing BMP-4 loaded MPs up-regulated Brachyury T and Flk1 expression compared to untreated control EBs. Brachyury-T and Flk1 are both mesoderm specific genes which are expressed very early in the onset of differentiation. Brachyury-T expression is sensitive to BMP4 and is useful for preliminary optimization of MP treatment. Pax6, a marker for neural ectoderm, was down-regulated in BMP-4 MP samples. The opposite trends were observed in EBs treated with Noggin loaded MPs. No significant differences were observed between Noggin loading conditions; however, BMP MPs loaded with the higher concentration of BMP-4 solution (25 µg/mL) were able to significantly alter gene expression of Brachyury-T and of Pax6. Therefore, for further investigation of BMP-4 delivery from MPs, the higher loading concentration was used and the lower concentration was used for Noggin delivery.

107
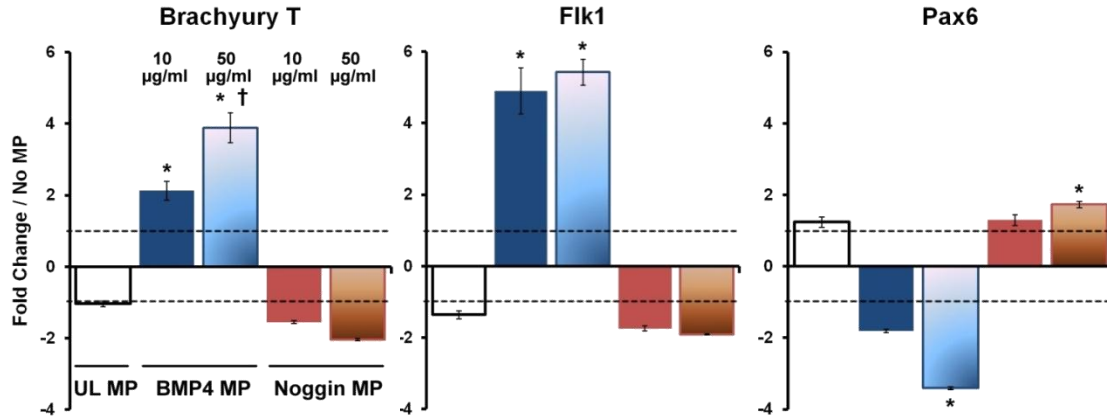
Figure 5.6 Gene expression analysis in response to growth factors delivered from gelatin MPs. Gelatin MPs were loaded with a 10 (dark bars) or 25 (shaded bars) µg/mL solution of BMP-4 or Noggin. MPs were then incorporated within EBs and gene expression was analyzed at day 4 of culture. EBs with BMP4 MPs demonstrated increased expression of mesoderm genes and decreased expression of Pax6, a neuroectoderm marker. EBs with Noggin MPs demonstrated the opposite trend with no significant dose response. $*$ = $p < 0.05$ compared to untreated EBs, $\dagger$ = $p < 0.05$ compared to 10 µg/mL BMP-4 MP.

EB morphology

EBs cultured with growth factor loaded MPs or with soluble treatment through the first four days if differentiation were further cultured for 6 days in suspension or plated on gelatin coated dishes. After 10 total days of differentiation, morphological differences were observed between groups (Figure 5.7). BMP MP treated EBs developed translucent outgrowths, observed in suspension and in plated EBs. In contrast, Noggin MP treated EBs formed small protrusions visible in suspension and in plated EBs. Differences in EB morphology observed after 10 days of differentiation suggested that MP based growth factor delivery had lasting effects on cell behavior. By day 14 of differentiation small ring-like structures were commonly observed in BMP-4 treated samples (Figure 5.8). These structures were not observed in untreated or noggin treated samples but instead neurite outgrowths were observed. This was consistent with early gene expression where

108

Pax6, a neuroectoderm marker, was up-regulated in Noggin samples and down-regulated in BMP-4 samples.

Discussion

The data presented here demonstrates that BMP-4 loaded gelatin MPs are capable of inducing mesoderm differentiation at comparable levels to soluble delivery of BMP-4. Gene expression of mesoderm markers, Brachyury-T and Flk1 were increased in EBs treated with soluble BMP-4 or MPs loaded with BMP-4 and quantification of Brachyury-T positive cells with flow cytometry confirmed mesoderm differentiation on a per cell basis. The morphology of EBs also demonstrated differences between the groups even after 10 to 14 days of culture. This suggests that cell fate can be influenced at an early stage of differentiation and that the effects will carry on after the differentiation cue is removed. Noggin treatment did not demonstrate effective directed differentiation either delivered solubly or from MPs. Noggin acts to prevent BMP4 signaling and because this study used a defined medium lacking BMP-4, it may be that Noggin treatment would be more effective at later time points of differentiation when cells begin to secrete endogenous BMP4. Alternatively, Noggin delivery could be useful when delivered simultaneously with BMP4. For example, Noggin would be beneficial in future studies utilizing dual growth factor release from multiple microparticle populations, spatially patterned to release BMP-4 and Noggin on opposite sides of a single EB. Further analysis of the amount of BMP-4 used soluble vs. MP delivery demonstrated that MP delivery of BMP-4 required 12 fold less growth factor. This is a significant savings in reagent and more importantly it suggests that factors presented via microparticle incorporation can more efficiently direct stem cell differentiation.

109

The release of BMP-4 from MPs fabricated from gelatin types A and B confirmed the important role of polyion complexation between the growth factor and the MP base material. BMP-4 was almost entirely released from type A particles after just 6 hours; however, heparin modification of type A particles resulted in delayed release kinetics which mirrored those of type B particles. Growth factor release from MPs in a cell-free assay gives valuable information when comparing between material types; however, the environment within EBs is such that release kinetics in cell-free assays cannot be equated to the release kinetics of growth factor within EBs. For example, Figure 5.3 demonstrates that fluorescently labeled BSA is released from gelatin MPs within EBs over a period of 4-6 days. In cell free assays, BSA release is similar to BMP-4 and is exhausted over a period of 24-48 hours. Characterization of release kinetics of growth factors from MPs within EBs would be useful for optimization of directed differentiation protocols. A complicating variable is endogenous BMP-4 production from cells within the EB, requiring the use of radio- or fluorescently-labeled growth factor to distinguish between exogenous and endogenous growth factor.

MP-based delivery of growth factors could be used as an "inside-out" approach to deliver morphogens within the EB with the goal being to create a homogeneous concentration of growth factor within the EB thereby directing differentiation towards a more homogeneous population of differentiated cells. Another application could be to locally deliver morphogens to the cells in the direct vicinity of the MPs. The goal could then be to create pockets of differentiated cells or to study growth factor gradients in a complex system.

110
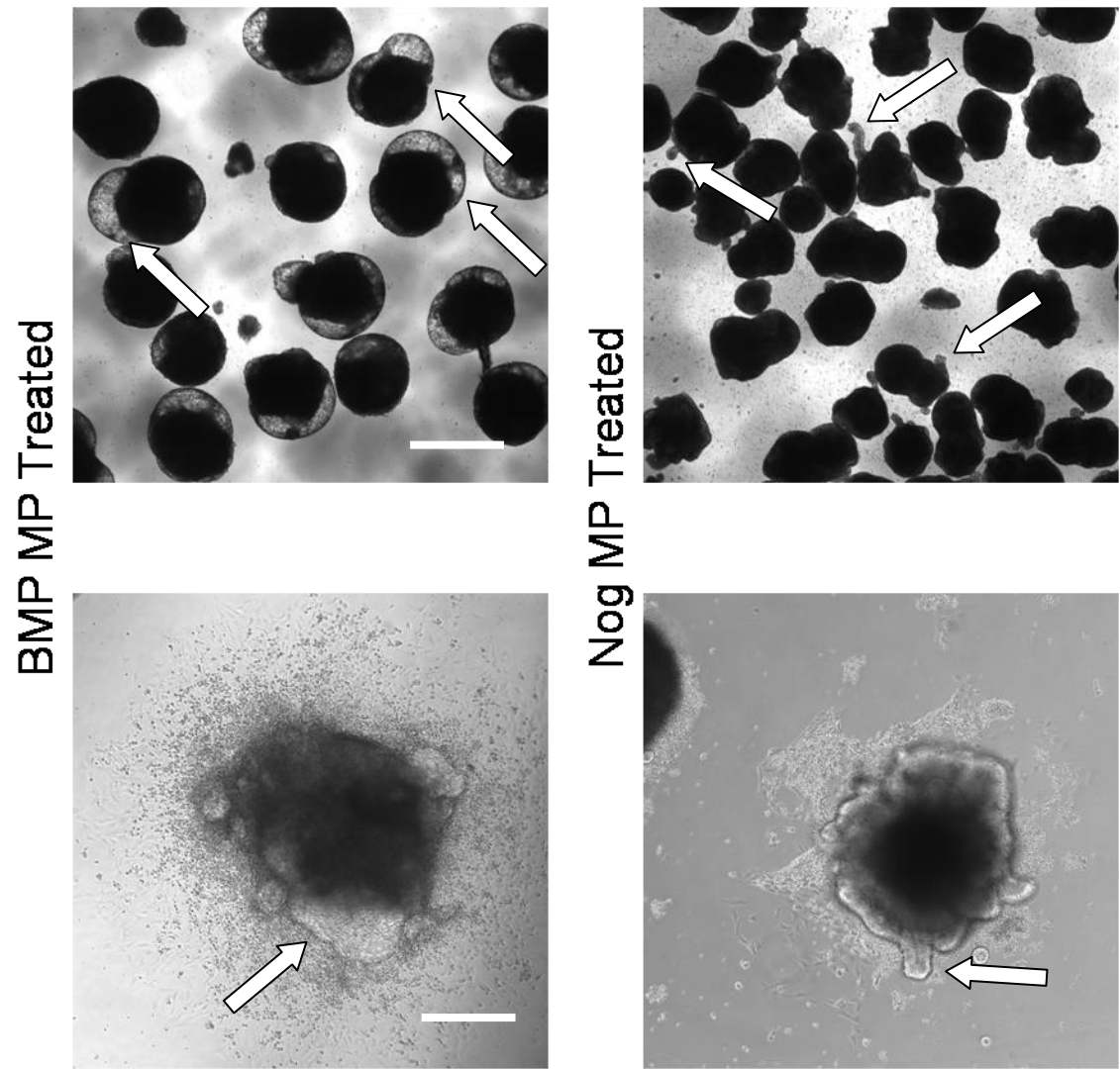
Figure 5.7 Phase images of BMP4 and Noggin MP treated EBs after 10 days of culture. BMP MP treated EBs formed optically translucent, bubble shaped outgrowths (arrows) both in suspension (top row) and in plated EBs (bottom row). Noggin MP treated EBs, however, were morphologically distinct with smaller protrusions (arrows) observed both in suspension (top row) or after plating (bottom row). Scale bars = 500 μm (top row) and 200 μm (bottom row)

No MP

BMP MP

Noggin MP

Neurite Outgrowth

Soluble BMP

Soluble Noggin
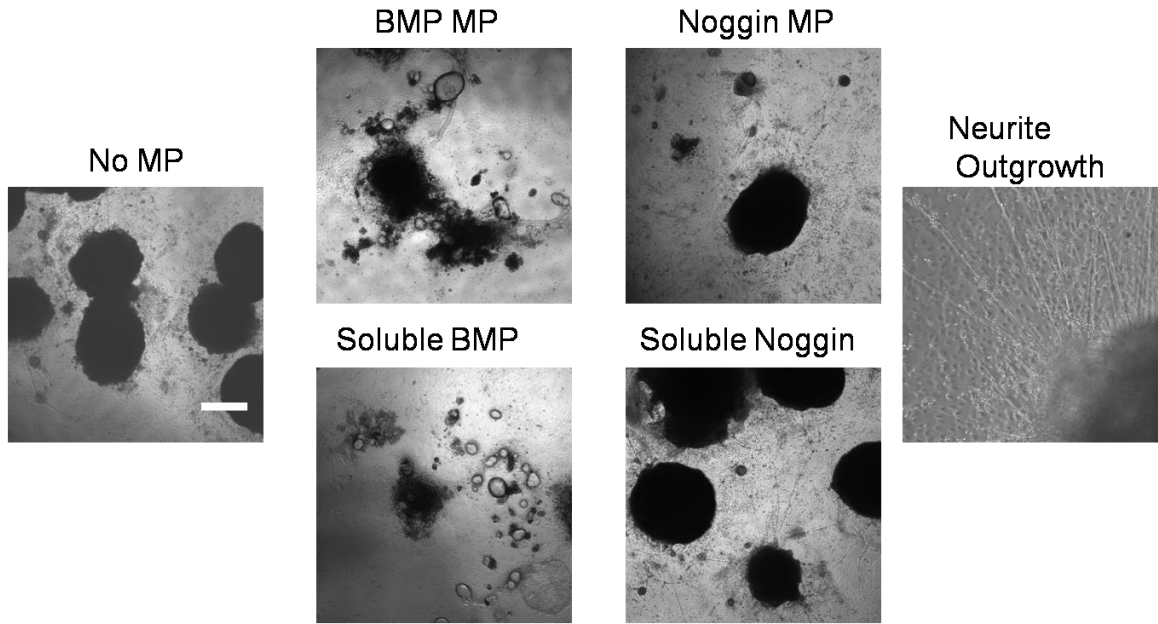
Figure 5.8 EBs plated for 14 days display differing morphology depending on treatment. EBs treated either with soluble BMP-4 or with BMP MPs demonstrated strikingly different morphologies after 14 days of culture. In both BMP-4 treated conditions, small, ring-like structures were frequently observed. These structures were not observed in untreated or noggin treated samples, but instead neurite outgrowths were observed. Scale bar = 200 µm.

CHAPTER 6

MICROPARTICLE INCORPOARTION WITHIN EBS FOR
MAGNETIC MANIPULATION AND SPATIAL PATTERNING[‡]

Introduction

Mammalian tissues are comprised of individual cells assembled in a hierarchical manner to form multi-cellular units that span micron to millimeter scales in order to coordinately contribute to tissue function[101]. The engineering of tissues *ex vivo* seeks to emulate the complexity of native tissues and organs by generating 3D multi-cellular constructs capable of serving as models of healthy and diseased tissues for use as novel diagnostic and drug-screening platforms[218] and potentially for organ replacement or regenerative therapies[109]. Construction of 3D multi-cellular neo-tissues requires directed assembly of both homogeneous and heterogeneous populations of cells. Current approaches to control the assembly and patterning of cells in 3D rely on intrinsic adhesive properties of the cells or engineering cellular interactions. Intercellular adhesion is mitigated through natural cell-cell adhesion mechanisms, such as cadherins[219, 220], or can be engineered by chemically modifying cell surface molecules to promote and stabilize multi-cellular assembly[221-223]. In some instances, otherwise non-adhesive cell types can be induced to form homotypic cell aggregates; however, engineering of aggregates with multiple cell types requires a step-wise building

---

process which has thus far been limited to the formation of small aggregates comprised of at most 2-4 cell layers[221]. One particular concern associated with engineering cell surface adhesion properties of stem cells is the possibility of attenuating or inhibiting signaling pathways important to differentiation that rely upon dynamic transmembrane binding events, including cell-cell and cell-ECM interactions. An alternative approach to controlling larger scale cell aggregation is to entrap cells within biomaterials, such as hydrogels, which can then be assembled by engineering the chemical and physical properties of the cell-laden material building blocks[224, 225]. Unlike modification of individual cells, cell encapsulation technologies can control the spatial assembly of multi-cellular modules (100s of µm to mm in size) into composite structures. However, cell encapsulation limits the interaction of cells in different modules and properties of hydrogel materials such as degradability, stiffness and ligand density can independently and cooperatively influence cell phenotype[226-228], thereby requiring that cell-specific design criteria potentially be considered for different stem and progenitor cell populations. In either case, engineering cell membrane properties and cell entrapment both require *a priori* design of parameters including complementary cell adhesion mechanisms or design of material properties based on the cell type and desired construct geometry. Thus, a robust method capable of geometrically controlled multi-scale assembly for a variety of cell types without the need for cell modification or *a priori* materials design would provide a novel and flexible route to study the biology of multi-cellular structures in 3D.

Magnetic forces can be broadly applied across multiple length scales to direct individual cells at the micro-scale (i.e. microtweezers[229] and microfluidics[230]) and

114

have long been used for larger scale applications including technologies for separation and sorting of cell populations[231, 232]. In general, approaches to magnetically label and direct cells have required surface modification of the magnetic particles and/or the cell plasma membranes in order to permit stable association between the materials and the cells[233]. Alternatively, the directed endocytosis of magnetic material can be utilized to induce magnetic sensitivity of individual cells[234]; however, endocytosis of sub-micron magnetic material can interfere with intracellular signaling and viability[235, 236]. In contrast, magnetic manipulation of multi-cellular aggregates with larger (>1 µm diameter) paramagnetic material incorporated within the extracellular space does not require cellular modification or material internalization and remains an attractive route to control cell behavior because of the inherently flexible and spatiotemporally controlled manner in which magnetic fields can be applied. Recently our lab has demonstrated that biomaterial microparticles (MPs) of varying sizes (1-20 µm) can be efficiently incorporated in a dose-dependent and homogeneous manner within the extracellular space of multi-cellular spheroids to engineer physicochemical properties of the 3D stem cell microenvironment[155, 161, 201]. However, to date, controlling the spatial incorporation and distribution of MPs or populations of different cells within multi-cellular aggregate environments has proven difficult. Thus, we aimed to incorporate magnetic microparticles (MPs) as a means to spatially control homogeneous and heterogeneous multi-cellular aggregates, without adversely impacting cell viability or phenotype.

We report here that magnetic MPs (magMPs) can be efficiently and stably incorporated in a dose-dependent manner in the extracellular environment of 3D stem cell

115

aggregates without the need for biochemical modification of the cell membrane or material adhesive properties.   MagMP entrapment within multi-cellular aggregates enables the directed movement and assembly of spheroids in suspension culture with an externally applied magnetic field to yield complex organization of 3D constructs across broad length and time scales. Therefore, this method can be used to address a variety of questions of relevance to stem cell and developmental biology, tissue engineering and cell bioprocessing.

Materials and methods

Spheroid formation and magMP incorporation

D3 murine embryonic stem cells (ESCs) were propagated on 0.1% gelatin-coated tissue culture dishes in DMEM media containing 15% FBS and 10^3 U/ml leukemia inhibitory factor (LIF; Millipore, Billerica, MA). Embryoid bodies (EBs) were formed using a single-cell suspension by forced aggregation in AggreWell^{TM} 400 inserts (Stem Cell Technologies, Vancouver, CA). Briefly 1.2×10^6 cells in 0.5 ml of medium were inoculated into AggreWell inserts, containing approximately 1,200 wells per insert, and centrifuged at 200 RCF for 5 minutes to pellet cells in the wells. Magnetic, polystyrene microparticles with a diameter of 4µm (SpheroTech, Lake Forest, IL) were washed 3x with ddH2O, diluted in 0.1 mL DMEM media, and subsequently added at a 1:10, 1:3, 1:1, and 3:1 microparticle-to-ESC ratio. To pellet microparticles in the wells, either a second centrifugation was performed at 200 RCF for 5 minutes or a magnet (10 lb pull strength) was applied below the plate for 5 minutes. All magnets used to create external magnetic fields were purchased from Gaussboys Super Magnets (Portland, OR). After 24

116

hours of culture, aggregates were removed from the wells using gentle pipetting and transferred to a suspension culture on a rotary orbital shaker (45 RPM) to maintain the homogeneous populations of spheroids[54].

Quantification of magMP incorporation in EBs

After 24 hours of culture, EBs containing magnetic microparticles were collected and transferred to a 48 well plate where they were first counted and then lysed in a 5% SDS solution. The magMPs remaining were counted using a Coulter Counter (Beckman Coulter, Brea, CA) using a collection window of 3.5-4.5 µm for each sample. The resulting count was divided by the number of EBs lysed to calculate the average incorporation of magMPs per EB.

Histological analysis and cell viability

Spheroids cultured for 2 days were collected and rinsed in PBS, fixed in 10% formalin and embedded in Histogel (Thermo Scientific), processed and paraffin-embedded. Sections of 5 µm in thickness were deparaffinized before staining with Fast Green. Histological samples were imaged using an 80i upright microscope (Nikon) and an SPOT Flex camera (15.2 64 MP Shifting Pixel, Diagnostic Instruments). Cell viability was analyzed after 2 days of EB differentiation using LIVE/DEAD staining (Invitrogen, Carlsbad, CA). Samples were incubated in serum-free, phenol red-free medium containing 1 mM calcein AM and 2 mM ethidium homodimer I at room temperature for 30 minutes. Spheroids were then washed three times with PBS and imaged using an LSM 510 confocal microscope (Carl Zeiss, Inc).

117

Spheroid translocation

Spheroids formed from 1:10 and 1:3 magMP:cell seed ratios were aligned linearly in a 100 mm suspension culture Petri dish using a bar magnet (65 lb pull strength) placed below the dish. The magnet was removed from directly below the magMP laden spheroid population and placed under the dish at a distance of 4 mm away from the linear array of cell aggregates. The movement of individual spheroids was recorded at 3 frames per second using an SPOT Flex camera mounted on an Elipse TE2000U phase microscope (Nikon).

Cell labeling

Adherent ESC monolayers were rinsed in PBS and incubated with a 5 ųM solution of CellTracker^{TM} (Blue, Red or Green, Invitrogen) in serum-free medium for 30 minutes. The CellTracker solution was aspirated and cells were incubated with serum containing medium for 30 minutes prior to trypsinization and spheroid formation.

Magnetic manipulation

4mm x 1mm nickel plated neodymium magnets were used to spatially confine the location of spheroids in rotary orbital suspension culture. The desired configurations of magnets were created by magnets held in place on opposing sides of the culture lid. The ability of the magnets to pattern the spheroids was dependent on the distance of the magnets to the level of culture medium, which could be adjusted by stacking magnets on top of each other to increase the thickness of the magnet layer. After the magnets were configured, the dish was placed on a rotary orbital shaker at 40-50 RPM. In order to

118

reversibly manipulate the translocation of individual spheroids between paramagnetic elements, iron rods were embedded in a PDMS gel approximately 4 mm in thickness such that the ends were spaced 2-3 mm apart and the opposite end of each iron element protruded at least 2 cm from the PDMS gel near the outside edge of the dish. Individual rods were transiently magnetized by contacting the free end of each with a 10 lb pull force bar magnet in a sequential manner such that after removing the magnet, one of the other rods could be magnetized. Individual spheroids were added in 1 ml of medium on top of the PDMS gel and imaged continuously as the rods were sequentially magnetized and demagnetized.

Spheroid merging

Spheroids were first formed from ESC populations labeled with CellTracker fluorescent dyes. For multi-aggregate assembly patterning, a 15mm x 2mm nickel plated neodymium magnet was applied underneath cell culture dishes to control spheroid location. Populations of spheroids were then added to the dish in small volumes of medium (100-500 μL) in the order shown in Figure 4 A,D. The EBs were then guided to a closely packed formation by swirling the magnet around the area occupied by the spheroids. After a population of spheroids was closely packed, spheroids labeled with a different color were added to the culture. For a stacked Venn diagram configuration, spheroids were sequentially added to the side of magnet each time, whereas for "bullseye" configuration, the spheroids were added in a circle around the magnet each time.

119

For merging of individual aggregates, single spheroids labeled green, red or blue were transferred from batch suspension culture to a 30 mm suspension culture Petri dish containing 500 µl of medium. A 3mm x 9mm nickel plated neodymium cylindrical magnet positioned beneath a Petri dish was used to direct the spheroids to the desired position. Merging of two spheroids was monitored at 37ºC via time lapse microscopy (Biostation IM, Nikon) with images taken every 3 minutes for a period of up to 15 hours. Merging of 3 and 4 spheroids composed of fluorescently labeled cells was performed similarly by adding different colored individual spheroids (one blue, red, green and no fluorescent label) sequentially to a culture dish. Each spheroid was then magnetically guided to the desired position and allowed to sit for 10 minutes before other spheroids were added. After spheroids were in contact with each other, the plate was placed in a cell culture incubator overnight and imaged using epifluorescent microscopy after 18-24 hours.

Statistical analysis

Experimental values are reported as mean ± standard deviation (n = 6). Statistical analysis was determined using one way ANOVA coupled with Tukey's post hoc analysis using Systat (v12, Systat Software Inc.). p-values < 0.05 were considered statistically significant.

120

Results

Magnetic microparticle incorporation in cell spheroids

Mouse ESCs and magMPs (4 μm diameter) were sequentially seeded in PDMS microwells through successive centrifugation or a combination of centrifugation and magnetic pull-down (Figure 6.1A). Immediately after centrifugation or magnetic pull-down, magMPs were clearly observed on top of the cell layer (Figure 6.1Bi, arrows) and were primarily visible along the edges of the wells (Figure 6.1Bii, arrows). Within 18-24 hours, multi-cellular aggregates formed within the wells (Figure 6.1Biii) with magMPs distributed throughout the entirety of the spheroids (Figure 6.1Biv). Time-lapse microscopy analysis indicated that cell movement during spheroid formation corresponded with displacement of the magMPs, but no significant differences were observed in the kinetics of spheroid formation with or without the introduction of magMPs.
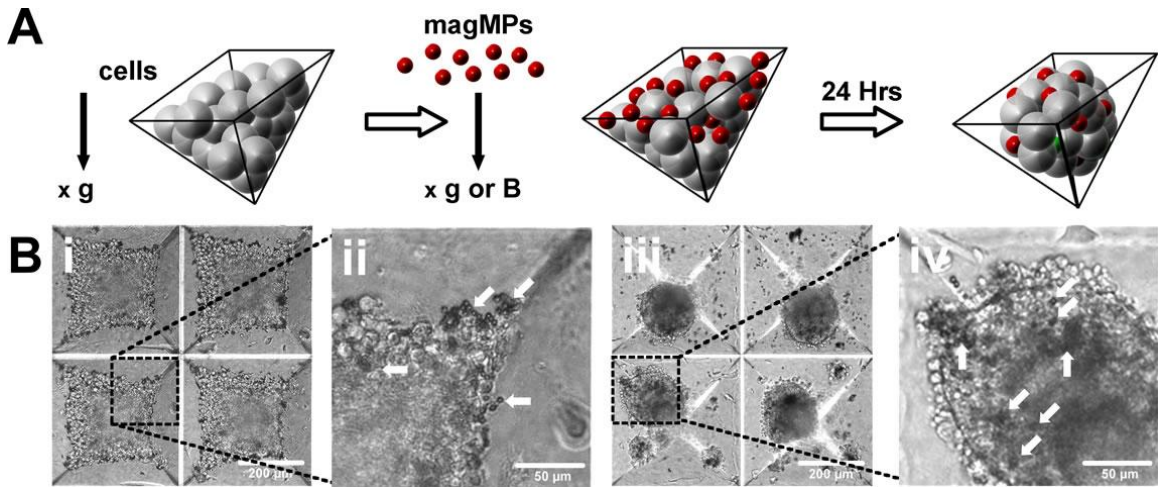
Figure 6.1 Magnetic MPs are incorporated in a dose dependent manner. (a) MagMPs were incorporated within stem cell spheroids within PDMS microwells (b) MagMPs (arrows) were observed after ESC and magMP centrifugation (i,ii) as well as throughout the spheroids that were formed after 18-24 hours of culture (iii,iv). Scale bars, 100μm (i,iv) and 50μm (ii,iii)

The number of magMPs incorporated within cell spheroids significantly ($p <$ 0.01) increased in a dose-dependent manner as a function of the microparticle-to-cell seed ratio (Figure 6.2). At a seed ratio of 3:1 (MPs : cells) approximately 1500 MPs were counted on average for each spheroid. This represents an incorporation efficiency of 41.6%. The upper limit of incorporation was not reached; however, it is likely that the probability of altering normal EB behavior (differentiation, cell viability, cell movement) increases with the number of incorporated MPs. The goal of the experiment was not to find an upper limit of incorporation but to investigate a range of incorporation values so that EBs could be fabricated with various magnetic sensitivities.
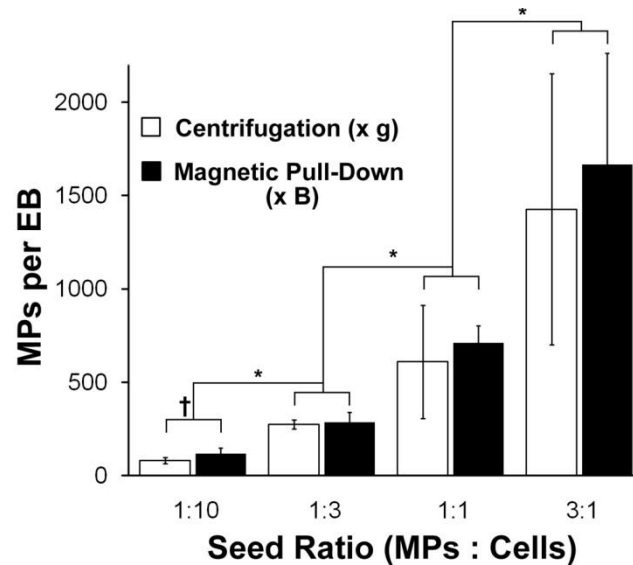
Figure 6.2 MagMP incorporation quantification. Spheroids were formed using centrifugation or magnetic pull-down and the number of MPs incorporated per spheroid was determined after 24 hours of culture. * $p \leq 0.05$ Comparison of loading ratios, † $p \leq 0.05$ comparison between pull-down and centrifugation.

After transferring the multi-cellular aggregates from the microwells to suspension culture, the resulting spheroid populations exhibited comparable sizes and shapes, and the magMPs (observed as opaque regions) remained readily apparent in contrast to the

122

translucent cells (Figure 6.3). EBs formed with a 1:10 and 1:3 seed ratio were sufficiently sensitive to magnetic manipulation; therefore, further analysis on the effects of magMP incorporation on EB morphology and cell viability were performed with these groups. Additionally, it is worth noting that EBs became difficult to maintain in culture at the higher incorporation levels (1:1, 3:1) confirming the idea that when the number of MPs approaches the number of cells in the EB, behavior is likely to be altered. Culture difficulty came from the fact that the EBs were prone to merging and were difficult to culture as homogeneous aggregates even under differing rotary speeds.

123
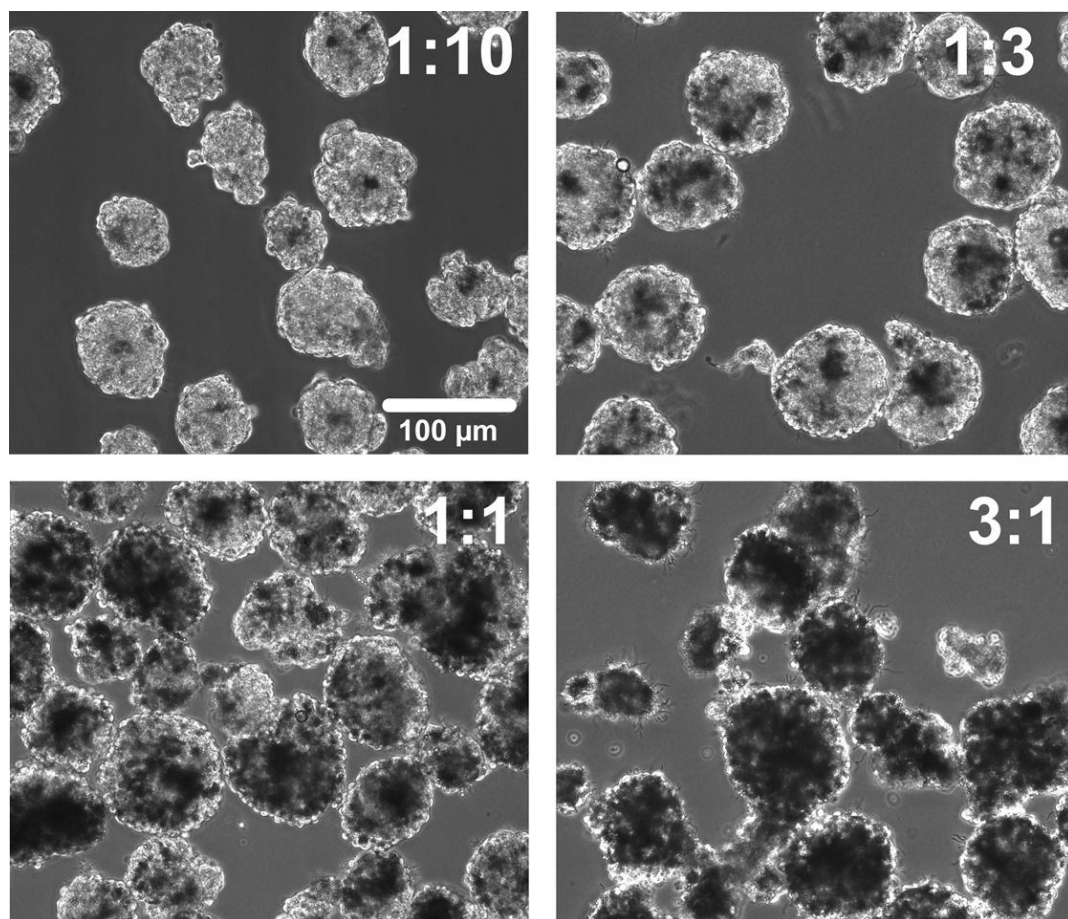
Figure 6.3 EBs formed with MagMPs. EBs formed at cell seeding ratios of 1:10 (i), 1:3 (ii), 1:1 (iii), 3:1 (iv) were of similar shape and size and dark regions of magMPs increased with the seeding ratio. Scale bar 100μm.
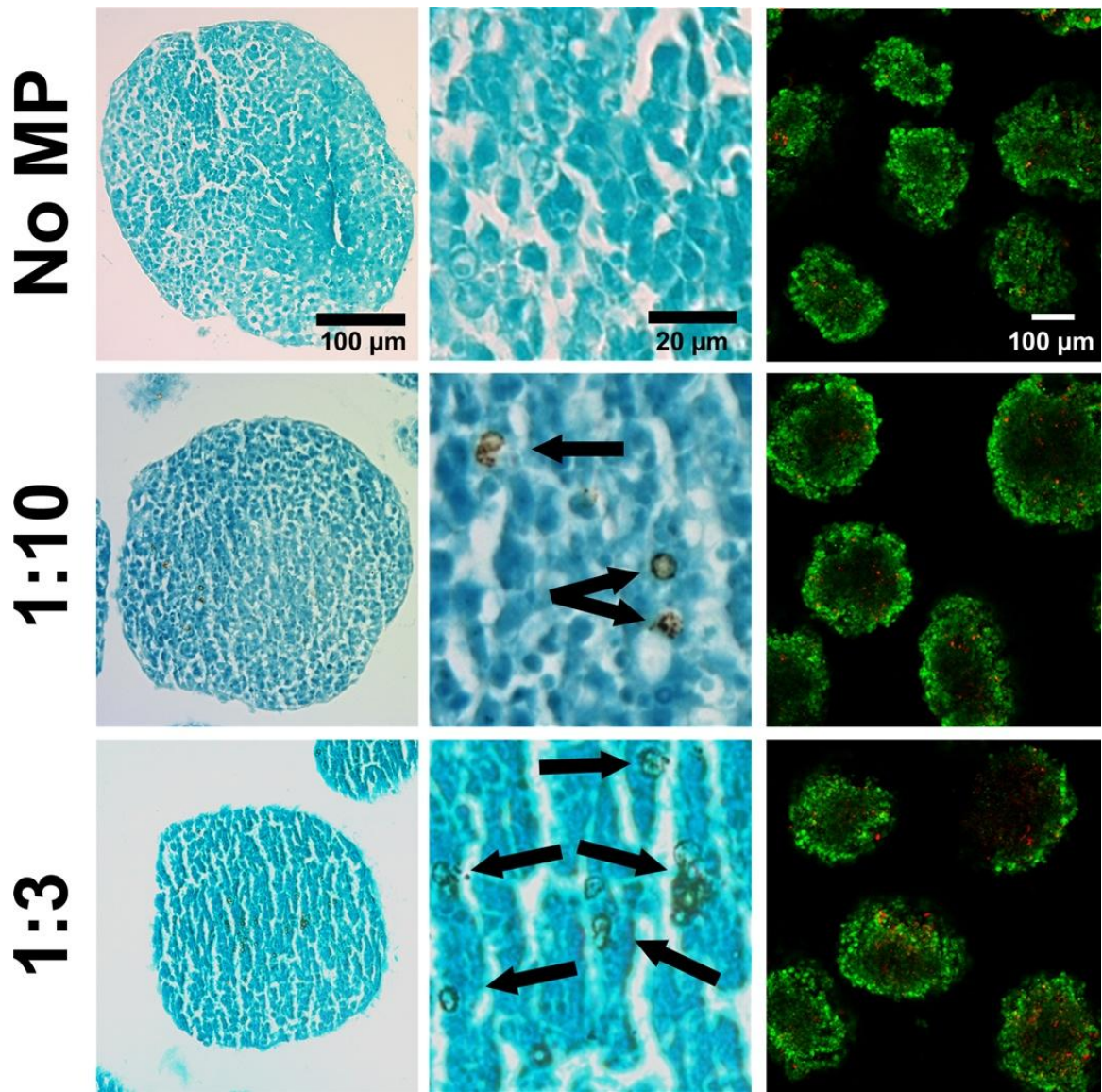
Figure 6.4 EB histology and viability. Histological sections stained with Fast Green stain revealed that magMP incorporation did not disrupt cellular arrangement or morphology. No differences in cell viability were observed for any of the groups (LIVE/DEAD assay, dead cells labeled red and live cells labeled green). Scale bar 100μm (i,iii,iv,vi,vii,ix), 25μm (ii,v,viii).

MagMPs in histological sections were visibly brown, due to their iron composition, and were clearly identifiable in the extracellular space of the cell spheroids in proportion to the respective seed ratio. The addition of magMPs (1:10 or 1:3) did not alter the cellular organization within EBs or affect the morphology of the cells in direct contact with the magMPs (Figure 6.4). Additionally, no difference in cell viability was observed between EBs with or without magMPs as assessed by LIVE/DEAD® staining after 2 days of culture.

Differentiation of EBs, with and without magMPs, was assessed by gene expression analysis of pluripotent and germ layer specific markers over seven days of culture in serum containing medium. The expression of pluripotent markers, Nanog and OCT4, decreased with differentiation time and temporal expression patterns of markers from each of the three germ lineages (Pax6 – ectoderm, Brachyury-T – mesoderm, and Gata4 – endoderm) appeared as expected, with no significant differences between the experimental groups indicating that the presence of magMPs did not interfere with the normal differentiation process (Figure 6.5).

MagMPs were also similarly incorporated within spheroids of human mesenchymal stem cells (Figure 6.6) and human induced pluripotent cells, indicating the broad applicability of this technique.
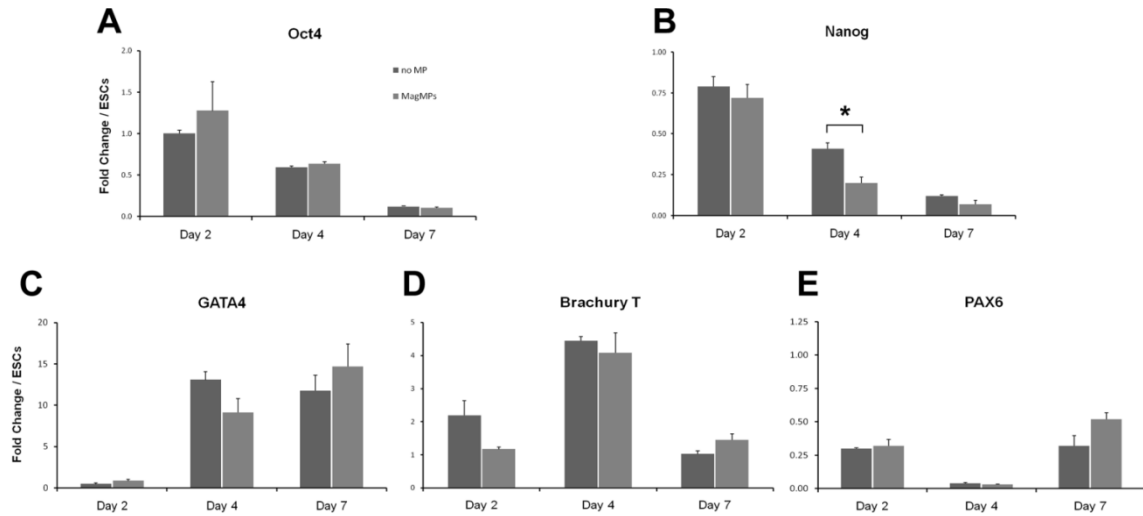
Fig 6.5 EB differentiation is unchanged in the presence of magMPs. EBs cultured in serum containing media for 7 days were sampled and gene expression was analyzed using RT-PCR and normalized to ESC values. Expression of pluripotent markers, Oct4 and Nanog, decreased with culture time (a,b) indicating the magMPs did not disrupt the kinetics of differentiation. Additionally, temporal expression patterns of germ layer differentiation markers, GATA4 – endoderm (c), Brachyury T – mesoderm (d), and PAX6 – ectoderm (e) appeared as expected, with no significant differences between the experimental groups. * = $p \leq 0.05$, n = 3

127
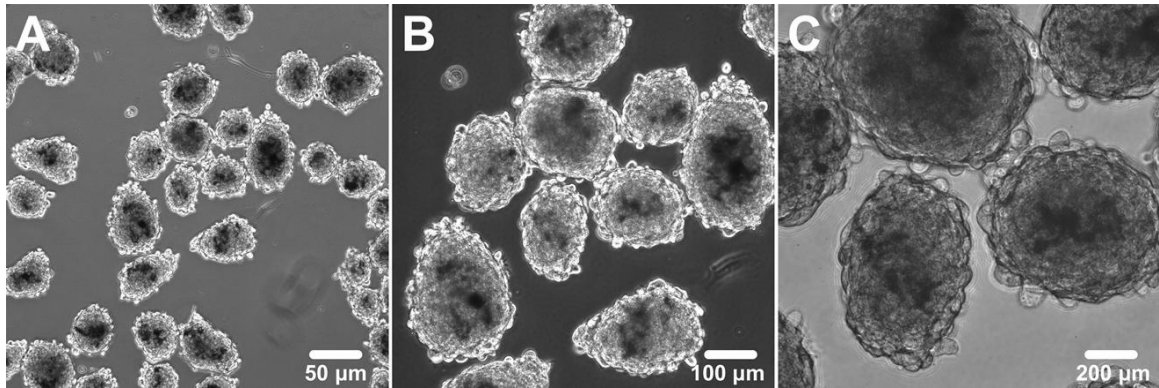
Figure 6.6 MagMP can be incorporated within human mesenchymal stem cell spheroids. Magnetic MPs, seeded in a 1:10 ratio, were incorporated within human mesenchymal stem cell spheroids using forced aggregation within microwells. Dark regions, consistent with those observed in ESC aggregates, were observed in all spheroids (a-c) indicating the presence of magMPs. Scale bars 50µm (a), 100 µm (b) and 200 µm (c).

Spatially directed translocation of EBs containing magMPs

Having demonstrated robust incorporation of magMPs within stem cell spheroids, the ability to manipulate the spatial positioning and translation of stem cell spheroids was examined in static and dynamic culture systems using externally applied magnetic fields. Under static culture conditions, entire fields of individual spheroids could be concentrated, translated and rotated based upon the relative location, direction and manner in which external magnetic fields were applied. As expected, spheroids containing a higher density of magMPs were more sensitive to applied magnetic fields (increased acceleration towards the magnet) compared to spheroids with a lower density of magMPs. In order to demonstrate the quantitative relationship between magMP incorporation and magnetic field strength, the positions of individual spheroids were tracked over time as they moved towards a magnet placed at a lateral distance of 4 mm (Figure 6.7A, D). Spheroids formed at a ratio of 1:3 (magMPs:cells) were translated

128

(Figure 6.7B) at an average speed of 451 ± 96 µm/s, whereas spheroids formed at a ratio of 1:10 moved at an average speed of 144 ± 80 µm/s in response to an identical magnetic field (500 Gauss). Spheroids with a lower seed ratio (1:10) demonstrated increased variability in their response to the magnet, presumably a consequence of the greater variability of magMPs per spheroid with lower seeding ratios. As expected, weaker or stronger magnets (10 – 65 lb pull strength) resulted in slower or faster translocation, respectively, of the same magMP-spheroid populations (data not shown). It was notable that the velocities of the distinct spheroid populations did not overlap (Figure 6.7B, C), suggesting that complex mixtures of different types of spheroids could be sorted and organized rapidly based simply on the number of magMPs incorporated in distinct multicellular aggregate populations.
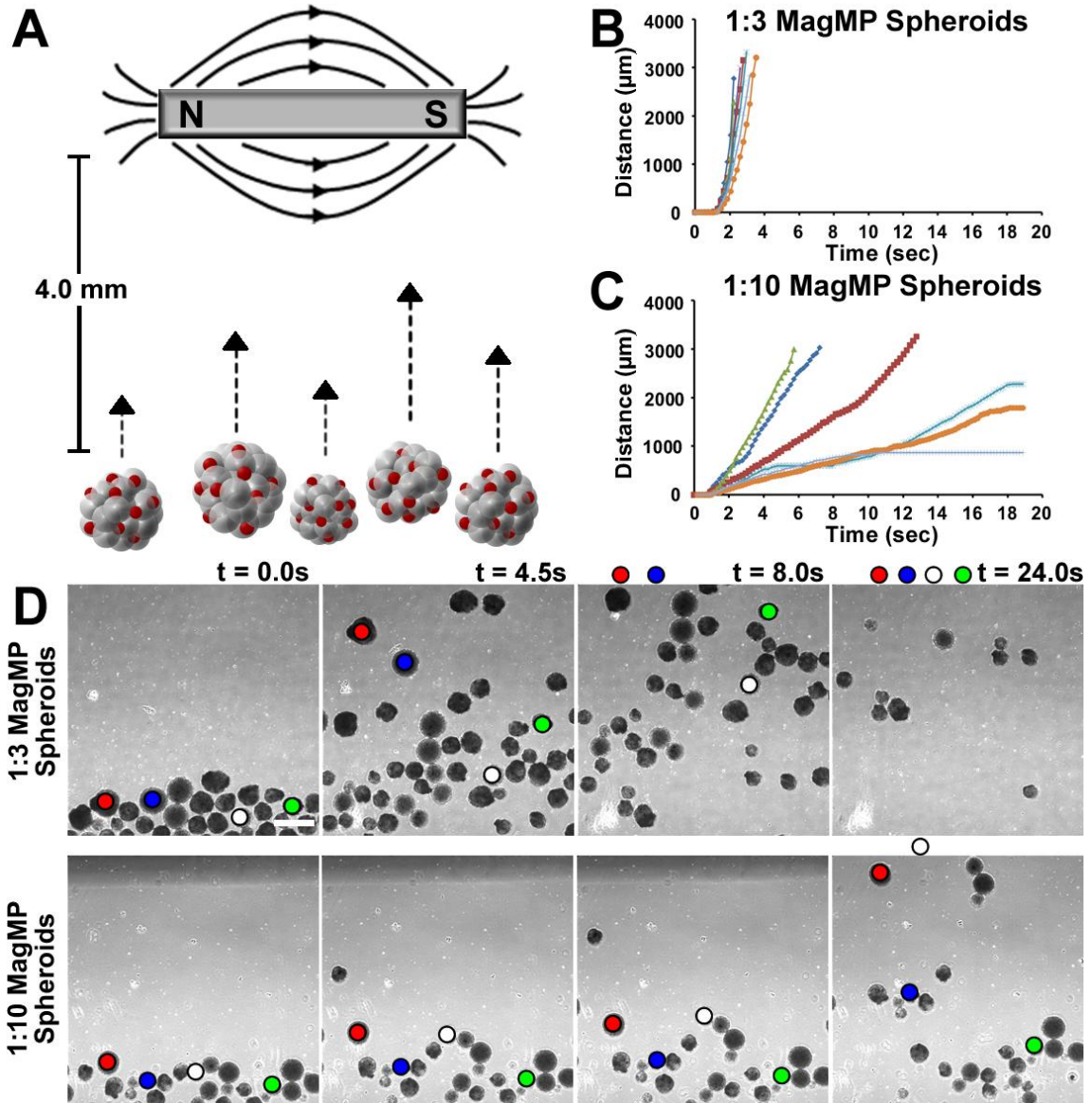
Figure 6.7 Spheroids with magMPs respond in a dose dependent fashion to magnetic fields. (a) Spheroids can be directed to move in a dish by an externally applied magnetic field. (b,c) Spheroids formed with a higher ratio (1:3) of magMPs to cells move faster and more uniformly relative to spheroids formed with a 1:10 seed ratio. (d) The distance moved between frames was tracked and suggests that the populations could be sorted based on magnetic sensitivity alone. Scale bar 500µm.

<u>Magnetic control of hydrodynamic suspension cultures</u>

Bioreactor culture is often utilized or envisioned in stem and progenitor cell culture as a means to produce high yields of cells thought to be required for large-scale biomanufacturing and clinical efficacy[64, 237]. The inability to control the spatial position of cells and aggregates under hydrodynamic conditions becomes problematic because shear forces, which can affect stem cell differentiation, vary as a function of position within individual mixed/stirred systems[55, 238]. As a simplified example, we examined the use of patterned magnetic fields to constrain spheroid location within rotary orbital culture. Our lab and others have previously reported the use of rotary orbital shaker culture of ESCs to create and maintain homogeneous populations of EBs in suspension culture conditions[54, 239, 240]. In rotary culture, spheroids generally occupy a focused region of the dish (Figure 6.5A) and are subjected to a range of shear forces depending on their precise location, which changes slightly with each revolution of the culture. By adhering magnets in a circular pattern on the lid of a Petri dish (Figure 6.5B), we observed that the distance of the EBs to the center of the dish could be confined exclusively to the region below the magnetic pattern, which constrains the range of shear forces experienced by the cell spheroids. Other patterns could also be imposed on dynamically cultured spheroids including discrete islands across the dish (Fig. 6.8Bii), a "four leaf clover" pattern (Figure 6.8Biii) or a straight line (Figure 6.8iv) by altering the configuration of the magnets on the lid of the Petri dish (shown in the insets of Figure 6.8B). Asymmetric geometries (Figure 6.8C) could also be formed and maintained by simply altering the externally applied magnetic field via the configuration of the magnets on the lid of the dish.

131

The transient application of magnetic fields was also investigated as a method to control the spatiotemporal localization and translocation of individual spheroids. A triangular configuration was created with iron rods embedded in a thin layer of PDMS approximately 1 mm apart (Figure 6.8D) and individual spheroids containing magMPs were placed in the center of the configuration on top of the PDMS (Figure 6.8Di). In the absence of an external magnetic field, a spheroid remained free-floating in the center of the configuration, but as soon as one of the iron rods was magnetized, the spheroid was immediately attracted by the magnetic field to the end of that particular rod. By sequentially magnetizing other rods, the spheroid could be rapidly and specifically translocated from point-to-point, demonstrating the ability to direct multi-cellular movement and location in suspension culture purely by alternating magnetic fields of paramagnetic elements (Figure 6.8Dii-iv).
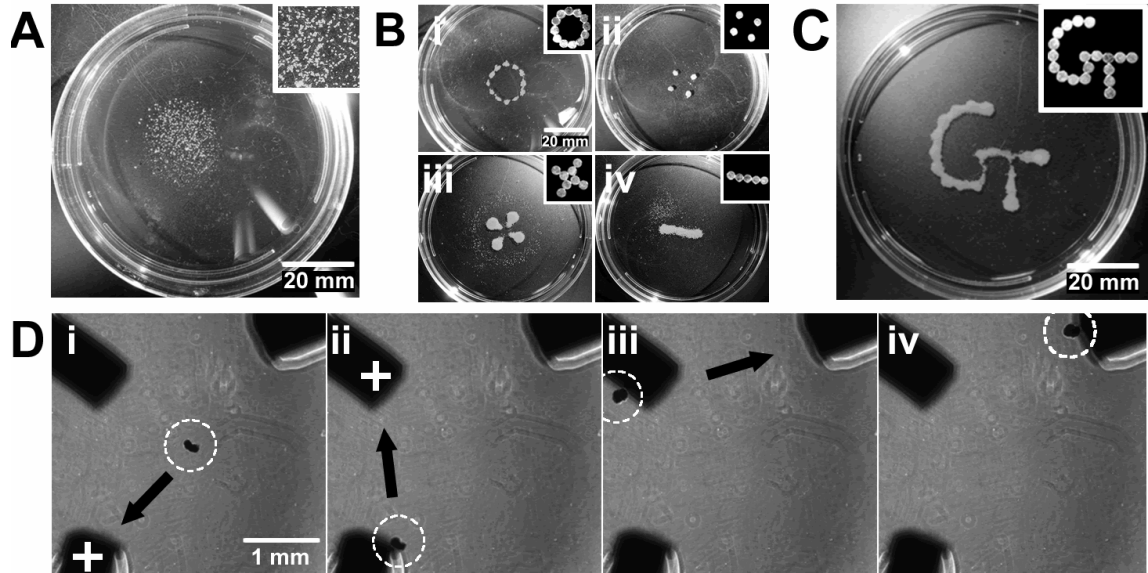
Figure 6.8 Spheroids location can be controlled in dynamic suspension culture. (a) Without magnets, spheroids cultured on a rotary orbital shaker (45 RPM) cluster in the center of the dish. Scale bar 20 mm. (b) The placement magnets on the lid of the dish (configuration shown in insets) could be used to confine the spheroids to (i) a defined radius, (ii) distinct islands, (iii) a four-leaf clover, (iv) or a line configuration. Scale bar 20 mm. (c). More complicated patterns, including the Georgia Tech logo, could be made at slower culture speeds. Scale bar 20mm. (d) In addition, the location of a single spheroid could be manipulated back and forth between iron pillars embedded in PDMS. The iron pillars were alternately magnetized (demonstrated by a "+" label), resulting in attraction of the spheroid to the magnetized pillar (i-iv). Scale bar 1mm.

Multi-scale complex assembly of spheroid units

The sequential assembly of bulk populations of magMP containing spheroids (hundreds to thousands of aggregates) was next examined using external magnetic fields in static culture environments. A single population of fluorescently labeled spheroids, indicated with a "1" in Figures 6.9A,D, was added to a Petri dish and aggregated into a circle using a magnet 5 mm in diameter. When subsequent populations, labeled "2", "3" were added only on one side of the magnet, the spheroids aggregated into a stacked Venn diagram pattern (Figure 6.9B). At the interfaces between the different spheroid populations little mixing was observed, demonstrating that geometry could be controlled with good pattern fidelity (Figure 6.9C). When subsequent aggregate populations were added around the entire circumference of a fixed magnet, large numbers of spheroids could be arranged in a "bullseye" pattern of concentric circles (Figure 6.9E). Again, higher magnification analysis revealed that the interface between different spheroid populations was largely conserved even in a construct as large as 5 mm in diameter (Figure 6.9F).

134
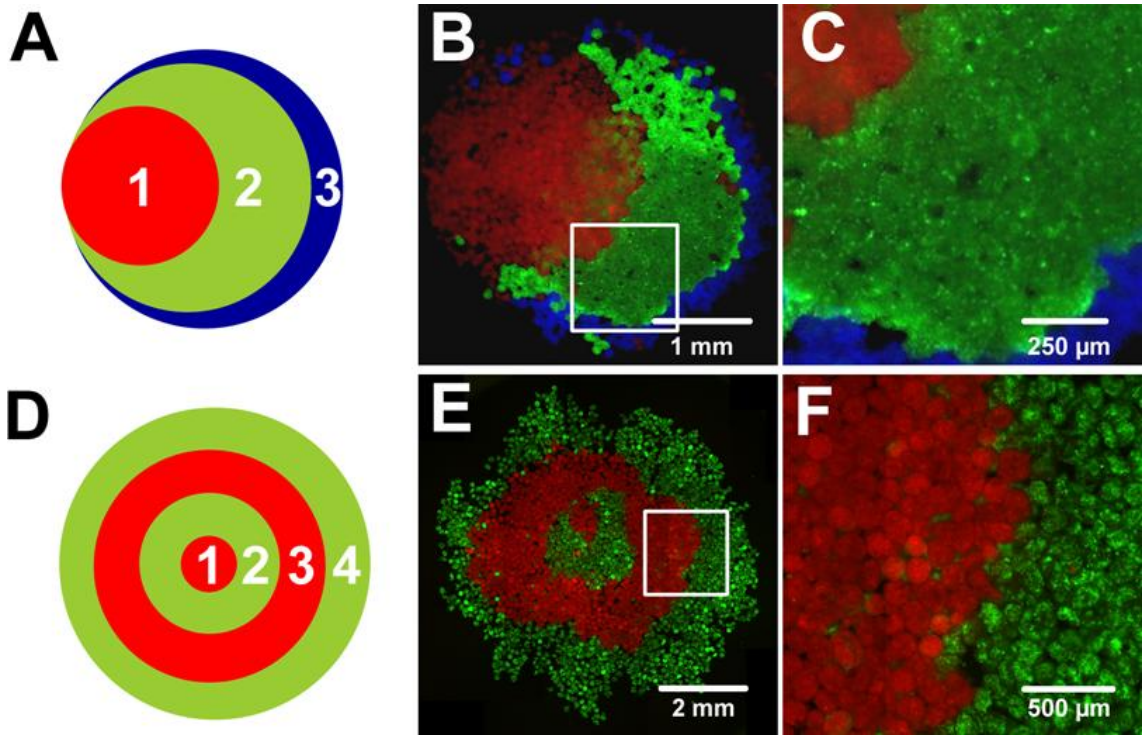
Figure 6.9 Macro manipulation of EB populations. Large populations of magMP spheroids were manipulated to form macroscopic patterns including a "stacked Venn diagram" shape (a-c) or a "bullseye" pattern (d-f). Populations of CellTracker labeled EBs were added sequentially as shown in panels a and d and were aggregated using a magnet applied underneath the Petri dish. Mixing between the layers was limited as demonstrated in panel c and f, magnified from the boxed areas in b and e. Scale bars 1mm (b), 250 μm (c), 2 mm (e), 500 μm (f).

Spatial patterning of magnetically sensitive spheroids can be applied to various cell types which can be grown as aggregates but embryonic stem cell spheroids are prone to E-cadherin mediated agglomeration during early stages of differentiation[55]. In general, agglomeration increases the heterogeneity of culture and is avoided; however, controlled agglomeration may yield a platform for local control of the spheroid microenvironment. In order to test this hypothesis, individual spheroids, pre-labeled with CellTracker^{TM} Red, Blue or Green (or not labeled), were magnetically guided within close proximity of each other (Figure 6.10Ai) and monitored continuously thereafter with time-lapse microscopy. After 5 hours of static culture, the individual spheroids remained in contact and began to merge along the interface adjoining adjacent aggregates (Figure 6.10Aii). After an additional 5 hours, the initially distinct spheroids continued to merge to form an oblong, oval structure (Figure 6.10Aiii) that eventually became a fully conjoined aggregate by ~15 hours (Figure 6.10Aiv). Interestingly, throughout the entirety of the merging process, the fluorescently labeled populations of cells remained largely in the same hemispheres corresponding to the initial relative location of their original respective spheroids. Based on the ability to assemble spheroids that retained the relative position of the original sub-units, the same process was applied to the step-by-step construction of more complex multi-spheroid aggregates (Figure 6.10B). Two spheroids were magnetically oriented adjacent to one another (Figure 6.10Bi-ii) before introducing a third (Figure 6.10Biii) and fourth spheroid (Figure 6.10Biv) on opposite sides. Within 18 hours the individual spheroids had merged to form a multi-quadrant aggregate, whose contributing multi-cellular units could be identified and distinguished by epifluorescent microscopy (Figure 6.10C).

136
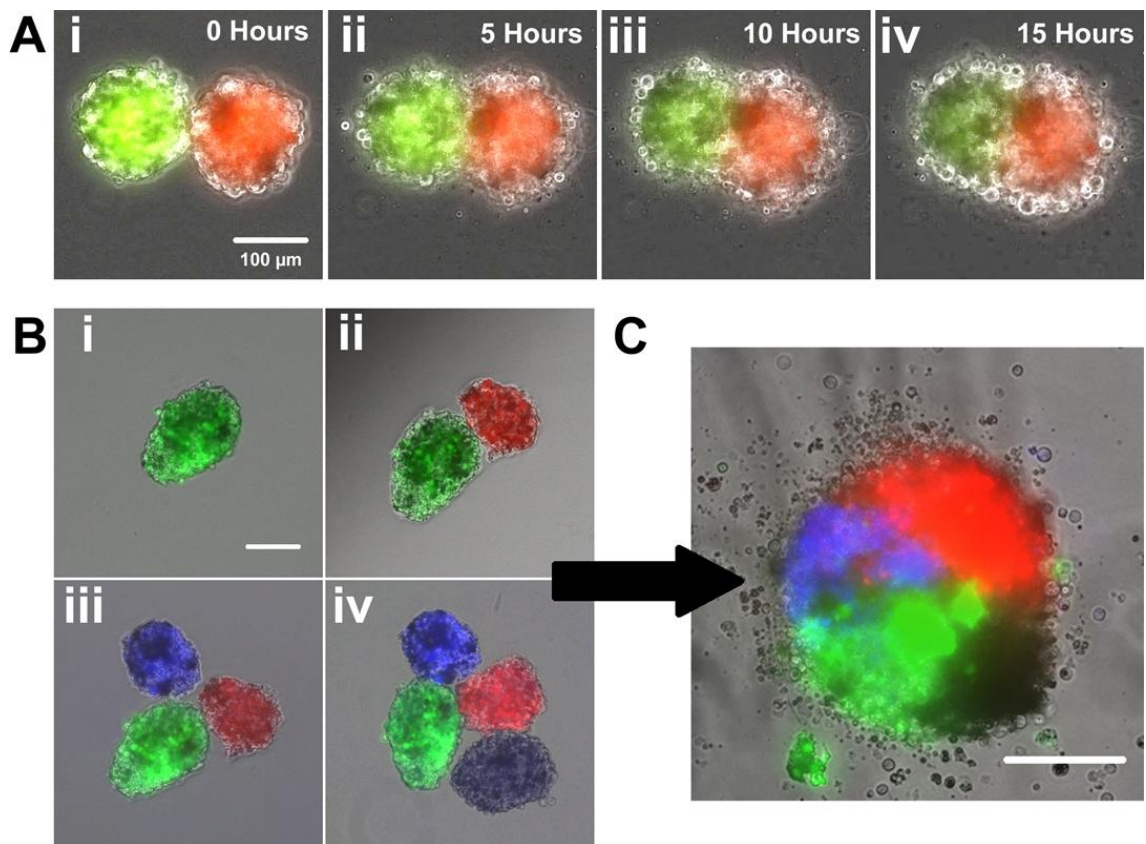
Figure 6.10 Merging of EBs can be spatially controlled on the single aggregate level.
(a) The merging process of two spheroids was visualized over a period of 15 hours using time lapse microscopy. Fluorescently labeled stem cell spheroids were brought in contact with one and other using a magnetic probe (i) and began to merge after 5 hours of culture (ii). The spheroids continued to merge after 10 hours (iii) and became more rounded after 15 hours (iv). Scale bar 100µm. (b) Merging of more than two spheroids could also be controlled by magnetic manipulation. Spheroids were drawn together magnetically in a sequential manner (i-iv) which maintained the position of the spheroids relative to each other. Scale bar 100µm. (c) After 24 hours of culture 4 spheroids merged to create a single construct consisting of four distinct quadrants of fluorescence. Scale bar 100µm.

137

Discussion

In these studies, we have shown that magnetic manipulation of stem cells in 3D cultures provides a simple approach to control the aggregation and design of multi-cellular geometries for neo-tissue constructs. The method described herein relies upon high-throughput formation of magnetically sensitive stem cell spheroids, which differs significantly from other lower-throughput methods[234, 241], in part because it is not dependent on engineered cell or material properties. Entrapment of magnetic microparticles can be conducted with various types of stem cells that are commonly grown as spheroids including embryonic[37], induced pluripotent[9], mesenchymal[242, 243] and neural stem cells[244, 245]. Magnetizing cells or cell spheroids generally requires internalization of sub-micron material or conjugation to the cell surface which can impede cell motility and induce cell death[235]. By simply physically entrapping magMPs within the extracellular space of stem cell spheroids, magnetic fields can be applied to induce multi-cellular aggregates to rapidly assemble into higher order structures without directly perturbing intracellular machinery and signaling pathways. In addition, the patterns that we report in these studies could all be created in static suspension culture using a relatively weak (10x weaker than a 3 tesla magnetic resonance imaging electromagnet) and transiently (1 min or less) applied magnetic field. In such case where a continuous magnetic field may be necessary, the effects of magnetic field strength on stem cell differentiation could be assayed, though adverse effects on viability are not expected, based on prior reports of ESCs and neural stem cells cultured in the continuous presence of a magnetic field for 48-72 hours[246, 247].

138

Patterning of spheroids in dynamic suspension culture systems, such as bioreactors, can be used for more uniform control of the extracellular environment and therefore offers advantages for stem cell bioprocessing. Spheroids with incorporated magMPs could be strictly confined to specific locations within dynamic suspension culture suggesting a possible route to study confined regions of shear forces for individual EBs. The distinct position of spheroids could also be controlled by magnetizing paramagnetic elements that could be physically integrated into the culture vessel design. This method introduces the possibility of automating electromagnetic field patterning for precise control of spheroid locations within a bioreactor to better direct stem cell differentiation in batch culture processes.

Another distinct advantage of incorporating magMPs within multi-cellular aggregates is the ability to manipulate their movement over multiple length scales, thereby providing new ways to study interactions of heterogeneous cell populations or homogeneous cells engineered within heterogeneous microenvironments. Distinct types of cells or preformed spheroids can be conjoined with control over the ratios of different cells, as well as their spatial organization with respect to one another in order to create more complex 3D spatial patterns[248]. The sensitivity of the spheroids in this study to magnetic manipulation was dependent on the number of magMPs incorporated. Therefore the magnetic sensitivity can be determined during the formation of spheroids and populations can be self-sorted in a rapid and scalable manner to form complex, organized structures from mixed populations of different types of spheroids. Magnetic field patterns could be specifically created with this purpose in mind to form hierarchical

139

tissue architectures with multiple cell types from a mixed population of multi-cellular aggregates.

The magMPs incorporated within multi-cellular aggregates are currently used for magnetic control of the spheroids; however, recent work from our lab and others has shown that MPs can also be used to deliver morphogenic factors locally within cell spheroids[154-156, 249]. Dual incorporation of magMPs and morphogen-laden MPs within pluripotent stem cell aggregates could be used to engineer the types of gradients observed during embryonic morphogenesis, a novel and powerful approach to study fundamental principles of developmental biology in a more controlled and tractable manner. This approach could also be complemented by encapsulation of individual 3D cell aggregates, like EBs, in engineered microgel niches to expose cells to patterned, heterogeneous environmental signals[250]. Specifically, a spheroid containing MPs loaded with a single morphogen could be merged together with three other spheroids each containing MPs loaded with complementary or antagonist molecules, as in Figure 6.10C, to pattern pluripotent cells in a polarized manner similar to what is observed in pre-gastrulation stage embryos. As such, spatiotemporal effects of controlled morphogen and inhibitor delivery could be studied to model aspects of human or mouse embryonic development and potentially be applied to the production of tissues from stem cells *ex vivo*.

Conclusions

The incorporation of magnetically sensitive microparticles within the extracellular environment of stem cell spheroids provides a facile means to control the subsequent

140

spatial location of spheroids in dynamic and suspension cultures using transiently applied magnetic fields. The number of magMPs incorporated could be controlled during the aggregate formation stages and determined the magnitude of aggregate response to applied magnetic fields. The method described herein was applied to single aggregates as well as large populations of spheroids without *a priori* design of materials or alterations to the cellular membrane. This work is suited to the construction of neo-tissues comprised of aggregates made from different cell types in which the spatial orientation is important to tissue function. In addition, combining magMPs with morphogen loaded MPs for localized delivery of multiple molecules within a single aggregate could be used for spatially controlled heterogeneous differentiation. Altogether, the incorporation of magMPs within stem cell spheroids represents an easily implemented method to further address significant questions of interest to the fields of stem cell biology, tissue engineering and cell bioprocessing.

CHAPTER 7

CONCLUSIONS

The formation of EBs is a reliable and commonly used method to induce the differentiation of ESCs into various somatic cell types. Hence, EB differentiation permits mechanistic studies of embryological development *in vitro*, including the examination of the effects of morphogenic cues on cell fate determination. Previous efforts to engineer the EB microenvironment have focused primarily on the regulation of EB size and cell-cell interactions, as well as addition of soluble factors, and ECM-molecules to EB cultures. The inherent 3D organization of EBs limits the effectiveness of 'outside-in' approaches which aim to affect differentiation of cells on the EB interior by controlling elements of the exterior EB environment. An alternative strategy to improve the control of the EB microenvironment in order to better direct ESC differentiation may be to use an 'inside-out' approach, such as integrating engineered biomaterials within the assembly of ESCs during EB formation. Engineering the interior of the EB microenvironment via molecularly engineered biomaterials to enhance the directed differentiation of ESCs could facilitate the production of large numbers of homogeneous cell populations useful to the development of regenerative cellular therapies and diagnostic cell-based technologies.

The work herein demonstrates the method of forced aggregation can be used to incorporate a variety of materials in pluripotent stem cell spheroids. Analysis of differentiation of EBs containing various types of unloaded MPs within aggregates demonstrated that the presence of materials themselves, in the absence of growth factors can modulate stem cell differentiation. With this conclusion in mind, gelatin MPs were

142

modified with the objective of achieving control of material-microenvironment interactions, specifically by conjugating heparin, a molecule with known growth factor interactions, to gelatin MPs. Incorporation of heparin-gelatin MPs within EBs resulted in increased changes in gene expression, growth factor secretion to the surrounding medium and localization of a marker for endothelial differentiation, VE-cadherin.

Gelatin MPs loaded with BMP-4 or Noggin and incorporated within EBs were investigated as a means to direct or inhibit mesoderm differentiation. Analysis of EBs containing growth factor loaded MPs demonstrated that gelatin MPs can be used to deliver BMP-4 within EBs to direct mesoderm differentiation. Analysis of growth factor release; however, demonstrated that gelatin MPs are not suitable for prolonged molecule release (longer than 24 hours) and other materials or methods of presentation may be necessary in protocols which require extended exposure to morphogens. This platform is not suited for differentiation which requires different stages of soluble factors, as release from gelatin MPs cannot be externally controlled once they are incorporated within EBs. EBs containing BMP-4 loaded MPs expressed higher amounts of mesoderm genes (Brachyury-T and Flk-1) as well as lower amounts of an ectoderm gene (Pax6). In addition to population based assays, formation of EBs using a Brachyury-T reporter ESC line demonstrated that the number of cells differentiated towards a mesoderm lineage was increased in BMP-4 gelatin MP treated EBs compared to solubly delivered BMP-4 and compared to untreated EBs. Importantly, analysis of the amount of growth factor used in MP based delivery vs. soluble delivery revealed that MP based delivery required 12 fold less growth factor. This finding is significant because the inefficiencies of currently used directed differentiation protocols combined with the large amount of cells needed for

143

development of clinically relevant therapies requires scalable processes for differentiation. MP based control of morphogenic factors is scalable because forced aggregation can be used to form EBs at a high density. These EBs can then be transferred to suspension cultures, which have a much higher culture area to volume ratio compared to monolayer cultures.

Formation of magnetically sensitive spheroids was successfully performed through the incorporation of magnetic MPs. Magnetic sensitivity was dependent on the number of MPs incorporated, a characteristic which could be useful in simple sorting of complex populations of EBs. Furthermore, control of the location of individual spheroids or populations of spheroids in dynamic or static suspension culture could be controlled with magnetic fields. This allowed for controlled agglomeration of single EBs or hundreds of EBs. Controlled heterogeneity within aggregates is expected to yield insights in the fields of developmental biology and tissue engineering, fields where the organization of multiple heterogeneous cell populations with respect to each other are vital to function.

CHAPTER 8

FUTURE WORK

In general, most of the strategies attempted thus far to direct EB differentiation have relied on an 'outside-in' approach to control aspects of the microenvironment. From the instant an aggregate of ESCs begins to form an EB, access to the interior intercellular environment and molecular composition of an EB becomes progressively restricted and 'outside-in' manipulation of cell fate within an EB becomes limited in its ability to direct cell differentiation. Although 2D differentiation of ESCs has been successfully used to spatially and temporally control the presentation of molecules for the differentiation of several cell phenotypes, the differentiation of some cells may require the synergistic effects of cell-cell and cell-ECM interactions provided within the context of EBs in 3D. Therefore, in order to efficiently control the 3D microenvironment of differentiating ESCs within EBs, further development of engineering technologies capable of directly influencing cell fates within EBs are needed.

Engineering the microenvironment within EBs is difficult because variables are difficult to isolate and control. Elements are constantly changing as the cells differentiate. Cells move within the EB and autocrine and paracrine signaling occurs as cells secrete morphogenic factors which can in turn affect differentiation. Additionally, cell-cell contacts are dynamic as the profile of cell adhesion molecule expression on the surface of the cells changes with differentiation. At later stages of EB differentiation, matrix production is an added variable. Extracellular matrix (ECM) molecules can regulate growth factor signaling by controlling molecule diffusion, and growth factor

145

binding availability and ECM molecules can present integrin binding sequences thereby providing another microenvironmental cue for cell behavior.

Work presented here demonstrates that forced aggregation is a flexible approach to incorporate various types of microparticles within stem cell spheroids and that the materials can present growth factors for directed differentiation. While MPs loaded with growth factors were capable of inducing mesoderm differentiation, areas of this work require further study.

2D vs. 3D differentiation

One topic that is of interest with respect to terminally differentiated somatic cell types derived from embryonic stem cells is whether or not they are truly mature, functional cells. Often cells derived from ESCs remain in an immature or embryonic-like state. For example, ESC-derived cardiomyocytes differ from adult cardiomyocytes in that they express immature action potentials, a characteristic which may be detrimental to their use in clinical treatments[251, 252]. Another example is neuronal cells derived from ESCs fail to generate functional, synchronously oscillating neuronal networks as do primary neural isolates[253]. *In vivo*, the cells from the inner cell mass, where ESCs are derived, go on to differentiate into each of the over 200 adult somatic cell types. Therefore conditions exist which could be used to differentiate mature, fully functional adult cells but it is likely that current differentiation protocols fail to completely mimic the complex, spatially and temporally controlled microenvironment required for maturation and complete functionality of certain cell types. The results presented in this work suggest that incorporation of biomaterials within stem cell aggregates may be a

146

method to better engineer the interior microenvironment. An important area for future study is the comparison between mature cell types derived from ESCs in a monolayer format vs. a 3D format with incorporated MPs. The hypothesis being that instructive cues provided by cell-cell and cell-ECM along with paracrine signaling from a heterogeneous population of cells will promote more mature differentiation of cell types.

Cellular movement within 3D constructs

One observation that deserves further study is the impact of MP incorporation on cell movement within spheroids. It was demonstrated that gelatin MP incorporation modulated phenotypic marker expression and this effect was dependent on the number of microparticles incorporated. Possible mechanisms for altered differentiation in the presence of gelatin MPs include integrin mediated signaling, alteration in cell-cell contacts and the ability of gelatin to act as a depot for secreted growth factors, thereby altering the local concentration of signaling molecules either by increased retention within the spheroid or by depletion of these same factors. One possible mechanism which may prove important even in the presence of morphogen delivery is the effect of adhesive materials on cellular migration during EB differentiation. It is well known that cellular migration plays a vital role in the progression of morphogenesis and tissue formation. For example, cell migration drives the process of gastrulation, critical for proper embryo development. In time lapse videos of EB formation, extensive cell movement was observed in the x, y and z planes. When microparticles were added to the cells, cellular movement appeared to decrease, dependent on the number of added MPs. Because EBs are often used as models of early mammalian development MP

147

incorporation could possibly be used to study the differentiation effects of stunted cell migration. Additionally, MPs engineered to present specific cell adhesion molecules, such as cadherins, could be utilized to study cell movement or to localize the delivered signal to cells expressing the same cadherin.

Another application of the magMP constructs could be to study cell migration. Interestingly, when EBs formed from fluorescently labeled ESC populations merge over a period of 24-48 hours, the fluorescent signal remains localized within the quadrant of the original EB (Figure 6.10C) suggesting that cell movement is limited or else the fluorescent cells would be completely mixed. Restricted cell movement is likely due to homotypic E-cadherin interactions between cells. This could be studied experimentally by reducing the concentration of calcium ions in the media thereby disrupting homotypic e-cadherin interactions in which calcium ion dependent hydrogen bonding is necessary[254]. If under low calcium conditions, the cells were able to migrate further the fluorescence from each ESC population would be mixed across the aggregate and fluorescence from each of the original populations would be diffuse throughout the aggregate. This same platform could be applied to study of developmental processes such as epithelial to mesenchymal transition (EMT) which occurs during gastrulation. During the EMT process, cells transition from an epithelial phenotype to migratory mesenchymal cells. In this case the fluorescence in the construct would change from localized quadrants to diffuse fluorescence as the cells down-regulate e-cadherin and differentiate towards mesoderm lineages. The EMT process is also implicated in a variety of diseases including tumor cell metastasis[255]. Because *in vitro* culture of explanted tumor cells are often cultured as spheroids, magMP incorporation could be

148

applied to study the process of metastasis within constructs composed of mixed populations of tumor cells and non-cancerous cell types. These constructs could be used to study the effects of cell co-culture or small molecule libraries and their effects on tumor cell migration and viability in a 3D model. High-throughput formation of cell constructs, as the one shown in Figure 6.10C would allow for screening of conditions promoting or inhibiting the EMT process. Microfluidic platforms would be advantageous both as a method for high-throughput formation of heterogeneous constructs and also for high-throughput fluorescent analysis, analogous to identification of desired mutants in *C. Elegans* populations[256, 257].

Next generation materials

During mammalian organogenesis, the spatial-temporal presentation of molecules is tightly regulated and exquisitely synched with processes such as cell migration, differentiation and maturation to direct the combination of both terminally differentiated cells and progenitor cells to form functioning organs. The work presented in this thesis focuses on the use of microparticles to deliver morphogens within 3D aggregates of pluripotent stem cells for directed differentiation. A long-term goal of the technology is to form neo-tissues *in vitro* from a starting population of ESCs. Two possible routes to this end include: either priming or "jumpstarting" differentiation towards cells of a specific lineage, such as mesoderm, thereby relying on the cells to produce their own autocrine and paracrine factors to produce mature cell types, or secondly, the materials could be engineered to deliver multiple morphogens with specific starting and stopping points.

149

A current limitation of gelatin, agarose and PLGA particles is that the materials are not stimuli responsive. Loaded morphogens are released continuously based on polymer degradation rate (PLGA) or diffusive mechanisms regulated in some respect by affinity interactions between the morphogen and hydrogel base material. Therefore, these materials are limited in their ability to temporally control morphogen delivery; delivery of loaded morphogens begins as soon as the materials come into contact with cells. It may be that the cells in an undifferentiated state do not express receptors necessary to respond to these signals and therefore, the signal is wasted or minimally effective. Equally important is the need to turn off signals or switch the delivered morphogen to guide the cell through various stages of differentiation. Work presented here serves as the framework to incorporate various materials and even to pattern multiple spheroids using magnetic manipulation to spatially pattern multiple populations of microparticles within single, merged spheroids. Likewise, proof-of-principle experiments have demonstrated that morphogens, such as BMP4, can be delivered from microparticles to direct stem cell differentiation. Therefore, attention should be given to design materials which are capable of responding to either cell based signals or externally applied signals.

An example of a cell-based trigger could be matrix metalloproteinase (MMP) sensitive linkers embedded in the microparticle material. The morphogen of interest would be freed from covalent attachment to the biomaterial after cell triggered cleavage of the linker, but only when the cell has differentiated to point that it is able to express the selected MMP[258, 259]. The MMP profile of spontaneously differentiating embryonic stem cells is as of yet not fully known and would require characterization before this

150

method could be implemented.   Early treatment with soluble factors or with microparticles delivering a soluble cue-- Noggin, for example, can induce specific MMP expression in ESCs[260]-- could be used to induce MMP expression.

As an alternative to cell-triggered responses, externally applied stimuli could be used to control the kinetics of morphogen release. Several reviews are available which discuss a variety of stimuli responsive materials[261-263], including those sensitive to the acidity of the microenvironment, temperature, light, applied electric and magnetic fields or changes in ion concentration. Of particular interest are methods which can be externally applied to microparticles incorporated in EBs.

Induction of VEGF production

The effects on differentiation of heparin-modified gelatin MPs, suggest that further study should be undertaken on what specific factors are interacting with the MPs. Several pieces of data led to the hypothesis that incorporation of heparin with the EB promoted endothelial cell differentiation, including increased secretion of VEGF and increased expression of VEGF receptors Flk-1 and Flk-1. To further test this hypothesis endogenous VEGF production could be induced by culture of EBs in hypoxic environment.   Hypoxic conditions induce VEGF production through the hypoxia-inducible factor-1 pathway[264]. Increased VEGF production by EBs with and without heparin-modified gelatin MPs would elucidate whether or not increased VEGF production in heparin-gelatin MP treated EBs is responsible for the localized expression of VE-cadherin expression observed at day 7. Increased VEGF expression could also be used to test whether the binding VEGF binding capacity of the heparin-gelatin MPs is

151

exhausted under normoxic conditions or whether increased VEGF production would further magnify the effects of heparin incorporation on ESC differentiation.

Paracrine capture

Just as endogenous growth factors secreted by differentiating ESCs can be used to direct ESC differentiation, these factors could possibly be captured for use in wound healing models. This would require retrieval of the MPs from the EBs after formation. Several possible routes to disrupt the spheroid for MP retrieval could be examined; with the requirement being that the treatment does not disrupt protein interactions with the heparin. This would exclude trypsin treatment but mechanical dissociation could still be used. Another hurdle is purification of the freed MPs from the disassociated cells, important because delivery of undifferentiated cells leads to teratoma formation. The MPs are of a different density than the cells and centrifugation separation could be used; however, an approach with likely a higher efficiency of purification would be to form the gelatin MPs with nano-sized magnetic material thereby making the MPs magnetically sensitive for purification purposes. Prior to MP formation, magnetic material could be mixed with the base polymer and physically entrapped within the MP during the emulsion stage and crosslinking stages. As an alternate approach, the entire population of EBs containing the heparin-gelatin MPs could be acellularized using the method previously reported by the McDevitt lab. The intent of acellularization is to create a biomaterial containing ECM and growth factors of an embryonic-like environment for wound healing or revascularization purposes. Acellularization of EBs containing particles capable of sequestering growth factors and limiting secretion of these factors

152

into the medium where they are washed away, would likely enhance the benefits observed from EBs acellularized without MPs. This idea could also be tested by first soaking the heparin-gelatin MPs in media conditioned from later time point EBs. The particles could then be delivered in a wound healing model as a preliminary test of growth factor capture.

Glycosaminoglycan based microparticles

It was demonstrated that heparin modification of gelatin MPs resulted in altered differentiation of EBs. It is likely that with biomaterials fabricated from other glycosaminoglycans (GAGs), such as chrondroitin sulfate or hyaluronic acid, will have differing growth factor interaction profiles. One recent study reported that methacrylation of chondroitin sulfate allowed for facile fabrication of microparticles composed entirely of chondroitin sulfate which could then be incorporated within stem cell aggregates[265]. A further application would be to combine methacrylated GAGs in various ratios, crosslinked together as MPs to create synthetic extracellular matrices for directed differentiation. Use of these MPs should be investigated in spheroids of other stem cell types including mesenchymal stem cells spheroids.

APPENDIX A

SYSTEMATIC ENGINEERING OF 3D PLURIPOTENT STEM CELL NICHES TO GUIDE BLOOD DEVELOPMENT[§]

Authors and affiliation:

Kelly A. Purpura[1,2], Andrés M. Bratt-Leal[5], Katy A. Hammersmith[5], Todd C. McDevitt[5,6], Peter W. Zandstra[1-4*]

[1] Chemical Engineering and Applied Chemistry, Univ. of Toronto, Toronto, ON

[2] Institute of Biomaterials and Biomedical Engineering, Univ. of Toronto, Toronto, ON

[3] McEwen Centre for Regenerative Medicine, University Health Network, Toronto, ON

[4] Heart and Stroke Richard Lewar Centre of Excellence, Toronto, ON

[5] The Wallace H. Coulter Department of Biomedical Engineering, Georgia Institute of Technology/Emory University, Atlanta, GA

[6] The Parker H. Petit Institute of Bioengineering and Bioscience, Georgia Institute of Technology, Atlanta, GA

*Corresponding Author:
Peter W. Zandstra, Ph.D., E-mail: peter.zandstra@utoronto.ca

Department of Chemical Engineering and Applied Chemistry, University of Toronto
Terence Donnelly CCBR, 160 College St., Office 1116
Toronto, Ontario, Canada M5S 3E1

Abstract

Pluripotent stem cells (PSC) provide insight into development and may underpin new cell therapies, yet controlling PSC differentiation to generate functional cells remains a significant challenge. In this study we explored the concept that mimicking the local in vivo microenvironment during mesoderm specification could promote the emergence of hematopoietic progenitor cells from embryonic stem cells (ESCs). First, we assessed early phenotypic markers of mesoderm differentiation (E-cadherin, brachyury, PDGFRα, Flk1; ETPF) and revealed that E-T+P+F+ cells have the highest capacity for hematopoiesis. Second, we determined how initial aggregate size influenced the emergence of mesodermal phenotypes (E-T+P+F+, E-T-P+/-F+, and E-T-P+F-) and discovered that colony forming cell (CFC) output was maximal with ~100 cells per PSC aggregate. Finally, we introduced these 100-cell PSC aggregates into a low oxygen environment (5 %; to upregulate endogenous VEGF secretion) and delivered two potent blood-inductive molecules, BMP4 and TPO (bone morphogenetic protein-4 and thrombopoietin), locally from microparticles to obtain a more robust differentiation response than soluble delivery methods alone. Approximately 1.7-fold more CFCs were generated with localized delivery in comparison to exogenous delivery, while combined growth factor use was reduced ~14.2-fold. By systematically engineering the complex and dynamic environmental signals associated with the in vivo blood developmental niche we demonstrate a significant role for inductive endogenous signaling and introduce a tunable platform for enhancing PSC differentiation efficiency to specific lineages.

155

Introduction

Many developing cell therapies and tissue engineering approaches seek to mimic aspects of development to produce therapeutic cells or promote healing within specific microenvironmental contexts. Pluripotent stem cells such as embryonic stem cells (ESCs) are a useful resource for elucidating mechanisms of development and offer tremendous potential for regenerative cell therapies. Although progress has been made in generating many cell types from PSC, the challenge to develop appropriate and scalable inductive processes for targeted cell generation still remains. Differentiation of pluripotent stem cells is commonly induced as 3D cell aggregates, termed embryoid bodies (EBs); a multicellular complex capable of recapitulating various morphogenetic cues from gastrulation and responding to exogenous factors relevant to lineage specification. EBs reproduce many of the temporal and spatial relationships found during normal embryogenesis[266], however, they lack critical developmental factors including biomechanical regulators[267], paracrine signals and the cellular migration that occurs within the murine yolk sac, embryo proper, and placenta[268, 269]. Herein we explore the prospective engineering of mesoderm and blood development inductive signals into differentiating aggregates of pluripotent cells, specifically focusing on environmental control of endogenous signaling and the local delivery of exogenous signaling factors.

During mouse gastrulation, morphogenetic movements coupled with cell proliferation and differentiation convert an embryo from two layers (primitive ectoderm and primitive endoderm) to a trilayered structure[270]. The epiblast cells (embryonic ectoderm) undergo an epithelial-to-mesenchymal transition (EMT), mobilize and migrate through a transient structure called the primitive streak. The primitive streak contains

156

nascent mesoderm that transiently expresses the T-box transcription factor, Brachyury (T) and acts as a specific site of cell ingression, as the three definitive germ layers, endoderm, mesoderm, and ectoderm form[271]. Undifferentiated ESCs express epithelial-cadherin (E-cad) which mediates initial EB formation, and is an indicator of pluripotency that is downregulated during differentiation and EMT events[272-274]. To measure the influence of diverse niche factors on mesodermal differentiation we first set out to determine an early mesoderm / CFC predictive phenotype associated with the primitive streak that could serve to accelerate our niche screening efforts. We investigated the phenotypes generated by combining E-cad staining with the pan mesodermal marker brachyury (T)[35, 275], and two receptor tyrosine kinases: platelet derived growth factor receptor-α (PDGFRα) and vascular endothelial growth factor (VEGF) receptor-2 (Flk1), that are expressed by early mesodermal cell types[276] and have been associated with axial, paraxial and lateral plate mesoderm.

We hypothesized that greater spatiotemporal control may allow quantitative contribution of normally convoluted niche parameters and provide insight into how to improve direct differentiation to desired lineages. The physical size of EBs has been reported to influence the proportion of cells differentiating toward specific lineages[48, 277] and impacts diffusion of soluble molecules[78]. We took advantage of recent advances to control EB size though forced centrifugation in micro-pyramidal wells[49] to influence endogenous interactions with the microenvironment. Using a range of mouse ESC aggregate sizes we assessed the predictive value of the identified mesoderm phenotypes (based on E-cad, T-GFP, PDGFRα, Flk1 expression: +/-ETPF) with respect to blood progenitor (CFC) output. We replaced exogenous soluble factors with local

157

delivery within the cell aggregate from microscale biomaterials to mimic factors normally delivered in a more systemic fashion[150, 157]. This approach has been used in hESC and mESC aggregates to control the release of small molecules and proteins within the local 3D microenvironment[154, 155, 161, 278]. These systems employed a variety of biomaterials, including poly (lactide-co-glycolide) (PLGA) or gelatin microparticles (MPs) capable of sustained release of molecules in a bioactive form. However, none of the previous systems used small aggregates of ESCs (more closely mimicking the developing embryo) or specifically induced cells towards the hematopoietic lineage.

Materials and Methods

Cell culture

Brachyury-GFP cells (E14.1, 129/Ola)[212] were maintained on 0.5 % gelatin coated flasks in a humidified 5 % CO_2 atmosphere, using the modified serum-free maintenance media and base differentiation media previously described[199]. Differentiation was initiated with 5 ng/mL BMP4, 25 ng/mL VEGF (Sigma-Aldrich, St.Louis, MO), and 50 ng/mL TPO (R&D Systems, Inc. Minneapolis, MN) in normoxia (20% O_2) from d0-2/4; only BMP4 and TPO were used in hypoxia (5% O_2).

Size controlled aggregation

Full or partial microwell inserts[49] were attached to 6- or 24-well plates using polydimethylsiloxane, and allowed to cure overnight at 37ºC. Plates were sterilized with UV and 70 % ethanol prior to coating with 5 % (w/v) Pluronic F-127 (Sigma). Wells were washed twice with PBS, and allowed to stand in media for a minimum of 30 min at

158

37ºC prior to seeding. Full-well inserts were seeded with a single cell suspension in differentiation medium (3.0 mL) at the desired number of cells/microwell and centrifuged for 5 min at 200g. Partial-well inserts were similarly seeded, however cells were suspended in 4-6 mL DMEM (Invitrogen) to minimize the effect of the uneven surface area of the well bottom. Cells not captured within the micropatterned square-pyramidal wells were carefully removed by aspiration and 3.0 mL of growth media was added. 200x200 μm wells were used to aggregate 1-20 cells (24000 agg/6-w insert), and 400x400 μm wells for 50-200 cells (6000 agg/6-w; 1200 agg/24-w).

<u>Encapsulation process</u>

To encapsulate 100 cell aggregates, 0.12×10^6 cells were seeded/well in a 24-well plate in a final volume of 1-1.5 mL differentiation media. Approximately 40 hours later, for each test condition triplicate wells were collected and settled to 100 μL. Encapsulation and washing was completed as previously described[199], except a lower vortex speed (7.25, Vortex-Genie2®, Scientific Industries Inc. Bohemia, NY) and centrifuge setting (350 g) was used. Aggregates were counted pre-and post-encapsulation in a gridded 35 mm petri dish or 24-well plate. Following encapsulation, the sBVT condition was split into one culture without factors and another with sBVT in normoxia or sBT in 5% O2 for a further two days (d2-4) as indicated. Aggregates with MPs were split between normoxia (with 25 ng/mL VEGF d2-4) and 5% O2.

Fluorescent automated cell sorting (FACS)

Flow cytometric analysis expression and cell sorting was carried out as described[279]. Staining of more than 5 samples was completed in a V-bottom 96 well plate with 20 µL of sample or control cells. Primary antibodies, E-cadherin (R&D) and PDGFRα-biotin (eBioscience Inc. San Diego, CA) were added at 1:100 for 25 min on ice before washing twice with HF (2% FBS in Hank's Buffered Salt Solution). Secondary or conjugated antibodies (BD, Franklin Lakes, NJ) were added at 1:200 for 35 min on ice: goat anti-mouse PECy7 (Santa Cruz Biotechnology Inc., Santa Cruz, CA), Stv-APC-Cy7, Flk1-APC or isotype rat IgG2 before washing twice and resuspending in 1µg/mL 7-amino-actinomycin D (7AAD, Molecular Probes® Invitrogen). Occasionally, PDGFRα-APC, Flk1-PE and their corresponding isotypes were used. Cells were analyzed on a BD FACSCanto (Firmware version 1.14), using BD FACSDiva software (Version 5.0.1) with positive staining defined as fluorescence emission > 99.1 % of negative control cells from the same starting population or undifferentiated cells. Cells were sorted on a BD FACSAria and collected in IMDM supplemented with 10 % serum, washed and resuspended in serum-free medium without growth factors.

Hematopoietic cell assays

EBs were dissociated with 0.25 % trypsin-EDTA (3 min, 37 °C, Sigma) before seeding the myeloid-erythroid colony forming cell assay (ME-CFC) at 100 000 c/mL in 35 mm duplicate plates (M3434, Stem Cell Technologies, Vancouver, BC) or at 60-100 000 c/mL in 24-well plates (0.5 mL duplicate wells). Previously sorted cells were

160

also seeded in 24-well plates, but at variable densities below 20 000 c/mL (2-3 wells with 0.3 mL). Colonies were enumerated 7-10 days after seeding as previously detailed[280].

Manufacturing and loading gelatin microparticles

Microparticles of type A (G1890) or B (G9391, Sigma) gelatin were generated using a water-in-oil emulsion method and fluorescently labeled as previously described[201]. Expected electrostatic interactions between the gelatin types and proteins were examined using ExPASy's Compute pI/MW program (www.phosphosite.org/psrSearchAction.do)[213, 281]. Heparin sodium salt (CalBiochem, San Diego, CA) was conjugated to gelatin type A MPs after MP formulation in the following manner. EDC and S-NHS (Thermo Scientific, Waltham, MA) were added to heparin at 10:1 and 25:1 molar ratios respectively, relative to heparin dissolved in 800 µL activation buffer (0.1M MES, 0.5M NaCl, pH 6.0) and reacted for 15 min at room temperature to modify the carboxyl groups of heparin to amine reactive S-NHS esters. The EDC/NHS reaction was quenched with 20 mM 2-mercaptoethanol and the activated heparin was added to 400 µL of particles in PBS at a 5:1 molar ratio of heparin to gelatin and allowed to react with agitation for 4 hours at 37ºC. Prior to cell culture, MPs were treated in 70 % ethanol for a minimum of 30 min before washing 3x with ddH$_2$O. Each MP batch was lyophilized and stored at -20 C. Growth factors were added to MPs at 5-5.5 µL/mg and kept overnight at 4 C, MPs were resuspended in differentiation media ($\leq$ 500 µL) and counted on a hemocytometer to estimate the concentration (ng/MP). For use with cells, BMP-MPs were loaded using 10-50 µg/mL stock solutions, and TPO-MPs were loaded with a 50 µg/mL stock.

161

Generating mixed aggregates: microparticles and cells

A single cell suspension was generated from undifferentiated T-GFP ESC and centrifuged into the microwells as described above; 200g for 5 min. Resuspended microparticles were added to the wells to obtain the desired factor concentration before centrifuging a second time at 200g for 5 min. This method of aggregate and MP formation has also been achieved with D3 ESC[201]. Aggregates were maintained with full media exchange in the microwells (daily or daily starting at 48h) prior to removal of soluble growth factors and transfer to Petri dishes on day 4. Alternatively, aggregates were removed 38-42 h after formation for encapsulation in agarose and/or dilution into 60-100 mm Petri dishes at approximately 300 aggregates/mL.

Human BMP4 ELISA

A quantitative sandwich enzyme immunoassay technique was used to determine BMP4 concentration after release from MPs suspended in PBS, based on the manufacturer's protocol (R & D, DBP400). Briefly, 2-5 mg of MPs were suspended in 750 μL of a 0.1% solution of BSA in PBS at 37ºC with rotation; at each sample time point 300 μL was removed following centrifugation of the microparticles and replaced with an equivalent volume.

Statistical analysis

Unless indicated, data are reported as mean ± standard deviation of the mean. Statistical significance was assessed using one-way ANOVA with Tukey's post hoc analysis, student's t-test, or nonparametric Mann-Whitney test (Minitab 15/16, State

162

College PA and OriginPro7.5 Northampton, MA). P-values of less than 0.05 were considered significant ($n \geq 3$).

RESULTS

Cell population phenotypes

We previously demonstrated that in serum-free conditions the addition of a trio of mesoderm inducing cytokines, BMP4, VEGF, and TPO (BVT) resulted in an induction of myeloid-erythroid colony forming cells (ME-CFC)[197]. In order to quantitatively measure the impact of our niche engineering efforts on hemogenic mesoderm generation we sought to develop a set of predictive phenotypic markers. Multiple cell lines respond to this differentiation strategy, however, to trace the dynamic process of mesodermal specification in greater detail we employed the Brachyury (T)-GFP line[212]. We postulated that the dynamic upregulation of brachyury and downregulation of E-cadherin, that appear to signal the upregulation of two mesodermal receptors (Flk1 and PDGFRα), could be used in combination to identify the putative hemogenic population for tracking purposes.

Monitoring the expression of E-cadherin, brachyury, PDGFRα, and Flk1 during differentiation distinguishes 16 possible phenotypes (Figure1 A). Once differentiation was initiated with BVT, E-cadherin expressing cells (E+T-P-F-) progressively downregulated that adhesive molecule while brachyury and both surface receptors were upregulated (Figure 1B). The presence of either one or both of the tracked receptors in the absence of brachyury was only observed after the initial peak of E-T+P+F+/- cells and may correspond to more differentiated cells (day 5, Figure 1B). Due to the rarity of

163

many of the phenotypic populations it is likely that they represent transient expression states during lineage specification.

We grouped the expression patterns into populations that could broadly be classified as having mesendoderm (ME), mesoderm (M), endoderm (E), or unknown potential, and differences in their gene expression profiles demonstrate this. We sorted the most abundant day 3.75 phenotypes associated with hemogenic mesoderm and assessed their colony forming capacity after 3 more days of suspension culture (the standard time to assess CFC). We found that the E-T+P+F+ population had the greatest hemogenic capacity, and was significantly enriched compared to the unsorted population and all other fractions (Figure 1C). The total number of colonies generated from the unsorted population was equivalent to the sum produced by the individual sorted fractions once the initial frequency of these phenotypes was taken into account. This analysis defined the starting population necessary to further track and optimize parameters of hemogenic mesoderm differentiation.

Aggregate size and mesodermal phenotype

Endogenous signals can impact differentiation[34] and it has been established with both 2 and 3D systems[282, 283] that the number of neighboring cells impacts autocrine and paracrine factors within the immediate media surrounding the cells[284, 285]. Thus, we examined how the initial number of cells per aggregate influenced mesoderm differentiation due to the interplay of endogenous stimulatory or inhibitory signals and exogenous factors (Figure 2A) utilizing a centrifugal forced-aggregation strategy[49] and assessing the resultant phenotypes and functional cell types. Total cell

164

density was controlled by seeding different cell numbers into 200 or 400 micron square-pyramidal well inserts that covered an eighth-, quarter-, half-, or full-well within 6-well plates (Figure 2B) to normalize the levels of nutrients and growth factors in the bulk media. The conditioning effect that occurs with larger cell aggregates during microwell differentiation was demonstrated by exchanging media between 10- and 100-cell aggregates. Media conditioned for two days by 100-cell aggregates boosted the CFC output of the smaller aggregates while no striking effect was observed with the reverse media exchange.

Mesoderm phenotypes associated with CFC potential were modestly enhanced with increasing aggregate size (Figure 2C). To insure that similar differentiation kinetics occurred across the different aggregate sizes we evaluated the CFC output of day 7-9 EBs; the greatest output occurred on day 7 for each size (Figure 2D). The hemogenic capacity of aggregates mirrored the trends of the combined phenotypic response and was maximal with 100-cell aggregates (1 in 145 ± 8 d7 cells). Uniformly sized aggregates initially seeded at 50-200 cells produced significantly more CFC ($p < 0.05$) than non-uniform LSC aggregates. Without inductive factors (BVT), spontaneous differentiation accounts for less than 0.5% of the CFC produced (data not shown). Thus, the addition of soluble factors is necessary to initiate hemogenic induction within the 100-cell aggregates. Based on the results of these studies, aggregate size was fixed at 100 cells for further investigations.

<u>Microparticle growth factor delivery</u>

Pluripotent populations demonstrate heterogeneity and plasticity in vitro and these properties can be modulated by extrinsic signaling[286], thus we sought to provide exogenous factors locally using growth factor delivery vehicles incorporated within the cell aggregates. Local delivery within multicellular aggregates may enhance the efficiency of differentiation by increasing the effective growth factor concentration and limiting the formation of gradients. We first confirmed that the physical incorporation of gelatin microparticles (MPs) within the extracellular space of 100 cell aggregates (Figure 3Ai) did not adversely influence aggregate formation, brachyury expression, or CD45 output. By varying the seed ratio of MP to cells, we noted that 1 MP to 3 or more cells produced stable aggregates with incorporated particles distributed throughout the volume of the 3D spheroids (Figure 3B, S4C).

The electrostatic affinity between charged biomolecules and gelatin species has been the impetus behind its use as a matrix for the controlled-release of bioactive molecules (reviewed in[287]). The characteristic isoelectric point (pI) of gelatin depends on the manufacturing conditions and it is expected that protein retention would be enhanced in gelatin of the opposite charge (Figure 3Aii). We tested the bioactivity of growth factor release from gelatin A or B MPs with 100-cell aggregates by seeding different amounts of BMP4-loaded MPs (B-MP, Figure 3B). To examine the inductive effect and release kinetics of BMP4, cells were grown in the wells until T-GFP was measured on day 4.5 with media exchange (ME) occurring daily or daily after an initial 48 hours of culture (d2ME). Brachyury expressing cells reached a plateau of ~70% with 2-15 ng/mL soluble BMP4 (sB) treatment in the presence of either gelatin A or B

166

unloaded MPs (U-MP, Figure 3B). Brachyury induction from both type A and B MPs was equivalent to soluble delivery if media was left standing for 2 days, however, with daily media exchange T-GFP and hence BMP4 release was significantly reduced (* p < 0.05). However, this robust response was only seen if media exchange began 48 hours after seeding, suggesting that BMP4 release kinetics were not optimal. Compared to continuous delivery, 24h soluble BMP4 reduced the percent of brachyury positive cells by ~10% (** p < 0.05), and a similar proportion of T-GFP cells was observed with gelatin A MPs (Figure 3B). BMP4 release from type A gelatin induced similar levels of T-GFP as 24h delivery of soluble BMP4, in contrast, type B gelatin was unable to induce Brachyury with daily media exchange, and T-GFP expression was significantly lower compared to both type A MPs with daily exchange and 24h († p < 0.05, Figure 3B), suggesting that not enough BMP4 was released due to stronger electrostatic interactions with the negatively charged gelatin. These dose responses indicate that MP delivery induced mesoderm differentiation similarly to bulk delivery. We next explored the capacity to increase cellular responses by tuning the release kinetics of our growth factor delivery vehicle through molecular engineering.

Growth factor release

To further investigate the interaction of BMP4 with gelatin A or B MPs we varied the stock concentration from 5-25 μg/mL and determined the characteristic release profiles by ELISA. Very rapid and full release from gelatin A MPs occurred within 24h when loaded with a 5 μg/mL BMP4 stock solution (Figure 3C). In contrast, only 35% BMP4 was released over the same time from gelatin B MPs. Neither of these release

167

kinetic profiles would be capable of sustained-release on the order of 4 days and allow

the cell aggregates to be transferred to bulk conditions for extended culture. Doubling

the stock concentration of BMP4 doubled its release from gelatin B, however, using a 25

µg/mL stock resulted in a more variable and intermediate extent of release (~50%)

(Figure 3C). The heparin binding domain of BMP4 has recently been identified[288],

thus, we conjugated heparin to type A gelatin MPs to take advantage of the total release

by enhancing the loading capacity via high affinity binding sites. We found that 35% less

BMP4 was detected in solution with heparinized type A gelatin MPs than untreated

gelatin A MPs and this was on the same order of release as gelatin B MPs (Figure 3C).

We hypothesized that using the heparinized type A MPs loaded with BMP4 from stocks

≥ 10 µg/mL would enhance the overall delivery and bioactivity of the heparin-bound

presentation of the morphogenic factor.

We successfully replaced soluble BMP4 with local delivery or presentation of

affinity-bound BMP4 using the heparinized gelatin A MPs in combination with sVT.

The MPs were seeded with 100 cells to form aggregates that were transferred to bulk

suspension culture on day two (Figure 3D). We next sought to integrate local factor

delivery with other cell inductive parameters in a manner that would lead to robust blood

cell development.

Low oxygen environment with growth factor delivery

We and others have shown that low oxygen tension (5 % O_2) is beneficial in

generating hemogenic mesoderm[289, 290] via a mechanism that dynamically tunes

VEGF signaling. We combined 5% oxygen tension with local factor delivery to enhance

168

blood development in the absence of exogenous VEGF. Gelatin microparticles were incorporated in 100-cell aggregates to support mesoderm development either loaded with BMP4 or TPO (previously shown to enhance CFC production), or as unloaded controls (Figure 4Ai). Cells were allowed to form stable aggregates for 32-42 hours before they were removed from the microwells and encapsulated in agarose to allow our engineered niche to be incorporated into suspension culture processes (Figure 4Aii). Brachyury induction was apparent after 3 days (Figure 4Aiii) and in addition to the soluble growth factor controls (BMP4, TPO), 25 ng/mL VEGF was provided for 4 days in normoxia (20% O_2) in order to match the CFC induction due to VEGF upregulation in 5% O_2.

Although thrombopoietin (pI 9.4) has a slightly higher pI than BMP4, we hypothesized that it would interact with the heparinized gelatin MPs in a similar fashion. We found that increasing the dose of BMP4 delivered by the MPs, while holding the dose of TPO relatively constant (range 9-15 ng), yielded an increasing number of CFCs (Figure 4B). The cells were split between normoxic and hypoxic conditions following encapsulation and similar trends were observed in both the phenotypic induction and CFC output in response to the B-MP and TPO-MP delivery regardless of oxygen tension, indicating that cells in low oxygen effectively upregulated endogenous VEGF to replace the exogenous delivery in normoxia.

In normoxic conditions 2-5 ng/well B-MP with TPO-MP delivery generated an increasing trend in CFC output but did not significantly differ from the soluble BVT (d0-2) control. Providing 8 ng/well B-MP provided a significant improvement over two days of soluble factors and was similar to the sBVT (d0-4) control. The highest CFC output occured with 12 ng/well of B-MP delivery. This indicates that depending on the

169

dose provided the factors were active following encapsulation (i.e. 8 ng, d0-4 and 12 ng, > 4 days). The early mesodermal phenotypes observed at day 4 (E-T+P+F+ and E-T-P+/-F+) correlated to the CFC producing cells present at day 7 (Figure 4C). Representative erythroid, myeloid and mixed colonies are shown from the 5 ng/well B-MP normoxic condition (Figure 4D). Altering the presentation of the growth factors, either from MP delivery or 5% O_2 induction, did not significantly alter the proportion of colony types produced by the majority of the different treatment conditions.

Seeding 8 or 12 ng BMP4 and ~12 ng TPO within the spatial context of 100-cell aggregates (1200 total) appears to induce comparable, if not greater, mesoderm differentiation than 5 ng/mL exogenous BMP4 and 50 ng/mL TPO. When the total growth factor loaded into the MPs and the additional media required for the soluble control following encapsulation (300 agg/mL) are accounted for, roughly 14x less BMP4 and TPO was required for local MP delivery/presentation than for bulk delivery.

In all, we have demonstrated that tracking the emergence of E-T+P+F+, E-T-P+/-F+, and E-T-P+F- phenotypes can predict the general capacity of a culture to produce CFC when seeded 3 days later, and aid in understanding the various microenvironmental factors capable of impacting CFC production. Aggregate size can be used to enhance CFC with soluble factors and manipulating the microenvironmental niche through controlled aggregation with microparticles that deliver BMP4 and TPO can generate greater numbers of CFCs than soluble delivery (~1.7x) of factors in both low oxygen (sBT) or normoxic (sBVT) environments. These results demonstrate that local delivery by affinity-bound presentation of growth factors from biomaterials can effectively induce mesoderm differentiation.

170

DISCUSSION

Modulating cell-cell interactions and the effects of autocrine, paracrine, and exogenous factors through initial aggregate size, oxygen tension, and local growth factor delivery, has provided insights into directed differentiation by monitoring both cellular phenotypes and functional responses. We first explored the differential expression of mesodermal cell phenotypes and the functional CFC response to exogenous growth factors in a serum-free media. We used a serum-free culture system that maintains the self-renewal of undifferentiated ESCs[197, 291] and the embryoid body system to model blood development as it induces differentiation similar to embryonic gastrulation. In an aim to better define and characterize subsets of nascent mesodermal cells for tracking and culture optimization purposes we monitored E-cadherin, brachyury, PDGFRα and Flk1.

Flk1 positive cells have been associated with hematopoiesis and vasculogenesis[212, 292, 293], as well as other mesodermal cell types[294-296]. Two-marker cell sorting strategies have demonstrated that P+F- cells have substantial muscle regeneration potential[297], while P^+F^+ cells demonstrate enhanced cardiac potential[298, 299], and P-F+ cells retain hematopoietic potential[299]. Monitoring E-cadherin and T-GFP[212] expression provided an indication that mesodermal differentiation was proceeding in our cultures and we combined these markers with PDGFRα and Flk1 expression to delineate potential hematopoietic progenitors. For the first time, we demonstrated that cells co-expressing brachyury, Flk1, and PDGFRα had the highest frequency of CFC formation when they did not express E-cadherin. Presumably the CFC output represents the cell autonomous capacity of the sorted phenotypes, as the cells were allowed to mature for an additional three days without the addition of exogenous growth

171

factors. Furthermore, the close link between the cardiac potential (P+F+) and hematopoietic potential (E-T+P+F+) raises the question whether a bi-potent cell population remains at the time we sorted. Insight from these phenotypes can be used to aid future developments in cell generation processes.

Focusing on parameters that may easily be incorporated into engineered systems to enhance hematopoietic specification, we next investigated the influence of local cell density. Examining the initial developmental stages leading up to the assessment of phenotypic expression, we showed an increasing proportion of hemogenic cells with increasing aggregate size (1-200 cells), with a maximum at 100-cell aggregates (Figure 2B). Aggregates seeded with 5-200 cells with or without growth factors continued to expand at similar growth rates, such that there were no significant differences in population doublings between the conditions. As the rate of aggregate growth was not strongly influenced by initial cell numbers, controlling both aggregate size and the total aggregates per well assured similar numbers of the bioactive molecules (BMP4, VEGF, or TPO) were available on a per cell basis in the bulk media or macroenvironment.

Taking advantage of the capacity for microenvironmental control from within the aggregate itself we incorporated gelatin MPs as a delivery vehicle to locally present BMP4[288]and TPO[300], which have known and presumed heparin binding domains and hemogenic induction capacity. Heparin has previously been used with scaffolds to sustain the release/presentation of heparin binding growth factors (HBGF)[301] and its use with particulate systems for controlled delivery of HBGF is an emerging area in tissue engineering[302]. In addition, although the specific heparin binding consensus sequence to various hematopoietic cytokines have not been established, cytokine-

172

immobilization using low molecular weight heparin was comparable for TPO, SCF and Flt-3 (both basic and acidic proteins) and ~32% remained after 6 days[300], suggesting that heparinized gelatin MPs are able to deliver a variety of morphogenic factors in a similar manner.

Finally, we established a system incorporating heparinized microparticle delivery of two factors, BMP4 and TPO, into 100-cell aggregates, which supports the generation of hematopoietic progenitors equivalently, if not to a greater extent (~1.7-fold more CFCs) than bulk exogenous delivery. Similar cell numbers were generated with or without the provision of growth factors and in the presence or absence of microparticles, thus differences in colony numbers and enhanced CFC output represent better process yields from the initial ESC input. In all, integration of a microparticle approach for bioactive molecule delivery within EBs provides the opportunity to deconvolute the complex biological signals which cells receive during blood development.

In the future, time-lapse imaging studies may be used to investigate the localization of the developing mesoderm with enriched CFC activity or the relation between the hemogenic and non-hemogenic endothelium produced by the mesodermal precursors. Furthermore with the establishment of this system, studies may now be designed to explore asymmetrical signals within the aggregate (by providing hemispherical delivery) and further mimic embryonic development or polar axis definitions. Overall, this approach based on engineered combinations of physical and biochemical signaling serves as a model to guide differentiation of pluripotent stem cells to specific mesoderm phenotypes, such as blood, as well as to quantitatively investigate

173

the contribution of normally convoluted niche parameters on pluripotent cell developmental fate decisions.

CONCLUSION

We have provided a model system that used mesodermal phenotype characterization with a forced aggregation technique to control aggregate size and to embed MPs to serve as local delivery vehicles. Under serum-free conditions, heparinized MPs incorporated prior to aggregate encapsulation were able to induce differentiation to levels that were similar or exceeded bulk delivery methods.

Figure 1. Monitoring mesodermal specification. **(A):** Four-colour FACS employing a T-GFP cell line sheds light onto pan mesoderm development by tracking the surface expression of E-cadherin, PDGFRα and Flk1. **(B):** Comparison of undifferentiated cells to cells after 3.75 or 5 days in serum free differentiation media with or without BVT highlights the dynamic progression of these lineage markers and demonstrates that not all phenotypic combinations occur. **(C):** Populations were sorted singly or in combination as indicated; the average efficiency of colony formation from $E^-T^+P^+F^+$ cells (no. of colonies/no. of seeded cells x 100) was significantly (*) higher than all other sorted fractions (n=4, except $E^-T^-P^+/F^+$ n=2; ANOVA with Tukey's post hoc analysis α=0.05).
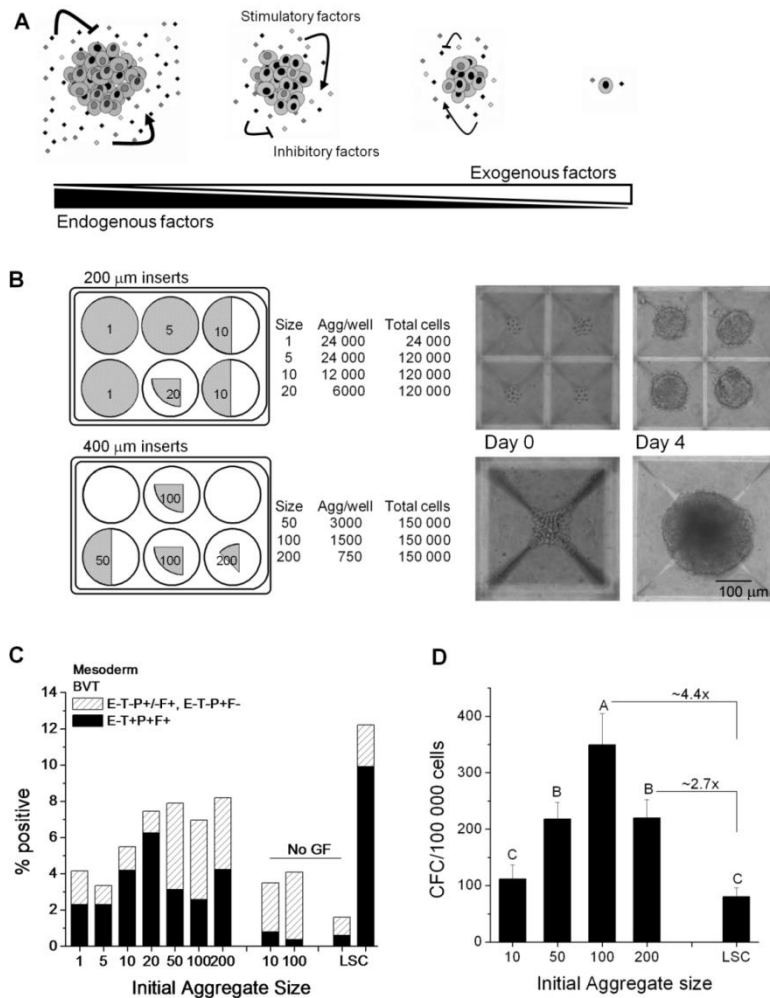
Figure 2. Controlling initial cell aggregate size influences mesodermal specification.
(A): The overall effect of endogenously produced factors would depend on the balance of stimulatory or inhibitory regulators that are secreted by the mixture of cell types. A higher local cell density would condition the microenvironment with more endogenous factors than lower density conditions. **(B):** Two sizes of micropatterned square-pyramidal wells and partial coverage allows similar overall cell densitites with constant volume to be compared. Initial 10-or 100-cell aggregates are shown in 200 and 400 μm inserts respectively, immediately after spinning down the cells and following four days of growth. **(C):** The mesodermal phenotypes associated most closely with CFC, are shown as a stacked percentage of expression for aggregates that were initially 1-200 cells or non-uniform aggregates, formed from liquid suspension culture (LSC). **(D):** The phenotypic expression increased with larger aggregate sizes, however, CFC are maximal with 100 cell aggregates. The average number of CFC ± standard error of the mean are shown. Means that do not share a letter are significantly different (n=6-8; ANOVA with Tukey's post hoc analysis α=0.05).
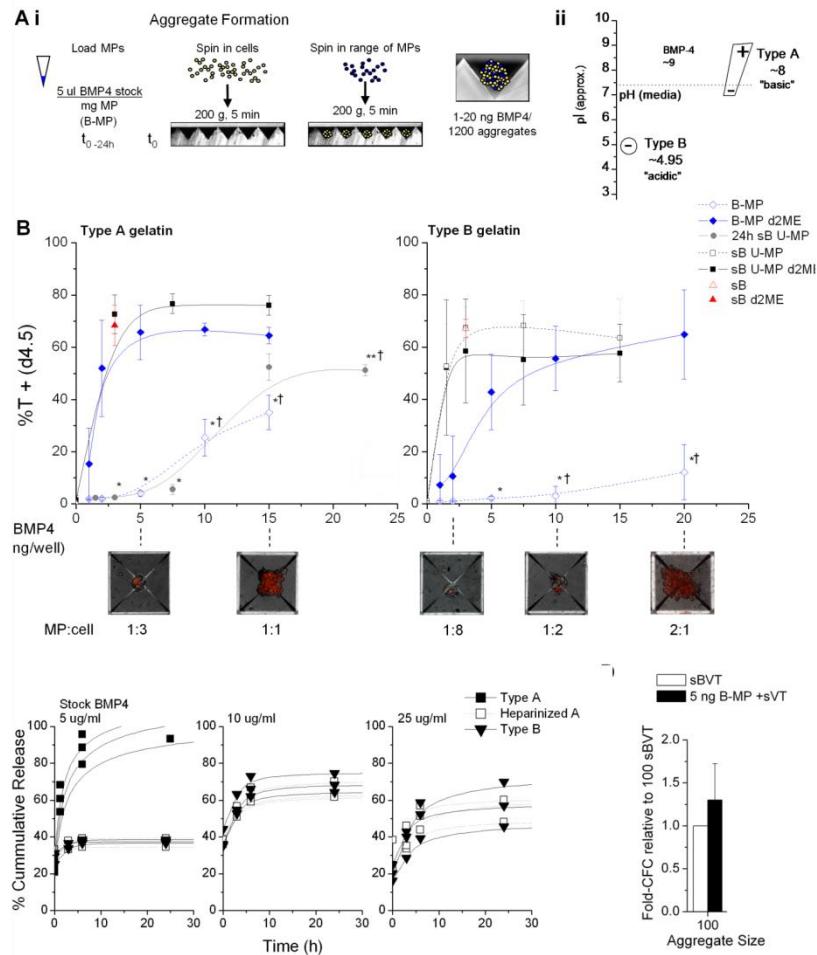
Figure 3. Gelatin microparticles do not interfere with cell aggregation and exogenous factors can be delivered locally. (Ai): A schematic of the aggregate formation process with BMP4 loaded gelatin MPs. **(Aii):** Both type A and type B gelatin MPs with characteristic pI were tested within the cell aggregates as it was expected BMP4 would have different inductive capacities depending on the electrostatic interaction between the gelatin and protein. **(B):** A range of BMP4 concentrations were tested by calculating the theoretical amount of BMP4 contained/MP. Brachyury (T-GFP) was assessed on day 4.5 (n=3; one-way ANOVA with Tukey's post hoc analysis, $\alpha = 0.05$). Open symbols: daily media exchange. Abbreviations: MP, microparticle; B-MP, BMP4-MP; U-MP, unloaded MP; sB, soluble BMP4; d2ME, daily media exchange from day two. $P < 0.05$ for comparison of: *daily exchange (open diamond) to sB (filled square☐) or d2ME of type A/B (filled diamond) gelatin respectively; **24h sB (filled grey circle) to continuous BMP4 (filled square☐ / diamond); †daily exchange type B (open diamond) to both type A MPs with daily exchange and 24h sBMP4 (filled grey circle☐). The MP:cell ratio used to deliver 1-20 ng BMP4 are shown below the axis; representative fluorescent images were taken 24h after seeding. **(C):** BMP4 was loaded into type A (square☐), typeB (triangle), and heparinized type A (☐ open square) MPs from 5,10 or 25 µg/mL stock solutions as indicated and its release into PBS was monitored by ELISA (n=3). **(D):** Delivery of 5 ng/well BMP4 with heparinized MPs was as effective as soluble delivery for 100 cell aggregates (n=4, student's t-test; 1200 aggregates, 24 well plate, 400 µm).

177
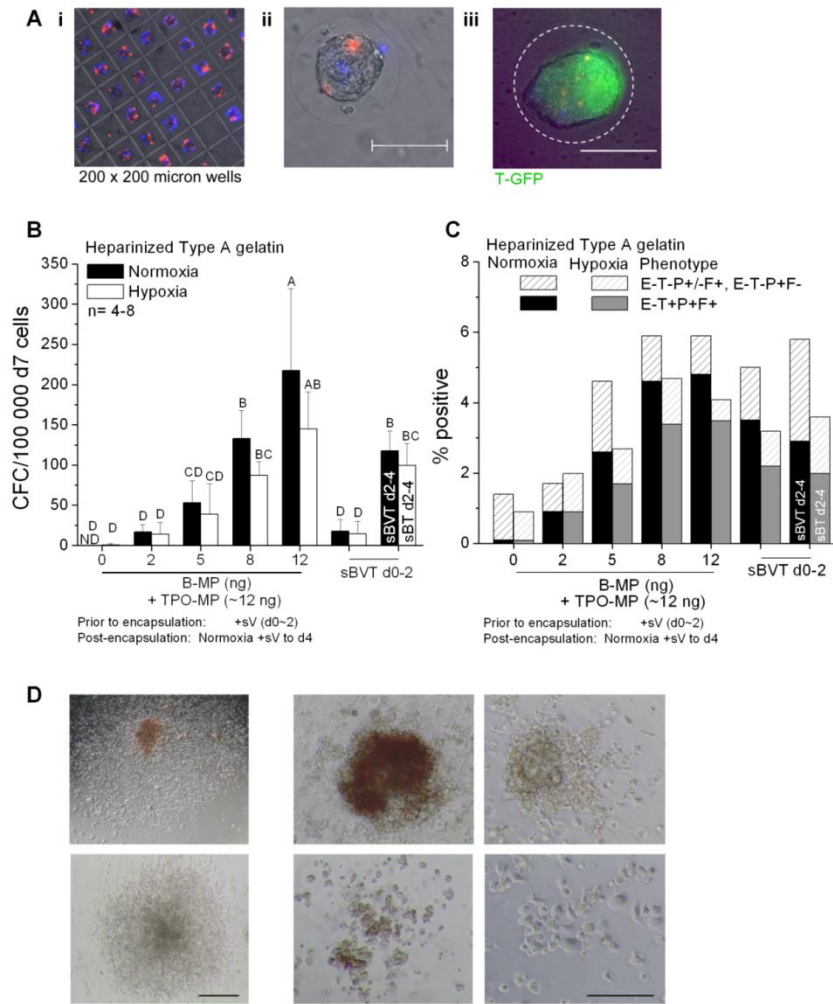
Figure 4. Combining local growth factor delivery with low oxygen supports mesodermal development. (Ai): Aggregates formed with blue and red microparticles can be removed and **(Aii):** encapsulated for further culture. **(Aiii):** The aggregates respond to media nutrients and soluble factors as this control aggregate seeded with unloaded MPs differentiated with BVT and expressed brachyury (T-GFP). The agarose shell is hightlighted with a dashed white ring. **(B):** BMP4 and TPO were delivered locally within 100 cell aggregates using heparinized type A gelatin MPs, while VEGF was provided in solution (d0-2) in normoxia. Means that do not share a letter are significantly different (n=4-8; one-way ANOVA with Tukey's post hoc analysis $\alpha = 0.05$). ND- not detected. **(C):** Assessing the phenotypes of the developing mesoderm at d3.75 as described earlier (ETPF), accurately predicts the general trend in CFC output from day seven cells in both 20% O_2 (black bars) and 5% O_2 conditions (grey bars). **(D):** Representative myeloid and erythroid colonies from dual BMP4 and TPO microparticle delivery are shown. Suppl. Figure 5 shows the distribution of colony types for each condition. All scale bars are 200 μm.

178

REFERENCES

[1] Martin GR. Isolation of a pluripotent cell line from early mouse embryos cultured in medium conditioned by teratocarcinoma stem cells. Proc Natl Acad Sci U S A. 1981;78:7634-8.

[2] Evans MJ, Kaufman MH. Establishment in culture of pluripotential cells from mouse embryos. Nature. 1981;292:154-6.

[3] Doetschman TC, Eistetter H, Katz M, Schmidt W, Kemler R. The in vitro development of blastocyst-derived embryonic stem cell lines: formation of visceral yolk sac, blood islands and myocardium. J Embryol Exp Morphol. 1985;87:27-45.

[4] Thomson JA, Kalishman J, Golos TG, Durning M, Harris CP, Becker RA, et al. Isolation of a primate embryonic stem cell line. Proc Natl Acad Sci U S A. 1995;92:7844-8.

[5] Thomson JA, Kalishman J, Golos TG, Durning M, Harris CP, Hearn JP. Pluripotent cell lines derived from common marmoset (Callithrix jacchus) blastocysts. Biol Reprod. 1996;55:254-9.

[6] Reubinoff BE, Pera MF, Fong CY, Trounson A, Bongso A. Embryonic stem cell lines from human blastocysts: somatic differentiation in vitro. Nature Biotechnology. 2000;18:399-404.

[7] Thomson JA, Itskovitz-Eldor J, Shapiro SS, Waknitz MA, Swiergiel JJ, Marshall VS, et al. Embryonic stem cell lines derived from human blastocysts. Science. 1998;282:1145-7.

[8] Takahashi K, Yamanaka S. Induction of pluripotent stem cells from mouse embryonic and adult fibroblast cultures by defined factors. Cell. 2006;126:663-76.

[9] Takahashi K, Tanabe K, Ohnuki M, Narita M, Ichisaka T, Tomoda K, et al. Induction of pluripotent stem cells from adult human fibroblasts by defined factors. Cell. 2007;131:861-72.

[10] Yu J, Vodyanik MA, Smuga-Otto K, Antosiewicz-Bourget J, Frane JL, Tian S, et al. Induced pluripotent stem cell lines derived from human somatic cells. Science. 2007;318:1917-20.

[11] Wernig M, Meissner A, Foreman R, Brambrink T, Ku M, Hochedlinger K, et al. In vitro reprogramming of fibroblasts into a pluripotent ES-cell-like state. Nature. 2007;448:318-24.

[12] Park IH, Zhao R, West JA, Yabuuchi A, Huo H, Ince TA, et al. Reprogramming of human somatic cells to pluripotency with defined factors. Nature. 2008;451:141-6.

[13] Gossler A, Doetschman T, Korn R, Serfling E, Kemler R. Transgenesis by means of blastocyst-derived embryonic stem cell lines. Proc Natl Acad Sci U S A. 1986;83:9065-9.

[14] Robertson E, Bradley A, Kuehn M, Evans M. Germ-line transmission of genes introduced into cultured pluripotential cells by retroviral vector. Nature. 1986;323:445-8.

[15] Ying QL, Stavridis M, Griffiths D, Li M, Smith A. Conversion of embryonic stem cells into neuroectodermal precursors in adherent monoculture. Nature Biotechnology. 2003;21:183-6.

[16] Nakano T, Kodama H, Honjo T. Generation of lymphohematopoietic cells from embryonic stem cells in culture. Science. 1994;265:1098-101.

[17] Wada T, Honda M, Minami I, Tooi N, Amagai Y, Nakatsuji N, et al. Highly efficient differentiation and enrichment of spinal motor neurons derived from human and monkey embryonic stem cells. PLoS One. 2009;4:e6722.

[18] Li X, Chen Y, Scheele S, Arman E, Haffner-Krausz R, Ekblom P, et al. Fibroblast growth factor signaling and basement membrane assembly are connected during epithelial morphogenesis of the embryoid body. J Cell Biol. 2001;153:811-22.

[19] Komura H, Ogita H, Ikeda W, Mizoguchi A, Miyoshi J, Takai Y. Establishment of cell polarity by afadin during the formation of embryoid bodies. Genes Cells. 2008;13:79-90.

[20] Wu X, Li S, Chrostek-Grashoff A, Czuchra A, Meyer H, Yurchenco PD, et al. Cdc42 is crucial for the establishment of epithelial polarity during early mammalian development. Dev Dyn. 2007;236:2767-78.

[21] Sato N, Sanjuan IM, Heke M, Uchida M, Naef F, Brivanlou AH. Molecular signature of human embryonic stem cells and its comparison with the mouse. Dev Biol. 2003;260:404-13.

[22] Ginis I, Luo Y, Miura T, Thies S, Brandenberger R, Gerecht-Nir S, et al. Differences between human and mouse embryonic stem cells. Dev Biol. 2004;269:360-80.

[23] Wei CL, Miura T, Robson P, Lim SK, Xu XQ, Lee MY, et al. Transcriptome profiling of human and murine ESCs identifies divergent paths required to maintain the stem cell state. Stem Cells. 2005;23:166-85.

[24] Maurer J, Nelson B, Cecena G, Bajpai R, Mercola M, Terskikh A, et al. Contrasting expression of keratins in mouse and human embryonic stem cells. PLoS ONE. 2008;3:e3451.

[25] Sun Y, Li H, Liu Y, Mattson MP, Rao MS, Zhan M. Evolutionarily conserved transcriptional co-expression guiding embryonic stem cell differentiation. PLoS ONE. 2008;3:e3406.

[26] Dang SM, Gerecht-Nir S, Chen J, Itskovitz-Eldor J, Zandstra PW. Controlled, scalable embryonic stem cell differentiation culture. Stem Cells. 2004;22:275-82.

[27] Dasgupta A, Hughey R, Lancin P, Larue L, Moghe PV. E-cadherin synergistically induces hepatospecific phenotype and maturation of embryonic stem cells in conjunction with hepatotrophic factors. Biotechnol Bioeng. 2005;92:257-66.

[28] Larue L, Antos C, Butz S, Huber O, Delmas V, Dominis M, et al. A role for cadherins in tissue formation. Development. 1996;122:3185-94.

[29] Chen Y, Li X, Eswarakumar VP, Seger R, Lonai P. Fibroblast growth factor (FGF) signaling through PI 3-kinase and Akt/PKB is required for embryoid body differentiation. Oncogene. 2000;19:3750-6.

[30] Esner M, Pachernik J, Hampl A, Dvorak P. Targeted disruption of fibroblast growth factor receptor-1 blocks maturation of visceral endoderm and cavitation in mouse embryoid bodies. Int J Dev Biol. 2002;46:817-25.

[31] Smyth N, Vatansever HS, Murray P, Meyer M, Frie C, Paulsson M, et al. Absence of basement membranes after targeting the LAMC1 gene results in embryonic lethality due to failure of endoderm differentiation. J Cell Biol. 1999;144:151-60.

[32] Coucouvanis E, Martin GR. Signals for death and survival: a two-step mechanism for cavitation in the vertebrate embryo. Cell. 1995;83:279-87.

[33] Murray P, Edgar D. Regulation of programmed cell death by basement membranes in embryonic development. J Cell Biol. 2000;150:1215-21.

[34] Keller GM. In vitro differentiation of embryonic stem cells. Curr Opin Cell Biol. 1995;7:862-9.

[35] Keller G, Kennedy M, Papayannopoulou T, Wiles MV. Hematopoietic commitment during embryonic stem cell differentiation in culture. Mol Cell Biol. 1993;13:473-86.

[36] Dvash T, Mayshar Y, Darr H, McElhaney M, Barker D, Yanuka O, et al. Temporal gene expression during differentiation of human embryonic stem cells and embryoid bodies. Hum Reprod. 2004;19:2875-83.

[37] Itskovitz-Eldor J, Schuldiner M, Karsenti D, Eden A, Yanuka O, Amit M, et al. Differentiation of human embryonic stem cells into embryoid bodies compromising the three embryonic germ layers. Mol Med. 2000;6:88-95.

[38] Martin GR, Evans MJ. Differentiation of clonal lines of teratocarcinoma cells: formation of embryoid bodies in vitro. Proc Natl Acad Sci U S A. 1975;72:1441-5.

[39] Kurosawa H. Methods for inducing embryoid body formation: in vitro differentiation system of embryonic stem cells. J Biosci Bioeng. 2007;103:389-98.

[40] Maltsev VA, Wobus AM, Rohwedel J, Bader M, Hescheler J. Cardiomyocytes differentiated in vitro from embryonic stem cells developmentally express cardiac-specific genes and ionic currents. Circ Res. 1994;75:233-44.

[41] Hopfl G, Gassmann M, Desbaillets I. Differentiating embryonic stem cells into embryoid bodies. Methods Mol Biol. 2004;254:79-98.

[42] Zhang SC, Wernig M, Duncan ID, Brustle O, Thomson JA. In vitro differentiation of transplantable neural precursors from human embryonic stem cells. Nat Biotechnol. 2001;19:1129-33.

[43] Klug MG, Soonpaa MH, Koh GY, Field LJ. Genetically selected cardiomyocytes from differentiating embronic stem cells form stable intracardiac grafts. J Clin Invest. 1996;98:216-24.

[44] Wiles MV. Embryonic stem cell differentiation in vitro. Methods Enzymol. 1993;225:900-18.

[45] Vittet D, Prandini MH, Berthier R, Schweitzer A, Martin-Sisteron H, Uzan G, et al. Embryonic stem cells differentiate in vitro to endothelial cells through successive maturation steps. Blood. 1996;88:3424-31.

[46] Liu H, Collins SF, Suggs LJ. Three-dimensional culture for expansion and differentiation of mouse embryonic stem cells. Biomaterials. 2006;27:6004-14.

[47] Gerecht S, Brudick JA, Ferreira L, Townsend SA, Langer R, Vunjak-Novakovic G. Hyaluronic acid hydrogel for controlled self-renewal and differentiation of human embryonic stem cell. Proc Natl Acad Sci U S A. 2007;104:11298-303.

[48] Ng ES, Davis RP, Azzola L, Stanley EG, Elefanty AG. Forced aggregation of defined numbers of human embryonic stem cells into embryoid bodies fosters robust, reproducible hematopoietic differentiation. Blood. 2005;106:1601-3.

[49] Ungrin MD, Joshi C, Nica A, Bauwens C, Zandstra PW. Reproducible, ultra high-throughput formation of multicellular organization from single cell suspension-derived human embryonic stem cell aggregates. PLoS One. 2008;3:e1565.

[50] Moeller HC, Mian MK, Shrivastava S, Chung BG, Khademhosseini A. A microwell array system for stem cell culture. Biomaterials. 2008;29:752-63.

[51] Mohr JC, de Pablo JJ, Palecek SP. 3-D microwell culture of human embryonic stem cells. Biomaterials. 2006;27:6032-42.

[52] Torisawa YS, Chueh BH, Huh D, Ramamurthy P, Roth TM, Barald KF, et al. Efficient formation of uniform-sized embryoid bodies using a compartmentalized microchannel device. Lab Chip. 2007;7:770-6.

[53] Cameron CM, Hu WS, Kaufman DS. Improved development of human embryonic stem cell-derived embryoid bodies by stirred vessel cultivation. Biotechnol Bioeng. 2006;94:938-48.

[54] Carpenedo RL, Sargent CY, McDevitt TC. Rotary suspension culture enhances the efficiency, yield and homogeneity of embryoid body differentiation. Stem Cells. 2007.

[55] Fok EY, Zandstra PW. Shear-controlled single-step mouse embryonic stem cell expansion and embryoid body-based differentiation. Stem Cells. 2005;23:1333-42.

[56] Gerecht-Nir S, Cohen S, Itskovitz-Eldor J. Bioreactor cultivation enhances the efficiency of human embryoid body (hEB) formation and differentiation. Biotechnology and Bioengineering. 2004;86:493-502.

[57] Zweigerdt R, Burg M, Willbold E, Abts H, Ruediger M. Generation of confluent cardiomyocyte monolayers derived from embryonic stem cells in suspension: a cell source for new therapies and screening strategies. Cytotherapy. 2003;5:399-413.

[58] Schroeder M, Niebruegge S, Werner A, Willbold E, Burg M, Ruediger M, et al. Differentiation and lineage selection of mouse embryonic stem cells in a stirred bench scale bioreactor with automated process control. Biotechnol Bioeng. 2005;92:920-33.

[59] Sargent CY, Berguig GY, McDevitt TC. Cardiomyogenic Differentiation of Embryoid Bodies is Promoted by Rotary Orbital Suspension Culture. Tissue Engineering. 2008;In Press.

[60] Kramer J, Hegert C, Guan K, Wobus AM, Muller PK, Rohwedel J. Embryonic stem cell-derived chondrogenic differentiation in vitro: activation by BMP-2 and BMP-4. Mech Dev. 2000;92:193-205.

[61] Bauwens CL, Peerani R, Niebruegge S, Woodhouse KA, Kumacheva E, Husain M, et al. Control of human embryonic stem cell colony and aggregate size heterogeneity influences differentiation trajectories. Stem Cells. 2008;26:2300-10.

[62] Maguire T, Novik E, Schloss R, Yarmush M. Alginate-PLL microencapsulation: effect on the differentiation of embryonic stem cells into hepatocytes. Biotechnology and Bioengineering. 2006;93:581-91.

183

[63] Magyar JP, Nemir M, Ehler E, Suter N, Perriard JC, Eppenberger HM. Mass production of embryoid bodies in microbeads. Annals of the New York Academy of Sciences. 2001;944:135-43.

[64] Randle WL, Cha JM, Hwang YS, Chan KL, Kazarian SG, Polak JM, et al. Integrated 3-dimensional expansion and osteogenic differentiation of murine embryonic stem cells. Tissue Eng. 2007;13:2957-70.

[65] Ferreira LS, Gerecht S, Fuller J, Shieh HF, Vunjak-Novakovic G, Langer R. Bioactive hydrogel scaffolds for controllable vascular differentiation of human embryonic stem cells. Biomaterials. 2007;28:2706-17.

[66] Hwang NS, Varghese S, Elisseeff J. Controlled differentiation of stem cells. Adv Drug Deliv Rev. 2008;60:199-214.

[67] Schuldiner M, Yanuka O, Itskovitz-Eldor J, Melton DA, Benvenisty N. Effects of eight growth factors on the differentiation of cells derived from human embryonic stem cells. Proc Natl Acad Sci U S A. 2000;97:11307-12.

[68] Czyz J, Wobus A. Embryonic stem cell differentiation: the role of extracellular factors. Differentiation. 2001;68:167-74.

[69] Takahashi T, Lord B, Schulze PC, Fryer RM, Sarang SS, Gullans SR, et al. Ascorbic acid enhances differentiation of embryonic stem cells into cardiac myocytes. Circulation. 2003;107:1912-6.

[70] Gajovic S, St-Onge L, Yokota Y, Gruss P. Retinoic acid mediates Pax6 expression during in vitro differentiation of embryonic stem cells. Differentiation. 1997;62:187-92.

[71] Buttery LD, Bourne S, Xynos JD, Wood H, Hughes FJ, Hughes SP, et al. Differentiation of osteoblasts and in vitro bone formation from murine embryonic stem cells. Tissue Engineering. 2001;7:89-99.

[72] Willerth SM, Faxel TE, Gottlieb DI, Sakiyama-Elbert SE. The effects of soluble growth factors on embryonic stem cell differentiation inside of fibrin scaffolds. Stem Cells. 2007;25:2235-44.

[73] Flaim CJ, Chien S, Bhatia SN. An extracellular matrix microarray for probing cellular differentiation. Nature Methods. 2005;2:119-25.

[74] Hwang YS, Randle WL, Bielby RC, Polak JM, Mantalaris A. Enhanced derivation of osteogenic cells from murine embryonic stem cells after treatment with HepG2-conditioned medium and modulation of the embryoid body formation period: application to skeletal tissue engineering. Tissue Eng. 2006;12:1381-92.

184

[75] Rathjen J, Lake JA, Bettess MD, Washington JM, Chapman G, Rathjen PD. Formation of a primitive ectoderm like cell population, EPL cells, from ES cells in response to biologically derived factors. J Cell Sci. 1999;112 (Pt 5):601-12.

[76] Tropepe V, Hitoshi S, Sirard C, Mak TW, Rossant J, van der Kooy D. Direct neural fate specification from embryonic stem cells: a primitive mammalian neural stem cell stage acquired through a default mechanism. Neuron. 2001;30:65-78.

[77] Gerrard L, Rodgers L, Cui W. Differentiation of human embryonic stem cells to neural lineages in adherent culture by blocking bone morphogenetic protein signaling. Stem Cells. 2005;23:1234-41.

[78] Sachlos E, Auguste DT. Embryoid body morphology influences diffusive transport of inductive biochemicals: a strategy for stem cell differentiation. Biomaterials. 2008;29:4471-80.

[79] Fujiwara T, Dehart DB, Sulik KK, Hogan BL. Distinct requirements for extra-embryonic and embryonic bone morphogenetic protein 4 in the formation of the node and primitive streak and coordination of left-right asymmetry in the mouse. Development. 2002;129:4685-96.

[80] Zhang H, Bradley A. Mice deficient for BMP2 are nonviable and have defects in amnion/chorion and cardiac development. Development. 1996;122:2977-86.

[81] Ma L, Lu MF, Schwartz RJ, Martin JF. Bmp2 is essential for cardiac cushion epithelial-mesenchymal transition and myocardial patterning. Development. 2005;132:5601-11.

[82] Inai K, Norris RA, Hoffman S, Markwald RR, Sugi Y. BMP-2 induces cell migration and periostin expression during atrioventricular valvulogenesis. Dev Biol. 2008;315:383-96.

[83] Sugi Y, Yamamura H, Okagawa H, Markwald RR. Bone morphogenetic protein-2 can mediate myocardial regulation of atrioventricular cushion mesenchymal cell formation in mice. Dev Biol. 2004;269:505-18.

[84] Behfar A, Zingman LV, Hodgson DM, Rauzier JM, Kane GC, Terzic A, et al. Stem cell differentiation requires a paracrine pathway in the heart. FASEB J. 2002;16:1558-66.

[85] Leschik J, Stefanovic S, Brinon B, Puceat M. Cardiac commitment of primate embryonic stem cells. Nat Protoc. 2008;3:1381-7.

[86] Zeineddine D, Papadimou E, Mery A, Menard C, Puceat M. Cardiac commitment of embryonic stem cells for myocardial repair. Methods Mol Med. 2005;112:175-82.

185

[87] Tomescot A, Leschik J, Bellamy V, Dubois G, Messas E, Bruneval P, et al. Differentiation in vivo of cardiac committed human embryonic stem cells in postmyocardial infarcted rats. Stem Cells. 2007;25:2200-5.

[88] Di-Gregorio A, Sancho M, Stuckey DW, Crompton LA, Godwin J, Mishina Y, et al. BMP signalling inhibits premature neural differentiation in the mouse embryo. Development. 2007;134:3359-69.

[89] Hawley SH, Wunnenberg-Stapleton K, Hashimoto C, Laurent MN, Watabe T, Blumberg BW, et al. Disruption of BMP signals in embryonic Xenopus ectoderm leads to direct neural induction. Genes Dev. 1995;9:2923-35.

[90] Linker C, Stern CD. Neural induction requires BMP inhibition only as a late step, and involves signals other than FGF and Wnt antagonists. Development. 2004;131:5671-81.

[91] McMahon JA, Takada S, Zimmerman LB, Fan CM, Harland RM, McMahon AP. Noggin-mediated antagonism of BMP signaling is required for growth and patterning of the neural tube and somite. Genes Dev. 1998;12:1438-52.

[92] Reversade B, Kuroda H, Lee H, Mays A, De Robertis EM. Depletion of Bmp2, Bmp4, Bmp7 and Spemann organizer signals induces massive brain formation in Xenopus embryos. Development. 2005;132:3381-92.

[93] Hay ED. Extracellular matrix. J Cell Biol. 1981;91:205s-23s.

[94] Juliano RL, Haskill S. Signal transduction from the extracellular matrix. J Cell Biol. 1993;120:577-85.

[95] Battista S, Guarnieri D, Borselli C, Zeppetelli S, Borzacchiello A, Mayol L, et al. The effect of matrix composition of 3D constructs on embryonic stem cell differentiation. Biomaterials. 2005;26:6194-207.

[96] Engler AJ, Sen S, Sweeney HL, Discher DE. Matrix elasticity directs stem cell lineage specification. Cell. 2006;126:677-89.

[97] Philp D, Chen SS, Fitzgerald W, Orenstein J, Margolis L, Kleinman HK. Complex extracellular matrices promote tissue-specific stem cell differentiation. Stem Cells. 2005;23:288-96.

[98] Fujiwara H, Hayashi Y, Sanzen N, Kobayashi R, Weber CN, Emoto T, et al. Regulation of mesodermal differentiation of mouse embryonic stem cells by basement membranes. J Biol Chem. 2007;282:29701-11.

[99] Garreta E, Genove E, Borros S, Semino CE. Osteogenic differentiation of mouse embryonic stem cells and mouse embryonic fibroblasts in a three-dimensional self-assembling peptide scaffold. Tissue Eng. 2006;12:2215-27.

[100] Silva GA, Czeisler C, Niece KL, Beniash E, Harrington DA, Kessler JA, et al. Selective differentiation of neural progenitor cells by high-epitope density nanofibers. Science. 2004;303:1352-5.

[101] Gumbiner BM. Cell adhesion: the molecular basis of tissue architecture and morphogenesis. Cell. 1996;84:345-57.

[102] Artavanis-Tsakonas S, Rand MD, Lake RJ. Notch signaling: cell fate control and signal integration in development. Science. 1999;284:770-6.

[103] Lai EC. Notch signaling: control of cell communication and cell fate. Development. 2004;131:965-73.

[104] Lowell S, Benchoua A, Heavey B, Smith AG. Notch promotes neural lineage entry by pluripotent embryonic stem cells. PLoS Biol. 2006;4:e121.

[105] Walsh J, Andrews PW. Expression of Wnt and Notch pathway genes in a pluripotent human embryonal carcinoma cell line and embryonic stem cell. APMIS. 2003;111:197-210; discussion -1.

[106] Fox V, Gokhale PJ, Walsh JR, Matin M, Jones M, Andrews PW. Cell-cell signaling through NOTCH regulates human embryonic stem cell proliferation. Stem Cells. 2008;26:715-23.

[107] Varnum-Finney B, Wu L, Yu M, Brashem-Stein C, Staats S, Flowers D, et al. Immobilization of Notch ligand, Delta-1, is required for induction of notch signaling. J Cell Sci. 2000;113 Pt 23:4313-8.

[108] Beckstead BL, Santosa DM, Giachelli CM. Mimicking cell-cell interactions at the biomaterial-cell interface for control of stem cell differentiation. Journal of Biomedical Materials Research A. 2006;79:94-103.

[109] Langer R, Vacanti JP. Tissue engineering. Science. 1993;260:920-6.

[110] Li WJ, Tuli R, Okafor C, Derfoul A, Danielson KG, Hall DJ, et al. A three-dimensional nanofibrous scaffold for cartilage tissue engineering using human mesenchymal stem cells. Biomaterials. 2005;26:599-609.

[111] Li WJ, Chiang H, Kuo TF, Lee HS, Jiang CC, Tuan RS. Evaluation of articular cartilage repair using biodegradable nanofibrous scaffolds in a swine model: a pilot study. J Tissue Eng Regen Med. 2009;3:1-10.

187

[112] Li WJ, Tuli R, Huang X, Laquerriere P, Tuan RS. Multilineage differentiation of human mesenchymal stem cells in a three-dimensional nanofibrous scaffold. Biomaterials. 2005;26:5158-66.

[113] Yang J, Cao C, Wang W, Tong X, Shi D, Wu F, et al. Proliferation and osteogenesis of immortalized bone marrow-derived mesenchymal stem cells in porous polylactic glycolic acid scaffolds under perfusion culture. J Biomed Mater Res A. 2009.

[114] Xin X, Hussain M, Mao JJ. Continuing differentiation of human mesenchymal stem cells and induced chondrogenic and osteogenic lineages in electrospun PLGA nanofiber scaffold. Biomaterials. 2007;28:316-25.

[115] Park K, Cho KJ, Kim JJ, Kim IH, Han DK. Functional PLGA scaffolds for chondrogenesis of bone-marrow-derived mesenchymal stem cells. Macromol Biosci. 2009;9:221-9.

[116] Tanaka T, Hirose M, Kotobuki N, Tadokoro M, Ohgushi H, Fukuchi T, et al. Bone augmentation by bone marrow mesenchymal stem cells cultured in three-dimensional biodegradable polymer scaffolds. J Biomed Mater Res A. 2009;91:428-35.

[117] Stiehler M, Bunger C, Baatrup A, Lind M, Kassem M, Mygind T. Effect of dynamic 3-D culture on proliferation, distribution, and osteogenic differentiation of human mesenchymal stem cells. J Biomed Mater Res A. 2009;89:96-107.

[118] Hofmann S, Knecht S, Langer R, Kaplan DL, Vunjak-Novakovic G, Merkle HP, et al. Cartilage-like tissue engineering using silk scaffolds and mesenchymal stem cells. Tissue Eng. 2006;12:2729-38.

[119] Meinel L, Hofmann S, Karageorgiou V, Zichner L, Langer R, Kaplan D, et al. Engineering cartilage-like tissue using human mesenchymal stem cells and silk protein scaffolds. Biotechnol Bioeng. 2004;88:379-91.

[120] Meinel L, Karageorgiou V, Hofmann S, Fajardo R, Snyder B, Li C, et al. Engineering bone-like tissue in vitro using human bone marrow stem cells and silk scaffolds. J Biomed Mater Res A. 2004;71:25-34.

[121] Kim HJ, Kim UJ, Kim HS, Li C, Wada M, Leisk GG, et al. Bone tissue engineering with premineralized silk scaffolds. Bone. 2008;42:1226-34.

[122] Li YJ, Chung EH, Rodriguez RT, Firpo MT, Healy KE. Hydrogels as artificial matrices for human embryonic stem cell self-renewal. J Biomed Mater Res A. 2006;79:1-5.

[123] Nur EKA, Ahmed I, Kamal J, Schindler M, Meiners S. Three-dimensional nanofibrillar surfaces promote self-renewal in mouse embryonic stem cells. Stem Cells. 2006;24:426-33.

188

[124] Levenberg S, Huang NF, Lavik E, Rogers AB, Itskovitz-Eldor J, Langer R. Differentiation of human embryonic stem cells on three-dimensional polymer scaffolds. Proc Natl Acad Sci U S A. 2003;100:12741-6.

[125] Levenberg S, Burdick JA, Kraehenbuehl T, Langer R. Neurotrophin-induced differentiation of human embryonic stem cells on three-dimensional polymeric scaffolds. Tissue Eng. 2005;11:506-12.

[126] Liu H, Roy K. Biomimetic three-dimensional cultures significantly increase hematopoietic differentiation efficacy of embryonic stem cells. Tissue Eng. 2005;11:319-30.

[127] Liu H, Lin J, Roy K. Effect of 3D scaffold and dynamic culture condition on the global gene expression profile of mouse embryonic stem cells. Biomaterials. 2006;27:5978-89.

[128] Willerth SM, Arendas KJ, Gottlieb DI, Sakiyama-Elbert SE. Optimization of fibrin scaffolds for differentiation of murine embryonic stem cells into neural lineage cells. Biomaterials. 2006;27:5990-6003.

[129] Karoubi G, Ormiston ML, Stewart DJ, Courtman DW. Single-cell hydrogel encapsulation for enhanced survival of human marrow stromal cells. Biomaterials. 2009;30:5445-55.

[130] Markusen JF, Mason C, Hull DA, Town MA, Tabor AB, Clements M, et al. Behavior of adult human mesenchymal stem cells entrapped in alginate-GRGDY beads. Tissue Eng. 2006;12:821-30.

[131] Ma HL, Hung SC, Lin SY, Chen YL, Lo WH. Chondrogenesis of human mesenchymal stem cells encapsulated in alginate beads. J Biomed Mater Res A. 2003;64:273-81.

[132] Connelly JT, Garcia AJ, Levenston ME. Inhibition of in vitro chondrogenesis in RGD-modified three-dimensional alginate gels. Biomaterials. 2007;28:1071-83.

[133] Park JS, Woo DG, Yang HN, Lim HJ, Park KM, Na K, et al. Chondrogenesis of human mesenchymal stem cells encapsulated in a hydrogel construct: Neocartilage formation in animal models as both mice and rabbits. J Biomed Mater Res A. 2009.

[134] Nuttelman CR, Tripodi MC, Anseth KS. In vitro osteogenic differentiation of human mesenchymal stem cells photoencapsulated in PEG hydrogels. J Biomed Mater Res A. 2004;68:773-82.

189

[135] Alhadlaq A, Tang M, Mao JJ. Engineered adipose tissue from human mesenchymal stem cells maintains predefined shape and dimension: implications in soft tissue augmentation and reconstruction. Tissue Eng. 2005;11:556-66.

[136] Hwang NS, Varghese S, Zhang Z, Elisseeff J. Chondrogenic differentiation of human embryonic stem cell-derived cells in arginine-glycine-aspartate-modified hydrogels. Tissue Eng. 2006;12:2695-706.

[137] Temenoff JS, Park H, Jabbari E, Sheffield TL, LeBaron RG, Ambrose CG, et al. In vitro osteogenic differentiation of marrow stromal cells encapsulated in biodegradable hydrogels. J Biomed Mater Res A. 2004;70:235-44.

[138] Siti-Ismail N, Bishop AE, Polak JM, Mantalaris A. The benefit of human embryonic stem cell encapsulation for prolonged feeder-free maintenance. Biomaterials. 2008;29:3946-52.

[139] Hwang NS, Varghese S, Theprungsirikul P, Canver A, Elisseeff J. Enhanced chondrogenic differentiation of murine embryonic stem cells in hydrogels with glucosamine. Biomaterials. 2006;27:6015-23.

[140] Bauwens C, Yin T, Dang S, Peerani R, Zandstra PW. Development of a perfusion fed bioreactor for embryonic stem cell-derived cardiomyocyte generation: oxygen-mediated enhancement of cardiomyocyte output. Biotechnol Bioeng. 2005;90:452-61.

[141] Chayosumrit M, Tuch B, Sidhu K. Alginate microcapsule for propagation and directed differentiation of hESCs to definitive endoderm. Biomaterials. 2009.

[142] Benoit DS, Schwartz MP, Durney AR, Anseth KS. Small functional groups for controlled differentiation of hydrogel-encapsulated human mesenchymal stem cells. Nat Mater. 2008;7:816-23.

[143] Nie Y, Bergendahl V, Hei DJ, Jones JM, Palecek SP. Scalable culture and cryopreservation of human embryonic stem cells on microcarriers. Biotechnol Prog. 2009;25:20-31.

[144] Fernandes AM, Marinho PA, Sartore RC, Paulsen BS, Mariante RM, Castilho LR, et al. Successful scale-up of human embryonic stem cell production in a stirred microcarrier culture system. Braz J Med Biol Res. 2009;42:515-22.

[145] Lock LT, Tzanakakis ES. Expansion and differentiation of human embryonic stem cells to endoderm progeny in a microcarrier stirred-suspension culture. Tissue Eng Part A. 2009;15:2051-63.

[146] Fernandes AM, Fernandes TG, Diogo MM, da Silva CL, Henrique D, Cabral JM. Mouse embryonic stem cell expansion in a microcarrier-based stirred culture system. J Biotechnol. 2007;132:227-36.

190

[147] Abranches E, Bekman E, Henrique D, Cabral JM. Expansion of mouse embryonic stem cells on microcarriers. Biotechnol Bioeng. 2007;96:1211-21.

[148] Frauenschuh S, Reichmann E, Ibold Y, Goetz PM, Sittinger M, Ringe J. A microcarrier-based cultivation system for expansion of primary mesenchymal stem cells. Biotechnol Prog. 2007;23:187-93.

[149] Wang C, Gong Y, Zhong Y, Yao Y, Su K, Wang DA. The control of anchorage-dependent cell behavior within a hydrogel/microcarrier system in an osteogenic model. Biomaterials. 2009;30:2259-69.

[150] Bratt-Leal AM, Carpenedo RL, McDevitt TC. Engineering the embryoid body microenvironment to direct embryonic stem cell differentiation. Biotechnol Prog. 2009;25:43-51.

[151] Alberti K, Davey RE, Onishi K, George S, Salchert K, Seib FP, et al. Functional immobilization of signaling proteins enables control of stem cell fate. Nat Methods. 2008;5:645-50.

[152] Jaklenec A, Wan E, Murray ME, Mathiowitz E. Novel scaffolds fabricated from protein-loaded microspheres for tissue engineering. Biomaterials. 2008;29:185-92.

[153] Patel ZS, Yamamoto M, Ueda H, Tabata Y, Mikos AG. Biodegradable gelatin microparticles as delivery systems for the controlled release of bone morphogenetic protein-2. Acta Biomater. 2008;4:1126-38.

[154] Mahoney MJ, Saltzman WM. Transplantation of brain cells assembled around a programmable synthetic microenvironment. Nat Biotechnol. 2001;19:934-9.

[155] Carpenedo RL, Bratt-Leal AM, Marklein RA, Seaman SA, Bowen NJ, McDonald JF, et al. Homogeneous and organized differentiation within embryoid bodies induced by microsphere-mediated delivery of small molecules. Biomaterials. 2009;30:2507-15.

[156] Ferreira L, Squier, T., Park, H., Choe, H., Kohane, D.S., Langer, R. Human Embryoid Bodies Containing Nano- and Microparticulate Delivery Vehicles. Advanced Materials. 2008;20:2285-91.

[157] Discher DE, Mooney DJ, Zandstra PW. Growth factors, matrices, and forces combine and control stem cells. Science. 2009;324:1673-7.

[158] Lutolf MP, Gilbert PM, Blau HM. Designing materials to direct stem-cell fate. Nature. 2009;462:433-41.

[159] Anderson DG, Levenberg S, Langer R. Nanoliter-scale synthesis of arrayed biomaterials and application to human embryonic stem cells. Nature Biotechnology. 2004;22:863-6.

[160] Valamehr B, Jonas SJ, Polleux J, Qiao R, Guo S, Gschweng EH, et al. Hydrophobic surfaces for enhanced differentiation of embryonic stem cell-derived embryoid bodies. Proc Natl Acad Sci U S A. 2008;105:14459-64.

[161] Carpenedo RL, Seaman SA, McDevitt TC. Microsphere size effects on embryoid body incorporation and embryonic stem cell differentiation. J Biomed Mater Res A. 2010;94:466-75.

[162] Fu K, Griebenow K, Hsieh L, Klibanov AM, LangerR. FTIR characterization of the secondary structure of proteins encapsulated within PLGA microspheres. J Control Release. 1999;58:357-66.

[163] Zhu G, Mallery SR, Schwendeman SP. Stabilization of proteins encapsulated in injectable poly (lactide- co-glycolide). Nat Biotechnol. 2000;18:52-7.

[164] Moribe K, Nomizu N, Izukura S, Yamamoto K, Tozuka Y, Sakurai M, et al. Physicochemical, morphological and therapeutic evaluation of agarose hydrogel particles as a reservoir for basic fibroblast growth factor. Pharm Dev Technol. 2008;13:541-7.

[165] Tabata Y, Hijikata S, Muniruzzaman M, Ikada Y. Neovascularization effect of biodegradable gelatin microspheres incorporating basic fibroblast growth factor. J Biomater Sci Polym Ed. 1999;10:79-94.

[166] Holland TA, Tabata Y, Mikos AG. In vitro release of transforming growth factor-beta 1 from gelatin microparticles encapsulated in biodegradable, injectable oligo(poly(ethylene glycol) fumarate) hydrogels. J Control Release. 2003;91:299-313.

[167] Carpenedo RL, Sargent CY, McDevitt TC. Rotary suspension culture enhances the efficiency, yield, and homogeneity of embryoid body differentiation. Stem Cells. 2007;25:2224-34.

[168] Wang N, Wu XS. Preparation and characterization of agarose hydrogel nanoparticles for protein and peptide drug delivery. Pharm Dev Technol. 1997;2:135-42.

[169] Dodla MC, Bellamkonda RV. Anisotropic scaffolds facilitate enhanced neurite extension in vitro. J Biomed Mater Res A. 2006;78:213-21.

[170] Sturn A, Quackenbush J, Trajanoski Z. Genesis: cluster analysis of microarray data. Bioinformatics. 2002;18:207-8.

[171] Pfaffl MW. A new mathematical model for relative quantification in real-time RT-PCR. Nucleic Acids Res. 2001;29:e45.

[172] Guilak F, Cohen DM, Estes BT, Gimble JM, Liedtke W, Chen CS. Control of stem cell fate by physical interactions with the extracellular matrix. Cell Stem Cell. 2009;5:17-26.

[173] Markway BD, Tan GK, Brooke G, Hudson JE, Cooper-White JJ, Doran MR. Enhanced Chondrogenic Differentiation of Human Bone Marrow-Derived Mesenchymal Stem Cells in Low Oxygen Environment Micropellet Cultures. Cell Transplantation. 2010;19:29-42.

[174] Sutherland RM. Cell and Environment Interactions in Tumor Microregions - the Multicell Spheroid Model. Science. 1988;240:177-84.

[175] Rahman N, Purpura KA, Wylie RG, Zandstra PW, Shoichet MS. The use of vascular endothelial growth factor functionalized agarose to guide pluripotent stem cell aggregates toward blood progenitor cells. Biomaterials. 2010.

[176] Yu XJ, Dillon GP, Bellamkonda RV. A laminin and nerve growth factor-laden three-dimensional scaffold for enhanced neurite extension. Tissue Engineering. 1999;5:291-304.

[177] Bellamkonda R, Ranieri JP, Aebischer P. Laminin Oligopeptide Derivatized Agarose Gels Allow 3-Dimensional Neurite Extension in-Vitro. Journal of Neuroscience Research. 1995;41:501-9.

[178] Fu K, Pack DW, Klibanov AM, Langer R. Visual evidence of acidic environment within degrading poly(lactic-co-glycolic acid) (PLGA) microspheres. Pharm Res. 2000;17:100-6.

[179] Chaudhry MA, Bowen BD, Piret JM. Culture pH and osmolality influence proliferation and embryoid body yields of murine embryonic stem cells. Biochemical Engineering Journal. 2009;45:126-35.

[180] Kenley RA, Lee MO, Mahoney TR, Sanders LM. Poly(Lactide-Co-Glycolide) Decomposition Kinetics Invivo and Invitro. Macromolecules. 1987;20:2398-403.

[181] Reed AM, Gilding DK. Biodegradable Polymers for Use in Surgery - Poly(Glycolic)-Poly(Lactic Acid) Homo and Co-Polymers .2. Invitro Degradation. Polymer. 1981;22:494-8.

[182] Adams JC, Watt FM. Regulation of development and differentiation by the extracellular matrix. Development. 1993;117:1183-98.

[183] Ma W, Tavakoli T, Derby E, Serebryakova Y, Rao MS, Mattson MP. Cell-extracellular matrix interactions regulate neural differentiation of human embryonic stem cells. BMC Dev Biol. 2008;8:90.

193

[184] Chazaud C, Yamanaka Y, Pawson T, Rossant J. Early lineage segregation between epiblast and primitive endoderm in mouse blastocysts through the Grb2-MAPK pathway. Dev Cell. 2006;10:615-24.

[185] Rula ME, Cai KQ, Moore R, Yang DH, Staub CM, Capo-Chichi CD, et al. Cell autonomous sorting and surface positioning in the formation of primitive endoderm in embryoid bodies. Genesis. 2007;45:327-38.

[186] Guo Y, Graham-Evans B, Broxmeyer HE. Murine embryonic stem cells secrete cytokines/growth modulators that enhance cell survival/anti-apoptosis and stimulate colony formation of murine hematopoietic progenitor cells. Stem Cells. 2006;24:850-6.

[187] Crisostomo PR, Abarbanell AM, Wang M, Lahm T, Wang Y, Meldrum DR. Embryonic stem cells attenuate myocardial dysfunction and inflammation after surgical global ischemia via paracrine actions. Am J Physiol Heart Circ Physiol. 2008;295:H1726-35.

[188] Baraniak PR, McDevitt TC. Stem cell paracrine actions and tissue regeneration. Regen Med. 2010;5:121-43.

[189] Bendall SC, Hughes C, Campbell JL, Stewart MH, Pittock P, Liu S, et al. An enhanced mass spectrometry approach reveals human embryonic stem cell growth factors in culture. Mol Cell Proteomics. 2009;8:421-32.

[190] Nair R. Acellular Matrices Derived From Differentiating Embryonic Stem Cells PhD Thesis: Georgia Institute of Technology; 2009.

[191] Nair R, Ngangan AV, McDevitt TC. Efficacy of solvent extraction methods for acellularization of embryoid bodies. J Biomater Sci Polym Ed. 2008;19:801-19.

[192] Ngangan AV, McDevitt TC. Acellularization of embryoid bodies via physical disruption methods. Biomaterials. 2009;30:1143-9.

[193] Webber MJ, Han X, Murthy SN, Rajangam K, Stupp SI, Lomasney JW. Capturing the stem cell paracrine effect using heparin-presenting nanofibres to treat cardiovascular diseases. J Tissue Eng Regen Med. 2010;4:600-10.

[194] Murry CE, Keller G. Differentiation of embryonic stem cells to clinically relevant populations: lessons from embryonic development. Cell. 2008;132:661-80.

[195] Laflamme MA, Chen KY, Naumova AV, Muskheli V, Fugate JA, Dupras SK, et al. Cardiomyocytes derived from human embryonic stem cells in pro-survival factors enhance function of infarcted rat hearts. Nat Biotechnol. 2007;25:1015-24.

[196] McCloskey KE, Lyons I, Rao RR, Stice SL, Nerem RM. Purified and proliferating endothelial cells derived and expanded in vitro from embryonic stem cells. Endothelium. 2003;10:329-36.

[197] Purpura KA, Morin J, Zandstra PW. Analysis of the temporal and concentration-dependent effects of BMP-4, VEGF, and TPO on development of embryonic stem cell-derived mesoderm and blood progenitors in a defined, serum-free media. Exp Hematol. 2008;36:1186-98.

[198] Zhang P, Li J, Tan Z, Wang C, Liu T, Chen L, et al. Short-term BMP-4 treatment initiates mesoderm induction in human embryonic stem cells. Blood. 2008;111:1933-41.

[199] Rahman N, Purpura KA, Wylie RG, Zandstra PW, Shoichet MS. The use of vascular endothelial growth factor functionalized agarose to guide pluripotent stem cell aggregates toward blood progenitor cells. Biomaterials. 2010;31:8262-70.

[200] Baker J, Liu JP, Robertson EJ, Efstratiadis A. Role of insulin-like growth factors in embryonic and postnatal growth. Cell. 1993;75:73-82.

[201] Bratt-Leal AM, Carpenedo RL, Ungrin MD, Zandstra PW, McDevitt TC. Incorporation of biomaterials in multicellular aggregates modulates pluripotent stem cell differentiation. Biomaterials. 2011;32:48-56.

[202] Hudalla GA, Kouris NA, Koepsel JT, Ogle BM, Murphy WL. Harnessing endogenous growth factor activity modulates stem cell behavior. Integr Biol (Camb). 2011;3:832-42.

[203] Hudalla GA, Murphy WL. Biomaterials that regulate growth factor activity via bioinspired interactions. Adv Funct Mater. 2011;21:1754-68.

[204] Kielman MF, Rindapaa M, Gaspar C, van Poppel N, Breukel C, van Leeuwen S, et al. Apc modulates embryonic stem-cell differentiation by controlling the dosage of beta-catenin signaling. Nat Genet. 2002;32:594-605.

[205] Risau W, Flamme I. Vasculogenesis. Annu Rev Cell Dev Biol. 1995;11:73-91.

[206] Faham S, Hileman RE, Fromm JR, Linhardt RJ, Rees DC. Heparin structure and interactions with basic fibroblast growth factor. Science. 1996;271:1116-20.

[207] Firth SM, Baxter RC. Cellular actions of the insulin-like growth factor binding proteins. Endocr Rev. 2002;23:824-54.

[208] Cardin AD, Weintraub HJ. Molecular modeling of protein-glycosaminoglycan interactions. Arteriosclerosis. 1989;9:21-32.

[209] Yamamoto M, Ikada Y, Tabata Y. Controlled release of growth factors based on biodegradation of gelatin hydrogel. J Biomater Sci Polym Ed. 2001;12:77-88.

[210] Ikada Y, Tabata Y. Protein release from gelatin matrices. Adv Drug Deliv Rev. 1998;31:287-301.

[211] Brunet LJ, McMahon JA, McMahon AP, Harland RM. Noggin, cartilage morphogenesis, and joint formation in the mammalian skeleton. Science. 1998;280:1455-7.

[212] Fehling HJ, Lacaud G, Kubo A, Kennedy M, Robertson S, Keller G, et al. Tracking mesoderm induction and its specification to the hemangioblast during embryonic stem cell differentiation. Development. 2003;130:4217-27.

[213] Bjellqvist B, Hughes GJ, Pasquali C, Paquet N, Ravier F, Sanchez JC, et al. The focusing positions of polypeptides in immobilized pH gradients can be predicted from their amino acid sequences. Electrophoresis. 1993;14:1023-31.

[214] Gasteiger E, Hoogland C, Gattiker A, Duvaud S, Wilkins MR, Appel RD, et al. Protein Identification and Analysis Tools on the ExPASy Server: Humana Press; 2005.
[215] Burdick JA, Khademhosseini A, Langer R. Fabrication of gradient hydrogels using a microfluidics/photopolymerization process. Langmuir. 2004;20:5153-6.

[216] Mayer M, Yang J, Gitlin I, Gracias DH, Whitesides GM. Micropatterned agarose gels for stamping arrays of proteins and gradients of proteins. Proteomics. 2004;4:2366-76.

[217] Yu X, Dillon GP, Bellamkonda RB. A laminin and nerve growth factor-laden three-dimensional scaffold for enhanced neurite extension. Tissue Eng. 1999;5:291-304.

[218] Khetani SR, Bhatia SN. Microscale culture of human liver cells for drug development. Nat Biotechnol. 2008;26:120-6.

[219] Takeichi M. Cadherins: a molecular family important in selective cell-cell adhesion. Annu Rev Biochem. 1990;59:237-52.

[220] Hynes RO, Lander AD. Contact and adhesive specificities in the associations, migrations, and targeting of cells and axons. Cell. 1992;68:303-22.

[221] Gartner ZJ, Bertozzi CR. Programmed assembly of 3-dimensional microtissues with defined cellular connectivity. Proc Natl Acad Sci U S A. 2009;106:4606-10.

[222] De Bank PA, Kellam B, Kendall DA, Shakesheff KM. Surface engineering of living myoblasts via selective periodate oxidation. Biotechnol Bioeng. 2003;81:800-8.

196

[223] Gothard D, Roberts SJ, Shakesheff KM, Buttery LD. Controlled embryoid body formation via surface modification and avidin-biotin cross-linking. Cytotechnology. 2009;61:135-44.

[224] Du Y, Lo E, Ali S, Khademhosseini A. Directed assembly of cell-laden microgels for fabrication of 3D tissue constructs. Proc Natl Acad Sci U S A. 2008;105:9522-7.

[225] McGuigan AP, Sefton MV. Vascularized organoid engineered by modular assembly enables blood perfusion. Proc Natl Acad Sci U S A. 2006;103:11461-6.

[226] Huebsch N, Arany PR, Mao AS, Shvartsman D, Ali OA, Bencherif SA, et al. Harnessing traction-mediated manipulation of the cell/matrix interface to control stem-cell fate. Nat Mater. 2010;9:518-26.

[227] Khetan S, Burdick JA. Patterning network structure to spatially control cellular remodeling and stem cell fate within 3-dimensional hydrogels. Biomaterials. 2010;31:8228-34.

[228] King WJ, Jongpaiboonkit L, Murphy WL. Influence of FGF2 and PEG hydrogel matrix properties on hMSC viability and spreading. J Biomed Mater Res A. 2010;93:1110-23.

[229] Alenghat FJ, Fabry B, Tsai KY, Goldmann WH, Ingber DE. Analysis of cell mechanics in single vinculin-deficient cells using a magnetic tweezer. Biochem Biophys Res Commun. 2000;277:93-9.

[230] Pamme N. Magnetism and microfluidics. Lab Chip. 2006;6:24-38.

[231] Melville D. Direct magnetic separation of red cells from whole blood. Nature. 1975;255:706.

[232] Molday RS, Yen SP, Rembaum A. Application of magnetic microspheres in labelling and separation of cells. Nature. 1977;268:437-8.

[233] Ho VH, Muller KH, Barcza A, Chen R, Slater NK. Generation and manipulation of magnetic multicellular spheroids. Biomaterials. 2010;31:3095-102.

[234] Souza GR, Molina JR, Raphael RM, Ozawa MG, Stark DJ, Levin CS, et al. Three-dimensional tissue culture based on magnetic cell levitation. Nat Nanotechnol. 2010;5:291-6.

[235] Berry CC, Wells S, Charles S, Aitchison G, Curtis AS. Cell response to dextran-derivatised iron oxide nanoparticles post internalisation. Biomaterials. 2004;25:5405-13.

197

[236] Pisanic TR, 2nd, Blackwell JD, Shubayev VI, Finones RR, Jin S. Nanotoxicity of iron oxide nanoparticle internalization in growing neurons. Biomaterials. 2007;28:2572-81.

[237] Kirouac DC, Zandstra PW. The systematic production of cells for cell therapies. Cell Stem Cell. 2008;3:369-81.

[238] Sargent CY, Berguig GY, Kinney MA, Hiatt LA, Carpenedo RL, Berson RE, et al. Hydrodynamic modulation of embryonic stem cell differentiation by rotary orbital suspension culture. Biotechnol Bioeng. 2010;105:611-26.

[239] Niebruegge S, Bauwens CL, Peerani R, Thavandiran N, Masse S, Sevaptisidis E, et al. Generation of human embryonic stem cell-derived mesoderm and cardiac cells using size-specified aggregates in an oxygen-controlled bioreactor. Biotechnol Bioeng. 2009;102:493-507.

[240] Singh H, Mok P, Balakrishnan T, Rahmat SN, Zweigerdt R. Up-scaling single cell-inoculated suspension culture of human embryonic stem cells. Stem Cell Res. 2010;4:165-79.

[241] Lin RZ, Chu WC, Chiang CC, Lai CH, Chang HY. Magnetic reconstruction of three-dimensional tissues from multicellular spheroids. Tissue Eng Part C Methods. 2008;14:197-205.

[242] Bartosh TJ, Ylostalo JH, Mohammadipoor A, Bazhanov N, Coble K, Claypool K, et al. Aggregation of human mesenchymal stromal cells (MSCs) into 3D spheroids enhances their antiinflammatory properties. Proc Natl Acad Sci U S A. 2010;107:13724-9.

[243] Steck E, Bertram H, Abel R, Chen B, Winter A, Richter W. Induction of intervertebral disc-like cells from adult mesenchymal stem cells. Stem Cells. 2005;23:403-11.

[244] Reynolds BA, Weiss S. Generation of neurons and astrocytes from isolated cells of the adult mammalian central nervous system. Science. 1992;255:1707-10.

[245] Uchida N, Buck DW, He D, Reitsma MJ, Masek M, Phan TV, et al. Direct isolation of human central nervous system stem cells. Proc Natl Acad Sci U S A. 2000;97:14720-5.

[246] Czyz J, Nikolova T, Schuderer J, Kuster N, Wobus AM. Non-thermal effects of power-line magnetic fields (50 Hz) on gene expression levels of pluripotent embryonic stem cells-the role of tumour suppressor p53. Mutat Res. 2004;557:63-74.

[247] Song M, Kim YJ, Kim YH, Roh J, Kim SU, Yoon BW. Using a neodymium magnet to target delivery of ferumoxide-labeled human neural stem cells in a rat model of focal cerebral ischemia. Hum Gene Ther. 2010;21:603-10.

[248] Elbert DL. Bottom-up tissue engineering. Curr Opin Biotechnol. 2011.

[249] Solorio LD, Fu AS, Hernandez-Irizarry R, Alsberg E. Chondrogenic differentiation of human mesenchymal stem cell aggregates via controlled release of TGF-beta1 from incorporated polymer microspheres. J Biomed Mater Res A. 2010;92:1139-44.

[250] Qi H, Du Y, Wang L, Kaji H, Bae H, Khademhosseini A. Patterned differentiation of individual embryoid bodies in spatially organized 3D hybrid microgels. Adv Mater. 2010;22:5276-81.

[251] Zeevi-Levin N, Itskovitz-Eldor J, Binah O. Functional properties of human embryonic stem cell-derived cardiomyocytes. Crit Rev Eukaryot Gene Expr. 2010;20:51-9.

[252] Dolnikov K, Shilkrut M, Zeevi-Levin N, Danon A, Gerecht-Nir S, Itskovitz-Eldor J, et al. Functional properties of human embryonic stem cell-derived cardiomyocytes. Ann N Y Acad Sci. 2005;1047:66-75.

[253] Illes S, Theiss S, Hartung HP, Siebler M, Dihne M. Niche-dependent development of functional neuronal networks from embryonic stem cell-derived neural populations. BMC Neurosci. 2009;10:93.

[254] Nagar B, Overduin M, Ikura M, Rini JM. Structural basis of calcium-induced E-cadherin rigidification and dimerization. Nature. 1996;380:360-4.

[255] Polyak K, Weinberg RA. Transitions between epithelial and mesenchymal states: acquisition of malignant and stem cell traits. Nat Rev Cancer. 2009;9:265-73.

[256] Stirman JN, Brauner M, Gottschalk A, Lu H. High-throughput study of synaptic transmission at the neuromuscular junction enabled by optogenetics and microfluidics. J Neurosci Methods. 2010;191:90-3.

[257] Crane MM, Chung K, Stirman J, Lu H. Microfluidics-enabled phenotyping, imaging, and screening of multicellular organisms. Lab Chip. 2010;10:1509-17.

[258] Ehrbar M, Djonov VG, Schnell C, Tschanz SA, Martiny-Baron G, Schenk U, et al. Cell-demanded liberation of VEGF121 from fibrin implants induces local and controlled blood vessel growth. Circ Res. 2004;94:1124-32.

[259] Sakiyama-Elbert SE, Panitch A, Hubbell JA. Development of growth factor fusion proteins for cell-triggered drug delivery. FASEB J. 2001;15:1300-2.

[260] Hong S, Kang JK, Park JJ, Ryu ES, Choi SS, Lee SH, et al. Association of matrix metalloproteinase-3 with cardiogenic activity during Noggin-induced differentiation of mouse embryonic stem cells. Int J Cardiol. 2010;141:49-60.

[261] de Las Heras Alarcon C, Pennadam S, Alexander C. Stimuli responsive polymers for biomedical applications. Chem Soc Rev. 2005;34:276-85.

[262] Jeong B, Gutowska A. Lessons from nature: stimuli-responsive polymers and their biomedical applications. Trends Biotechnol. 2002;20:305-11.

[263] Lee K, Silva EA, Mooney DJ. Growth factor delivery-based tissue engineering: general approaches and a review of recent developments. J R Soc Interface. 2011;8:153-70.

[264] Forsythe JA, Jiang BH, Iyer NV, Agani F, Leung SW, Koos RD, et al. Activation of vascular endothelial growth factor gene transcription by hypoxia-inducible factor 1. Mol Cell Biol. 1996;16:4604-13.

[265] Lim JJ, Hammoudi TM, Bratt-Leal AM, Hamilton SK, Kepple KL, Bloodworth NC, et al. Development of nano- and microscale chondroitin sulfate particles for controlled growth factor delivery. Acta Biomater. 2011;7:986-95.

[266] Leahy A, Xiong JW, Kuhnert F, Stuhlmann H. Use of developmental marker genes to define temporal and spatial patterns of differentiation during embryoid body formation. J Exp Zool. 1999;284:67-81.

[267] Adamo L, Naveiras O, Wenzel PL, McKinney-Freeman S, Mack PJ, Gracia-Sancho J, et al. Biomechanical forces promote embryonic haematopoiesis. Nature. 2009;459:1131-5.

[268] Ferkowicz MJ, Yoder MC. Whole embryo imaging of hematopoietic cell emergence and migration. Methods Mol Biol. 2011;750:143-55.

[269] Yoshimoto M, Montecino-Rodriguez E, Ferkowicz MJ, Porayette P, Shelley WC, Conway SJ, et al. Embryonic day 9 yolk sac and intra-embryonic hemogenic endothelium independently generate a B-1 and marginal zone progenitor lacking B-2 potential. Proc Natl Acad Sci U S A. 2011;108:1468-73.

[270] Tam PP, Behringer RR. Mouse gastrulation: the formation of a mammalian body plan. Mech Dev. 1997;68:3-25.

[271] Gadue P, Huber TL, Nostro MC, Kattman S, Keller GM. Germ layer induction from embryonic stem cells. Exp Hematol. 2005;33:955-64.

200

[272] Acloque H, Adams MS, Fishwick K, Bronner-Fraser M, Nieto MA. Epithelial-mesenchymal transitions: the importance of changing cell state in development and disease. J Clin Invest. 2009;119:1438-49.

[273] Spencer H, Keramari M, Ward CM. Using cadherin expression to assess spontaneous differentiation of embryonic stem cells. Methods Mol Biol. 2011;690:81-94.

[274] Spencer HL, Eastham AM, Merry CL, Southgate TD, Perez-Campo F, Soncin F, et al. E-cadherin inhibits cell surface localization of the pro-migratory 5T4 oncofetal antigen in mouse embryonic stem cells. Mol Biol Cell. 2007;18:2838-51.

[275] Wilkinson DG, Bhatt S, Herrmann BG. Expression pattern of the mouse T gene and its role in mesoderm formation. Nature. 1990;343:657-9.

[276] Yoshida H, Takakura N, Hirashima M, Kataoka H, Tsuchida K, Nishikawa S, et al. Hematopoietic tissues, as a playground of receptor tyrosine kinases of the PDGF-receptor family. Dev Comp Immunol. 1998;22:321-32.

[277] Hwang YS, Chung BG, Ortmann D, Hattori N, Moeller HC, Khademhosseini A. Microwell-mediated control of embryoid body size regulates embryonic stem cell fate via differential expression of WNT5a and WNT11. Proc Natl Acad Sci U S A. 2009;106:16978-83.

[278] Ferreira L, Squier T, Park H, Choe H, Kohane DS, Langer R. Human embryoid bodies containing nano- and microparticlulate delivery vehicles. Adv Mater. 2008;20:2285-91.

[279] Dang SM, Kyba M, Perlingeiro R, Daley GQ, Zandstra PW. Efficiency of embryoid body formation and hematopoietic development from embryonic stem cells in different culture systems. Biotechnol Bioeng. 2002;78:442-53.

[280] Eaves C, Fraser C, Udomsakdi C, Sutherland H, Barnett M, Szilvassy S, et al. Manipulation of the hematopoietic stem cell in vitro. Leukemia. 1992;6 Suppl 1:27-30.

[281] Gasteiger E, Hoogland C, Gattiker A, Duvaud S, Wilkins MR, Appel RD, et al. Protein Identification and Analysis Tools on the ExPASy Server. Totowa: Humana Press Inc.; 2005.
[282] Davey RE, Zandstra PW. Spatial organization of embryonic stem cell responsiveness to autocrine gp130 ligands reveals an autoregulatory stem cell niche. Stem Cells. 2006;24:2538-48.

[283] Hoelker M, Rings F, Lund Q, Phatsara C, Schellander K, Tesfaye D. Effect of embryo density on in vitro developmental characteristics of bovine preimplantative embryos with respect to micro and macroenvironments. Reprod Domest Anim. 2010;45:e138-45.

201

[284] Groebe K, Mueller-Klieser W. Distributions of oxygen, nutrient, and metabolic waste concentrations in multicellular spheroids and their dependence on spheroid parameters. Eur Biophys J. 1991;19:169-81.

[285] Peerani R, Onishi K, Mahdavi A, Kumacheva E, Zandstra PW. Manipulation of signaling thresholds in "engineered stem cell niches" identifies design criteria for pluripotent stem cell screens. PLoS One. 2009;4:e6438.

[286] Pera MF, Tam PP. Extrinsic regulation of pluripotent stem cells. Nature. 2011;465:713-20.

[287] Young S, Wong M, Tabata Y, Mikos AG. Gelatin as a delivery vehicle for the controlled release of bioactive molecules. J Control Release. 2005;109:256-74.

[288] Choi YJ, Lee JY, Park JH, Park JB, Suh JS, Choi YS, et al. The identification of a heparin binding domain peptide from bone morphogenetic protein-4 and its role on osteogenesis. Biomaterials. 2010;31:7226-38.

[289] Ramirez-Bergeron DL, Runge A, Dahl KD, Fehling HJ, Keller G, Simon MC. Hypoxia affects mesoderm and enhances hemangioblast specification during early development. Development. 2004;131:4623-34.

[290] Purpura KA, George SH, Dang SM, Choi K, Nagy A, Zandstra PW. Soluble Flt-1 regulates Flk-1 activation to control hematopoietic and endothelial development in an oxygen-responsive manner. Stem Cells. 2008;26:2832-42.

[291] Ying QL, Smith AG. Defined conditions for neural commitment and differentiation. Methods Enzymol. 2003;365:327-41.

[292] Shalaby F, Ho J, Stanford WL, Fischer KD, Schuh AC, Schwartz L, et al. A requirement for Flk1 in primitive and definitive hematopoiesis and vasculogenesis. Cell. 1997;89:981-90.

[293] Niwa A, Umeda K, Chang H, Saito M, Okita K, Takahashi K, et al. Orderly hematopoietic development of induced pluripotent stem cells via Flk-1(+) hemoangiogenic progenitors. J Cell Physiol. 2009;221:367-77.

[294] Yamashita JK, Takano M, Hiraoka-Kanie M, Shimazu C, Peishi Y, Yanagi K, et al. Prospective identification of cardiac progenitors by a novel single cell-based cardiomyocyte induction. Faseb J. 2005;19:1534-6.

[295] Motoike T, Markham DW, Rossant J, Sato TN. Evidence for novel fate of Flk1+ progenitor: contribution to muscle lineage. Genesis. 2003;35:153-9.

[296] Nakayama N, Duryea D, Manoukian R, Chow G, Han CY. Macroscopic cartilage formation with embryonic stem-cell-derived mesodermal progenitor cells. J Cell Sci. 2003;116:2015-28.

[297] Darabi R, Gehlbach K, Bachoo RM, Kamath S, Osawa M, Kamm KE, et al. Functional skeletal muscle regeneration from differentiating embryonic stem cells. Nat Med. 2008;14:134-43.

[298] Hirata H, Kawamata S, Murakami Y, Inoue K, Nagahashi A, Tosaka M, et al. Coexpression of platelet-derived growth factor receptor alpha and fetal liver kinase 1 enhances cardiogenic potential in embryonic stem cell differentiation in vitro. J Biosci Bioeng. 2007;103:412-9.

[299] Kattman SJ, Witty AD, Gagliardi M, Dubois NC, Niapour M, Hotta A, et al. Stage-specific optimization of activin/nodal and BMP signaling promotes cardiac differentiation of mouse and human pluripotent stem cell lines. Cell Stem Cell. 2011;8:228-40.

[300] Kishimoto S, Nakamura S, Nakamura S, Hattori H, Oonuma F, Kanatani Y, et al. Cytokine-immobilized microparticle-coated plates for culturing hematopoietic progenitor cells. J Control Release. 2009;133:185-90.

[301] Wu JM, Xu YY, Li ZH, Yuan XY, Wang PF, Zhang XZ, et al. Heparin-functionalized collagen matrices with controlled release of basic fibroblast growth factor. J Mater Sci Mater Med. 2011;22:107-14.

[302] Joung YK, Bae JW, Park KD. Controlled release of heparin-binding growth factors using heparin-containing particulate systems for tissue regeneration. Expert Opin Drug Deliv. 2008;5:1173-84.